


For Reference

NOT TO BE TAKEN FROM THIS ROOM

Ex LIBRIS
UNIVERSITATIS
ALBERTAEASIS





Digitized by the Internet Archive
in 2023 with funding from
University of Alberta Library

<https://archive.org/details/Jugdutt1977>

THE UNIVERSITY OF ALBERTA

RELEASE FORM

NAME OF AUTHOR

Bodh I. Jugdutt

TITLE OF THESIS

Echocardiographic assessment of peak aortic velocity
and acceleration and left ventricular contractility
from the mitral valve echogram in dogs and man

DEGREE FOR WHICH THESIS WAS PRESENTED

M.Sc.

YEAR THIS DEGREE GRANTED

1977

Permission is hereby granted to THE UNIVERSITY OF ALBERTA LIBRARY
to reproduce single copies of this thesis and to lend or sell such copies for private,
scholarly or scientific research purposes only.

The author reserves other publication rights, and neither the thesis nor
extensive extracts from it may be printed or otherwise reproduced without the author's
written permission.

THE UNIVERSITY OF ALBERTA

ECHOCARDIOGRAPHIC ASSESSMENT OF PEAK AORTIC VELOCITY
AND ACCELERATION AND LEFT VENTRICULAR CONTRACTILITY
FROM THE MITRAL VALVE ECHOGRAM IN DOGS AND MAN

by



Bodh I. Jugdutt, MB., Ch.B.

A THESIS

SUBMITTED TO THE FACULTY OF GRADUATE STUDIES AND RESEARCH
IN PARTIAL FULFILMENT OF THE REQUIREMENTS FOR THE DEGREE
OF MASTER OF SCIENCE (MEDICINE)

IN

DEPARTMENT OF MEDICINE

EDMONTON, ALBERTA

SPRING, 1977

THE UNIVERSITY OF ALBERTA
FACULTY OF GRADUATE STUDIES

The undersigned certify that they have read, and recommend to the Faculty of Graduate Studies for acceptance, a thesis entitled Echocardiographic assessment of peak aortic velocity and acceleration and ventricular contractility from the mitral valve echogram in dogs and man, submitted by Bodh I. Jugdutt, M.B., Ch.B., in partial fulfilment of the requirements for the degree of Master of Science (Medicine).

ABSTRACT

Conventional quantitative echocardiographic methods for estimating left ventricular (LV) function from measurements of internal diameters are limited by their reliance on (1) satisfactory echograms of the LV cavity so that the minor axis can be measured, and on (2) assumptions of prolate ellipsoid configuration and uniformity of contraction.

Hemodynamic measurements of the rate of rise of left ventricular pressure (dp/dt), or the aortic ejection velocity (V), or aortic acceleration (dV/dt) have been used to characterize myocardial contractile function, but they also suffer from drawbacks, depend on loading conditions, and require invasive methodology.

In this study the easily recorded mitral valve echogram was used to study LV function. It was proposed that the dynamics of anterior mitral valve leaflet (AMVL) closure are determined by the same forces, in early LV contraction, which generate pressure and culminate in aortic ejection.

In order to determine whether or not the AMVL echogram could reflect alterations in dp/dt and d^2p/dt^2 , and V and dV/dt , simultaneous mitral echo, LV pressure and aortic ejection velocity were recorded in 18 dogs and the signals were differentiated electronically. In 52 patients undergoing diagnostic cardiac catheterization the mitral echoes were recorded in all, and together with high fidelity LV pressure and velocity in 10 patients.

The echocardiographic measurement of peak mitral closing velocity (peak ds/dt) corresponded to the BC slope of AMVL closure, and in the dogs correlated significantly ($p < 0.001$) with peak dp/dt ($r = 0.73$, $N = 380$), peak d^2p/dt^2 ($r = 0.62$, $N = 311$), peak V ($r = 0.82$, $N = 295$), and peak dV/dt ($r = 0.67$, $N = 288$). The peak mitral closing

acceleration (d^2s/dt^2) also correlated significantly with peak dp/dt ($r = 0.75$, $N=330$), peak d^2p/dt^2 ($r = 0.63$, $N = 309$), peak V ($r = 0.83$, $N = 295$), and peak dV/dt ($r = 0.66$, $N = 288$) in the dogs. The average peak ds/dt and d^2s/dt^2 were 26.96 ± 9.04 (SD) cm/sec and 1526 ± 582 cm/sec² respectively under basal conditions, 39.7 ± 15 cm/sec and 2244 ± 890 cm/sec² respectively after isoprenaline, and 20.9 ± 10 cm/sec and 1140 ± 624 cm/sec² after propranolol. These changes followed directional changes in peak dp/dt , V and dV/dt with the interventions.

In the human study, the average peak ds/dt was 25.5 ± 1.6 cm/sec in 6 normal subjects, 26.0 ± 8.3 cm/sec in 24 patients with coronary artery disease (CAD) but normal resting LV end-diastolic pressure (LVEDP) and 16.9 ± 4.3 cm/sec in 12 CAD patients with elevated LVEDP (> 14 mmHg).

Again peak ds/dt correlated with peak dp/dt ($r = 0.93$, $N = 6$) and V ($r = 0.81$, $N = 10$). Also peak d^2s/dt^2 correlated with peak dp/dt ($r = 0.76$, $N = 6$) and V ($r = 0.91$, $N = 8$).

The manually derived values of the BC slope from the strip chart recordings of the mitral echo at speeds of 200 mm/sec correlated with the electronically derived peak ds/dt ($r = 0.93$, $N = 40$) in both man and dogs.

Thus, peak mitral closing velocity and acceleration of the AMVL echo can be used in the non-invasive estimation of peak aortic ejection velocity, peak aortic acceleration, and peak dp/dt , providing non-invasive indices of myocardial contractile function.

ACKNOWLEDGEMENTS

This thesis would not have been made possible without the help of numerous friends, and I would like to mention them in this section.

I could never have hoped to study the problem without the suggestion, guidance and support of Dr. Simon J. K. Lee. Besides being generous with his time and advice in the planning of the experimental design of the study, using the available instrumentation and equipment, he was above all a friend who offered constant encouragement.

The animal studies were made possible with the technical assistance of Mr. Alan Wells, Mr. Ted Germaine, Mr. John Henriksen, Mr. Alvin Todd and others. They performed as a team to ensure the successful completion of these long experiments. I am grateful to Dr. K. Kovaletvski for permitting me to use the facilities at the Surgical and Medical Research Institute, and to Dr. Garner King for the use of the magnetic tape recorder.

In performing the human studies, I am grateful to the Staff of the Cardiac Catheterization Laboratory and the Division of Cardiac Radiology for their cooperation, patience and help in my gathering of data during the performance of routine catheterization. I am especially grateful to Mr. Lou Lnenicka for technical assistance in these studies.

The members of the Medical Electronics Department at the University of Alberta Hospital, especially Mr. Don MacFarlane and Mr. Bert Van Mechelen, were very helpful at all times, offering considerable assistance with the instruments used for the recordings. Mr. MacFarlane selflessly assisted me in playing back the data from the magnetic tape, in some cases on sunny weekends of

August, 1976.

At the Johns Hopkins Hospital, Baltimore, I am indebted to Mrs. Rosemary Hopkins, Mrs. Gail Sullivan, Mrs. Janet Lewis, Ms. Helen Shamroth and Ms. Lisa Grue for typing the manuscript and for labelling the numerous graphs in spite of their busy schedule, and to Mr. Leroy Warthen for the photographic work.

Finally, I am especially indebted to my wife Catherine, and children (Asha, Sunita, and Sunil) for their devotion, patience, understanding and ability to tolerate my schedule.

Bodh I. Jugdutt, M.B., Ch.B.

Cardiology Division,
The Johns Hopkins Hospital,
March 21, 1977

TABLE OF CONTENTS

	PAGE
Introduction.....	1
Background information and review of the literature	
1. Cardiac dynamics and indices of left ventricular function.....	3
2. Aortic ejection velocity and acceleration as indices of contractility.....	9
3. Echocardiographic evaluation of left ventricular function from measurements on the ventricle.....	12
4. Myocardial performance from the mitral valve echogram.....	16
5. Role of ventricular contraction on the dynamics of mitral valve closure.....	22
Statement of the problem.....	31
1. Principal problems.....	31
2. Subsidiary problems.....	31
Methods and Procedure.....	32
1. Animal study.....	34
2. Human study.....	42
Results.....	44
Discussion.....	59
Conclusions.....	63
Tables.....	64
Figures.....	114
Bibliography.....	145

LIST OF TABLES

	PAGE
Table	Description
I	Summary of values of late closure velocity of the anterior mitral valve leaflet from the literature..... 64
II	Hemodynamic and echo data on 18 dogs. The manually obtained mitral closure slope and electronically derived peak mitral closing velocity and acceleration, peak aortic velocity and acceleration, and the peak of first and second derivatives of pressure rise are tabulated for (a) Dogs 1 to 3, (b) Dogs 4 to 6, and (c) Dogs 7 to 18 65
III	Summary of hemodynamic and echo data in 18 dogs..... 102
IV	Summary of correlation coefficients in the animal study..... 106
V	Hemodynamic and mitral echo data in 41 human subject..... 107
VI	Mitral echo, aortic velocity, high fidelity ventricular pressure and ejection fraction data in the remaining 15 human subjects.... 111
VII	Summary of correlation coefficients in the human study..... 113

LIST OF FIGURES

	PAGE
1. Relation between aortic acceleration to aortic velocity and peak dp/dt . Computer plot of data from Noble et al ⁽²⁷⁾	114
2. The animal model and assembly of instruments.....	115
3. Measurement of BC slope manually from echo recordings on strip chart and the Electronics for Medicine recorder.....	116
4. Recording of mitral echo on the Electronics for Medicine recorder: Anterior mitral leaflet (right) and ring (left).....	117
5. The playback assembly for echo, pressure, and velocity signals from magnetic tape.....	118
6. First and second derivatives of AMVL echo and timing with pressure and velocity signals.....	119
7. Mechanical alternans in the anaesthetized dog.....	120
8. Comparison of AMVL closure velocity obtained by manual and electronic methods.....	121
9. Comparison of peak aortic ejection velocity recorded by the electromagnetic cuff versus the catheter-tip probes.....	122
10. Relation between peak mitral closing velocity and peak aortic ejection velocity in 12 dogs (cuff probe).....	123
11. Individual relationships between peak mitral closing velocity and peak aortic ejection velocity by cuff probe in 4 dogs.....	124
12. Relation of peak mitral closing velocity to peak aortic acceleration in 12 dogs.....	125
13. Individual relationships between peak mitral closing acceleration and peak aortic velocity by cuff probe in 4 dogs.....	126
14. Relation of peak mitral closing acceleration to peak aortic ejection velocity by cuff probe in 12 dogs.....	127
15. Relation of peak mitral closing acceleration to peak aortic acceleration in 12 dogs with cuff probes.....	128

	PAGE
16. Relation of peak mitral closing velocity to peak dp/dt in 4 separate dogs.....	129
17. Relation of peak mitral closing velocity to peak left ventricular dp/dt in 17 dogs.....	130
18. Relation between peak mitral closing velocity and peak d^2p/dt^2 in 12 dogs.....	131
19. Relation between peak mitral closing acceleration and peak dp/dt in 15 dogs.....	132
20. Relation between peak mitral closing acceleration and peak d^2p/dt^2 in 12 dogs.....	133
21. Relation between peak aortic ejection velocity and peak dp/dt in 13 dogs.....	134
22. Relation between peak aortic acceleration and peak dp/dt in 12 dogs..	135
23. Relation between peak aortic velocity and peak aortic acceleration in 12 dogs.....	136
24. Relation between peak dp/dt and peak d^2p/dt^2 in 12 dogs.....	137
25. Relation between peak mitral closing velocity and peak mitral closing acceleration in 15 dogs.....	138
26. Angiographic left ventricular ejection fraction and the mitral echo, end-diastolic pressure and peak dp/dt in man.....	139
27. Relation between peak mitral closing velocity and acceleration and cardiac output in patients with various disease states except valvular disease.....	140
28. Grouping of patients by peak mitral closing velocity and acceleration and the underlying disease.....	141
29. Relation between peak mitral closing velocity and acceleration and resting left ventricular end-diastolic pressure in coronary artery disease.....	142
30. Relation of peak mitral closing velocity and acceleration to peak dp/dt in man.....	143
31. Relation of peak mitral closing velocity and acceleration to peak aortic ejection velocity in man.....	144

INTRODUCTION

A non-invasive method is proposed for the assessment of myocardial left ventricular function in man by the analysis of the mitral valve echocardiogram obtained by M-mode echocardiography. The major currently used echocardiographic methods (1-12) for assessing left ventricular function utilize measurements of left ventricular internal dimensions to calculate either volume or circumference. Both methods are adopted from the angiographic method (3-4, 13) and therefore assume that the ventricle is a prolate ellipse. They also assume that the ventricle contracts uniformly. Furthermore, the formula for calculating volume assumes that the long axis is approximately twice the short axis and that the echocardiographic dimension approximates the minor axis (2-3), while the formula for calculating the mean rate of circumferential fibre shortening (mean V_{CF}) assumes that the left ventricle is circular in its short axis and requires ejection time to be measured from the carotid pulse or the aortic valve echogram. Since mean V_{CF} attempts to estimate overall performance while looking at only two areas of the left ventricle, the measurements are distorted in the presence of segmental ventricular disease.

Because significant errors result in the estimation of cardiac output (21) from echocardiographic volumes, investigators in this institution (22,23) have recently used echocardiographic measurements of the systolic closure slope of the anterior mitral valve leaflet (AMVL), the aortic root diameter, and ejection time from the aortic root echogram to estimate cardiac output. The assumption was made in this method that the systolic closure velocity of the AMVL was a measure of the mean aortic ejection velocity. Statistically better correlation was demonstrated between

resting cardiac outputs by the standard Fick method and that derived by using this echographic method ($r = 0.90$) than by using the volume method ($r = 0.58$).

However, the measurement of cardiac output at rest is not an accurate index of cardiac performance and is often normal in the presence of diseased ventricles (24). Other conventional indices of cardiac function based on the force-velocity-length relation also have limitations set by assumptions of ellipsoidal geometry and validity of the models used in their formulation (25-26). It has recently been suggested that the maximum acceleration of the blood ejected into the aorta in ventricular systole may be a more sensitive index of myocardial performance (27-33).

The purpose of this study was, therefore, to explore the hemodynamic correlates of mitral valve closure, and to define the relation between mitral valve closing velocity and acceleration to aortic ejection velocity and acceleration, and to indices of left ventricular contractility. Thus, it was proposed to determine whether the mitral valve echo from M-mode echocardiography can be used as an estimate of overall left ventricular performance and contractile function in dogs and in the clinical setting in man.

BACKGROUND INFORMATION

Cardiac dynamics and indices of left ventricular function

Since the major function of the heart is to pump blood, methods to assess cardiac function have centered on techniques that examine the heart's action as a pump. Abbott and Mommaerts (34), Sonnenblick and others (35,36) provided the physiologic basis for such methods by applying Hill's force-velocity-length relation of skeletal muscle (38) to cardiac muscle, that is, the velocity of shortening is inversely proportional to the magnitude of developed tension.

There are two important consequences of this step. Firstly, a basic difference between skeletal and cardiac muscle physiology became evident. Thus, in skeletal muscle there is a single, essentially fixed, force-velocity curve at a given length, so that force and velocity are always related to each other in the same manner. Contractile activity of skeletal muscle is increased by recruitment of additional fibers while the contractility of each individual fibre remains constant. In contrast, the number of cardiac cells activated during each contraction remains constant, and contractile activity of the myocardium may be shifted by changes in end-diastolic fibre length and in contractility, both of which shift the myocardial force-velocity curve (38-40).

Secondly, since contractile activity of muscle may be expressed in only one of two ways, shortening and development of tension, the thrust of cardiovascular research has been the development of approaches for analysing performance of the intact heart quantitatively and reproducibly in terms of changes in length or volume, and tension. As a result, three major factors (24,25) influencing ventricular pump

function have emerged: (1) Preload, which is related to the end-diastolic volume or end-diastolic fibre length of the ventricle as determined by the force or stress in the wall during diastole. (2) Afterload, which is related to aortic pressure and represents the resistance or load which the ventricular muscle encounters once it begins to eject, and is also a function of ventricular size, geometry, wall thickness and intracavitary pressure. (3) Contractility, or inotropic state of the ventricle, related to the maximum velocity of contraction (V_{max}). A fourth factor (25) is coronary blood flow, which influences myocardial performance in the presence of contraction abnormalities in ischemic heart disease.

Attempts to isolate these factors in defining cardiac function in intact heart have not been successful (25). The three currently used methods measure consequences of shortening and tension development in terms of volumes, flow rates and pressures in pre-ejection and ejection phases of systole (41-42).

The first approach consists of the application of the Frank-Starling mechanism to measure directional changes in cardiac output, filling pressure, and ejection fraction at rest and under stress in diseased versus normal ventricles. Stress is an important factor in this approach because values of these hemodynamic variables under resting conditions are often within the normal range in diseased states (24). Unfortunately, there is a limit to the amount of stress that can be safely used, so that theoretically useful indices, such as the maximum cardiac output which a patient's heart can attain cannot be measured.

The second approach consists of the angiographic quantitation of myocardial contractile function. Thus Gault, Ross and Braunwald (43) showed that by

measuring left ventricular dimensions throughout contractions from high speed cineangiography together with high fidelity intraventricular pressure to derive myocardial wall forces, fibre length, and characteristics of fibre shortening, specific abnormal contractile patterns in left ventricular disease can be identified which are due mainly to decrease in extent and velocity of fibre shortening associated with decrease of wall tension during contraction. The sensitivity of the method is evident from their demonstration of similar cardiac outputs in the presence of decreased velocity of myocardial fibre shortening (V_{CF}) at any level of tension in primary myocardial disease without valvular regurgitation.

The same investigators ⁽⁴³⁾ estimated the velocity of contractile element shortening (V_{CE}) from the measured V_{CF} . Since the coefficient of series elastic element in man is not known and may differ in the normal and abnormal left ventricles the problem is circumvented by considering the point of maximum tension. At this point, stress reaches a maximum and is not changing, so that the rate of stretch of the elastic element is zero ($V_{SE} = 0$ where $dp/dt = 0$) and V_{CF} equals V_{CE} (from $V_{CF} = V_{CE} + V_{SE}$). Although V_{CE} provides an accurate measure of myocardial contractile state ⁽²⁴⁾, both V_{CE} and V_{CF} are load-dependent ⁽²⁵⁾.

The third approach attempts to characterize the contractile state of the myocardium by measuring the peak of the first time derivative of ventricular pressure rise, or peak dp/dt ⁽⁴⁴⁻⁴⁵⁾, and this depends on the use of special catheters with high-fidelity micromanometers at their tips or direct ventricular needle-puncture. Although peak dp/dt is a sensitive index of the contractile properties of the heart, being augmented by positive inotropic agents and diminished by myocardial ischemia

and cardiac depressant drugs, many variables unrelated to the inotropic state affect peak dP/dt , especially loading conditions (44-48). Thus peak dP/dt is increased by increasing preload (end-diastolic pressure and volume), or afterload (raising arterial diastolic pressure and thus delaying aortic valve opening), or heart rate (partly by intrinsic increase in contractility or Bowditch effect, and partly by increased sympathetic stimulation). In addition, it is affected by the pattern of ventricular activation. Efforts to find a better index of contractility which is not load-dependent have led to the use of new indices as the time to peak dP/dt (46), or the second time derivative of tension development peak d^2P/dt^2 (49,50). A different approach has been to correct for end-diastolic volume changes by normalizing the first and second derivatives of left ventricular pressure to the simultaneous isovolumic pressure (48,50), and to correct for aortic diastolic pressure changes by normalizing to the maximal developed isovolumic pressure common to control and altered states (51). Thus, Nejad, Klein, Mirsky and Lown (50) showed that there was no significant change in the normalized peak dP/dt or peak d^2P/dt with varying afterloads and end-diastolic pressures from 4.5 to 14.0 mm Hg.

However, the rationale that the normalized first derivative, $(dP/dt)/P$ may be employed as an index of contractility (50) also derives from the Hill model for skeletal muscle contraction, and the assumption of ellipsoid geometry of the ventricle.

$$\text{Thus: } V_{CE} = V_{CF} + V_{SE} = (db/dt)/b + (d\sigma/dt)/K\sigma$$

where V_{CE} = Contractile element shortening velocity,

V_{CF} = Circumferential fibre shortening velocity,

V_{SE} = Rate of lengthening of the series elastic component,

- and b = midwall radius at the equator of an ellipsoid of revolution, the assumed shape of the ventricle,
- k = stiffness constant obtained from both papillary muscle and intact dog experiments (35,52)

During isometric or isovolumic contraction, $V_{CF} = 0$, and therefore:

$$V_{CE} = V_{SE} = (d\sigma/dt)/K\sigma$$

Since stress (σ) is the product of pressure and geometry, it may be written as :

$$\sigma = C_p, \text{ where } C = \text{constant which depends on ventricular geometry.}$$

Substituting for σ , we obtain:

$$V_{CE} = (d\sigma/dt)/K\sigma = C (dp/dt)/KC_p = (dp/dt)/KP$$

Although extrapolation of the force-velocity curve, or the V_{CE} versus pressure curve to zero load yields an approximation to the maximal intrinsic velocity of contractile elements (34,35,53), or V_{max} , Nejad et al (50) found that although V_{max} remained constant at low-end-diastolic pressures, it was depressed by as much as 25% at higher values, namely 10.5 to 14.5 mm Hg. This confirms findings of others that directional changes in V_{max} tended to parallel those in peak $(dp/dt)/P$ over the normal range of end-diastolic pressures and volumes (24,53). Peak $(dp/dt)/P$ and peak $(d^2p/dt^2)/P$ thus provide simple means of evaluating contractility, but require that high fidelity ventricular pressure tracings are obtained (50,54,55). Extrapolation to zero pressure, which does not exist in the left ventricle during isovolumic contraction, can therefore be avoided in failing hearts with high end-diastolic pressures, when extrapolation over large distances to V_{max} would give low values (56,57).

Nevertheless, a specific index of contractility which is entirely independent of load is yet to be found (58-62). Kreulen et al (62) compared several indices and concluded that a combination of methods are required to detect all ventricular dysfunction. Peterson et al (42) compared isovolumic and ejection indices of contractility and found that while isovolumic indices as V_{max} and $(dp/dt)/P$ separated normal and diseased populations, ejection phase indices as mean VCF and mean normalized systolic ejection rate were better.

Aortic ejection velocity and acceleration as indices of contractility

An alternative approach to assess ventricular performance is the measurement of aortic blood flow velocity, an ejection phase index. Rushmer ⁽⁶³⁾ first drew attention to the fact that the ventricles acted as impulse generators and that the initial ventricular impulse, defined as the product of force and time, was a useful index of ventricular performance. Spencer and Greiss ⁽⁶⁴⁾ related the rapid acceleration of blood in the aorta to the driving pressure gradient across the aortic valve. The pressure difference reached its peak during the first part of systole, at the same time as the peak ejection velocity of about 88 cm/sec was achieved under an initial average acceleration of 4650 cm/sec^2 . This peak was followed by a progressive decline in flow rate and a deceleration of flow, leading to reversal of the pressure gradient. Thus, it became apparent that left ventricular ejection of blood not only requires tension to be developed and maintained during shortening, but the energy must be imparted to the blood to develop velocity and acceleration. It follows from Newton's second law of motion, $\text{Force} = \text{mass} \times \text{acceleration}$, that the maximum acceleration is proportional to the force applied to overcome the inertia of blood. The maximum acceleration in the ejection phase is a function of the force developed in the isovolumic phase.

The relation between aortic acceleration and contractility was studied by Noble and his associates ⁽²⁷⁾. They demonstrated in conscious dogs that changes in peak (dp/dt) produced directional changes in the maximum force exerted by the heart in initial systole (stroke work and power) and in peak acceleration (peak dV/dt). Computer plots of their data are shown in Figure 1. That such a relationship exists is not surprising as can be seen from Levine and Britman's ⁽⁶⁵⁾ equation for

the derivation of V_{CF} . They assumed the ventricle to be spherical, so that its volume is given by $V = (4/3)\pi r^3$ and the circumference by $2\pi r$. By differentiation, one obtains:

$$dV/dt \text{ (Aortic flow rate)} = 4\pi r^2 (dr/dt)$$

and substituting for $V_{CF} = 2\pi r (dr/dt)$,

$$V_{CF} = \text{Aortic flow rate} / 2r^2$$

Noble et al (27) also found that following myocardial ischemia, decrease in peak acceleration occurred earlier and were larger than decreases in peak dp/dt , suggesting that peak acceleration was a more sensitive index of myocardial contractility.

The force necessary to overcome inertia in early systole has been the subject of various studies (66-68). Thus Noble, Gabe and Trenchard (67) collected data to confirm the inertial effect of initial rise of aortic pressure, while Wilcken, Charlier and Hoffman (68) showed that an inverse relation existed between resistance to ejection, stroke volume and peak flow rate. Later Noble et al (69) showed that increasing preload leads to an increase in the active portion of systole during which accelerative forces are applied to ejected blood, thus producing higher peak velocity.

In 1974, further evidence to support aortic acceleration as a useful index of myocardial function came from four other groups of investigators (29-32). In 1976, Kolettis et al (29) found that while aortic velocity and acceleration correlated well with stroke volume, they did not correlate with the peak dp/dt . Moreover, support of the concept that the force for ventricular ejection develops in the pre-ejection period (PEP) came from Reitan et al (28), who found a close correlation between peak aortic acceleration and the inverse square of the pre-ejection period ($1/(\text{PEP})^2$).

The measurement of aortic velocity, however, has inherent problems because electromagnetic flow meters assume an axisymmetric flow profile, so that it is necessary to ascertain that the tip of the catheter lies in the middle of the stream of ejection for reliable measurements as done by Katz and Mills (70). Another problem is the distance of the catheter-tip from the aortic valve because of the complexity of fluid dynamics in the aorta (71) due to its shape, wall properties and its effect on pulse transmission. Three other methods of recording velocity are based on different principles and they also have limitations: the pressure gradient method (72) meets with difficulties when pressures are small; the thermal devices (73) are unable to sense directional flow and are non-linear, and the Doppler ultrasonic method (74) uses a catheter-tipped device.

Echocardiographic evaluation of left ventricular function from measurements on the ventricle.

The growing interest in echocardiography and expansion in its applications have suggested that it could be used in the non-invasive evaluation of left ventricular function.

Three quantitative methods are currently available and each of them have serious limitations. The first widely used method ⁽¹⁻¹²⁾ is the determination of left ventricular volume (LVV) from echo measurement of the left ventricular internal dimension (LVID). Volume is calculated from the formula ⁽¹⁾:

$$LVV = \frac{4\pi}{3} \frac{2(LVID)}{(2)} \frac{(LVID)}{(2)} \frac{(LVID)}{(2)} = 1.047 (LVID)^3$$

Reliability of this method depends on five assumptions ⁽⁵⁾ made in using the formula, and these are: (1) that the shape of the left ventricular cavity is a prolate ellipse, as in angiographic methods ⁽¹³⁾ and deriving indices of contractility ⁽²⁵⁾; (2) that the left ventricular chamber contracts uniformly; (3) that the two short axes are equal, that is the short axis of the left ventricle is circular; (4) that the echocardiographic internal dimension approximates the short axis, because this correlates best with angiographic measurements, while in fact it is most likely intermediate between the short and long axis; and (5) that the long axis is twice the length of the short axis.

The first major assumption requires to be corrected for in the presence of very small or dilated ventricles. A formula has been introduced ⁽¹¹⁾ in an attempt to correct for departures from the prolate ellipsoid model when the long axis is no longer equal to twice the short axis :
$$V = 7.0 / (2.4 + LVID)^3$$

However, the second assumption that the left ventricle contracts uniformly is the greatest source of theoretical and practical limitation of the method because of the sampling problem. Thus two areas are sampled and the manner in which they contract is used to reflect the motion of the rest of the ventricle. Erroneous estimates can therefore be expected in the presence of segmental abnormalities commonly present in coronary artery disease, as Teicholz, Kreulen, Herman and Gorlin (11), and others (7,8) have demonstrated. The error is specially marked during systole, so that estimates of stroke volume and ejection fraction, which are derived using the systolic left ventricular internal dimension (LVIDs), will be distorted in the presence of non-contracting segments. The advantage of estimating ejection fraction non-invasively is somewhat minimized in the presence of segmental disease. The diastolic internal dimension (LVIDd), however, is an accurate and valuable measurement, and correlates well with diastolic ventricular volume even in patients with coronary artery disease (75-76).

The second widely used measurement is that of the mean rate of circumferential fibre shortening (mean V_{CF}) (12, 14-20), and it measures circumference change rather than volume change. It requires the additional measurement of ejection time (ET), which was originally derived from the rise of the posterior left ventricular endocardium, while the carotid pulse or the aortic valve echo is now used. The formula used is based on the same assumptions made in measuring internal dimensions:

$$\text{Mean } V_{CF} = \frac{\pi \text{LVIDd} - \pi \text{LVIDs}}{\pi \text{LVID} \times \text{ET}} = \frac{\text{LVIDd} - \text{LVIDs}}{\text{LVIDd} \times \text{ET}}$$

Since it is adopted from quantitative angiography, this measurement suffers from the same drawbacks as the estimate of ejection fraction from volumes. A third

approach has been to measure the rate of rise of the posterior wall echo (19,77-82) to quantitate myocardial performance. Unfortunately, the dominant echo in the earlier studies probably involved the left ventricular epicardium, although Cooper and his associates (14) have recently suggested that the rate of motion of the posterior endocardium may be useful in assessing myocardial contractility. Again this approach has drawbacks in the presence of segmental abnormalities.

Some investigators have correlated left ventricular wall thickness by echo with measurements obtained from angiography, surgery and autopsy (83,84). It appears the echo measurement may be superior to angiographic measurements which are prone to errors during systole, due to the presence of trabeculation or variable amounts of pericardial effusion present in patients with heart disease. Other investigators have used estimates of left ventricular wall thickness and volume to derive left ventricular mass. Although the value of these measurements in studying cardiac performance is doubtful, altered systolic thickening in ischemic myocardium ⁸⁶, and segmental abnormalities in wall and septal motion ⁸⁷ in coronary artery disease using M-mode sector scanning provide useful quantitative information. It may be possible in the future to quantify these abnormalities.

Thus, in patients whose ventricles contract uniformly and have no gross distortion of shape, as in valvular heart disease or cardiomyopathy, echo measurements of internal dimensions to derive volumes and V_{CF} are useful in estimating overall left ventricular performance. But in the presence of segmental abnormalities, as commonly found in coronary artery disease, these echo measurements are often erroneous. Nevertheless, besides limitations set by theoretical assumptions made in the formulas, errors can arise from poor technique and improper placement and angulation of the

echo transducer (88). Thus, the success in obtaining satisfactory echograms varied between 60% and 80% in two studies (7,9).

Echocardiographic evaluation of left ventricular function from the mitral valve echogram

Eversince Edler (89,90) drew attention to the characteristic pattern of motion of the mitral valve leaflets and its distortion in disease, the mitral valve has occupied a central position in echocardiography. There are several reasons for this: (1) its characteristic "M" - appearance in diastole is easily recognized, (2) it is the easiest structure to localize and record, (3) it serves as a landmark in identifying other structures, (4) it provides information about transducer direction and helps to ascertain that the same portion of the left ventricle is traversed in measuring ventricular dimensions, and (5) it is useful in the diagnosis of various forms of valvular and congenital heart diseases.

However, attempts to use various parameters derived from the mitral echo to estimate left ventricular function have not achieved the popularity that measurements of left ventricular dimensions have. This may partly reflect the fact that the mitral valve is a complex structure with a complex motion pattern. In 1967, Zaky, Grabhorn and Feigenbaum (91) observed that the echo from the mitral valve ring resembled the inverted pattern of the ventricular volume curve and postulated that its motion was related to the stroke volume. In 1975, important contributions from two other groups of investigators (92-94) indicated that indices derived from mitral valve motion may give hemodynamic information concerning overall ventricular performance. They found that the timed pattern of motion of the anterior mitral valve leaflet (AMVL) echo is strikingly similar to the timed patterns of transmitral flow (92) and to the radiographically recorded motion of radio opaque clips placed

on the mitral valve ⁽⁹³⁾. These findings validate that the mitral echo indeed reflects the AMVL motion ⁽⁹³⁾, and that leaflet motion follows the blood flow pattern across the valve ⁽⁹²⁾.

The same two groups of investigators ⁽⁹²⁻⁹⁴⁾ provided additional evidence to support that characteristics of the AMVL motion reflect myocardial performance. Thus, Laniado's group ⁽⁹²⁾ showed good correlation between the diastolic closure slope (EF) and cardiac output ($r = 0.99$), and confirmed previous findings ⁽⁹⁵⁾ that flow across the mitral valve starts as soon as left atrial pressure exceeds left ventricular pressure. They also found that the EF slope can be reduced in other disease states besides mitral stenosis, in support of findings by Duchak and others ⁽⁹⁶⁾ who described the "false" mitral stenosis pattern in patients with decreased left ventricular compliance and decreased rate of filling. In these patients, the distance or area between the anterior and posterior leaflets is slightly reduced because of reduced flow ⁽⁹⁷⁾. Pennock and his associates ⁽⁹⁸⁾ found that the opening slope (DE) is also a possible indicator of mitral flow, and it is decreased in the presence of elevated filling pressures ⁽⁹⁹⁾.

While Laniado's group ⁽⁹²⁾ concerned themselves mainly with early and mid-diastolic events, Pohost and his associates ⁽⁹³⁻⁹⁴⁾ have provided the precise echocardiographic definition of mitral opening and closure in the dog and man. Mitral valve closure was previously thought to occur either at the most posterior point on the AMVL echo, called point C ⁽¹⁰⁰⁻¹⁰³⁾ or before point C ⁽¹⁰⁴⁾, or at the point of coaptation of anterior and posterior leaflets, also called point C ^(99, 103). Parisi and Milton ⁽¹⁰⁵⁾, on the other hand, demonstrated that mitral closure preceded

the mitral component of the first heart sound by 20 msec. The findings of Pohost et al (93,94) clarify this apparent controversy. They found that the mitral echo was a reliable indicator of the hemodynamic markers of opening and closure. They recognized that the conventional C point was occasionally difficult to define and coincided best with the mitral component of the first heart sound (100-104), which is known to lag the hemodynamic crossover by 25 to 30 msec (100). Furthermore, they labelled the termination of the final rapid posterior motion of the AMVL in end-diastole as C_o , and showed that C_o preceded the hemodynamic marker of mitral valve closure, that is, the onset of left ventricular systole by 18 to 37 msec in man (94) and 20 msec in dogs (93).

Qualitative analysis of mitral valve motion has provided further understanding of the mitral valve closure mechanism. The interplay between left atrial pressure and left ventricular pressures have repeatedly been demonstrated to influence both opening and closure. The finding of striking premature closure in patients with severe aortic regurgitation and elevated left ventricular end-diastolic pressures (99) was thus probably related to regurgitant aortic blood elevating the left ventricular end diastolic pressure beyond the left atrial pressure, an alternative explanation being that the backflow alone closed the mitral valve. However, in one patient who was in sinus rhythm, the leaflets could be seen to abruptly come closer together but they still remained separated until final closure after depolarization (99). It may be that partial closure was also followed by final closure in the other patients as well but could not be easily recognized from the echo because of problems in resolution.

Nevertheless, striking features appear in the AC portion of AMVL closure with elevation in left ventricular end diastolic pressure (LVEDP). In the normal patient,

the final closure of the AMVL represented by the A to C portion reflects a combination of two events, atrial relaxation and isovolumic ventricular systole⁽¹⁰³⁾. The mitral A wave follows the P wave of the electrocardiogram (ECG), and the A point (or often A') marks the beginning of atrial relaxation. The AC portion is usually smooth, so that the B point corresponding to the R wave of the QRS complex on the ECG may not be obvious from records made at conventional speeds (25 to 50 mm/sec). The leaflets are thought to close completely to point C after the onset of ventricular systole.

In the presence of elevated LVEDP (99, 107, 108) secondary to marked rise in left atrial pressure, as is usually seen with decreased ventricular compliance in hypertrophy, fibrosis or coronary artery disease, there is a rapid rise in left atrial pressure following atrial systole with instantaneous rise in left ventricular pressure, followed by an early crossover of left atrial and ventricular pressure curves resulting in an early onset of mitral valve closure and an early A point. The pressures nearly equalize prior to ventricular systole so that mitral valve closure is interrupted at point B coinciding with the onset of the QRS or the R wave on the ECG. The final closure, from point B' to C, or B' to C₀, occurs at a higher left ventricular pressure, as a result of which the AC interval is prolonged and a BB' shoulder appears.

Konecke et al ⁽⁹⁹⁾ have found by recording echocardiograms simultaneous with cardiac catheterizations that a PR minus AC interval less than 60 msec can be taken to indicate an LVEDP greater than 20 mm Hg and an atrial component of at least 8 mm Hg provided the PR interval is greater than 140 msec. Since the left ventricular diastolic pressure is initially low, the DE slope and amplitude of mitral valve opening

in these patients was found to be normal. Using computer analysis of AMVL and left ventricular wall echo motion in early diastole, Upton et al (109,110) found abnormal ventricular dimension during isovolumic relaxation.

An alternative explanation for the prolongation of C noted by Konecke et al⁽⁹⁹⁾ is that it is caused by altered contractility rather than increased LVEDP. However, Feigenbaum and associates⁽¹¹¹⁾ also found that the duration of the BB' shoulder was prolonged by increasing LVEDP. Thus they showed that the BB' interval decreased from 0.06 to 0.02 sec as LVEDP decreased after amyl nitrite in one patient, and increased from 0.01 to 0.04 sec after the afterload was increased with neo-synephrine in another patient.

Nevertheless, the exact relation between mitral valve closure and LVEDP remains unsettled, and Yow and Reichle⁽¹¹²⁾ were unable to reproduce the findings of Feigenbaum and his associates. This may be due to the heterogeneity of the population of patients with elevated LVEDP. Thus, while some have LVEDP due to an elevated atrial component, others have an initially high LVEDP⁽⁹⁹⁾. In these patients, the mitral valve opens against a high LVEDP and blood flows into a dilated ventricle which is only partly emptied, the DE slope is diminished, and a larger percentage of ventricular filling may follow atrial systole so that AC amplitude may be increased⁽¹⁰⁸⁾.

While most investigators measured slopes in early or mid diastole, a method was developed in this institution^(22,23) utilizing the systolic closure slope of the AMVL, defined as AC or BC, to calculate cardiac output. The formula was derived from the conventional hydraulic formula, but the assumption was made that the closure slope

measured the mean aortic ejection velocity. Thus:

$$\text{Cardiac output} = \text{Aortic area} \times \text{Ejection time} \times \text{Heart rate} \times \text{Mitral closure slope}$$

A good correlation ($r = 0.90$) was demonstrated between cardiac outputs derived by this method and the standard Fick method in patients with or without asynergy determined by angiography. Cardiac outputs derived from the conventional echo method showed a lesser correlation. Thus, simultaneous echocardiographic and hemodynamic observations have revealed various abnormalities in the mitral valve echo. Attention has recently been drawn to the final closure of the anterior mitral valve leaflet and attempts are being made to use the slope as a measure of myocardial performance.

Role of ventricular contraction on the dynamics of mitral valve closure

Studies of mitral valve motion using a variety of different techniques have indicated that the valve opens widely in diastole, moves steadily towards mid-diastolic closure, and then reopens with atrial systole before resumption of closure in end-diastole (92-95, 97, 113-118).

Three mechanisms which depend on ventricular filling have been suggested for the mid-diastolic closure. Firstly, blood flowing into the ventricle is thought to cause negative pressure changes (Bernoulli effect) which reverses the polarity of gradient across the valve (113, 117, 119, 120). Secondly, resistance to ventricular filling is thought to generate vortices which apply forces on the ventricular surfaces of leaflets (113, 119, 121, 122). Finally, the distension of the ventricle after rapid filling is thought to pull the roots of the papillary muscles away from the ring and transmission of this pull through the chordae to the edges of the leaflets draw them towards each other (114, 121).

Three major mechanisms have also been suggested for the closure in late diastole. The first two were proposed by Henderson and Johnson (119) in 1912. They believed that the primary mechanism was mediated by negative pressures created by the forward acceleration that followed atrial contraction and forced the leaflets into apposition, as for mid-diastolic closure. They also believed that ventricular contraction provided the secondary mechanism to complete valve closure. The third mechanism was proposed by Bellhouse (113) and Taylor (123) who emphasized the role of vortices behind the valve leaflets in enhancing closure velocity.

Evidence to support all three mechanisms of late diastolic closure have accumulated. Thus, in 1916, Dean ⁽¹²⁴⁾ used a perfused cat heart with a delicate lever system and confirmed that the mitral valve started to close in atrial systole and that final effective closure was rapidly completed in ventricular systole. The role of ventricular systole is supported by findings of three other groups of investigators. In 1956, Rushmer, Finlayson and Nash ⁽¹²¹⁾ observed cusp movements by silver clips on the mitral valve in vivo, and found movements were small in diastole and more marked at the beginning of ventricular systole. In 1968, Padula, Cowan and Camishion ⁽¹¹⁴⁾ obtained a cinefilm of the mitral valve in a beating heart and showed that the cusps remained in mid-position towards the end of diastole, with the cusp orifice approximately half the diameter of the mitral ring, presumably being held by papillary muscles in diastole as suggested by Rushmer ⁽¹²¹⁾. Finally, in 1974, Gordon, Mathieu, Lipton and Tsakiris ⁽¹¹⁸⁾ observed AMVL closure, using cineangiography to track radio-opaque markers sutured on the mitral cusps, in isolated atrial systole and normal sinus rhythm. They found that at comparable heart rates, closure was slow (10 ± 4.5 cm/sec), ineffective and mostly partial (40-95%), and of short duration (10-30 msec) after isolated atrial contractions while with normal sinus rhythm it was more rapid (33 ± 13 cm/sec), effective (100%) and of longer duration (250-430 msec).

In contrast, in 1966, Brockmann ⁽¹¹⁷⁾ measured pressure differences across the mitral valve in dogs and concluded that atrial contraction produced presystolic closure of the mitral valve by propagating a pressure front towards the ventricle which made the pressure difference positive and tended to close the valve. The atrial

mechanism is also supported by Sarnoff's (120) and Luisada's groups (125).

On the other hand, in 1972, Bellhouse (113) reported some important observations made using a model of the left ventricle with aortic and mitral valves. He not only confirmed the double opening and closure of the mitral valve, but was able to define four forces acting on the valve cusps. Firstly, a ring vortex occupying the left ventricle tended to close the valve. Secondly, acceleration of flow through the valve ring tended to open the valve while deceleration tended to close it. Thirdly, a Venturi effect tended to move the cusps parallel. And finally, there was a resistance to opening and closure of the valve, and it depended on cusp angular velocity and acceleration. He also found that the anterior cusp closed before the posterior cusp, unless the ventricle was dilated, in which case they closed together. When the ventricle was small, a strong ring-vortex, which was symmetrical with its main strength concentrated behind the anterior cusp, tended to close the mitral valve in diastole and was formed within the ventricle. When the ventricle was dilated, this vortex was of negligible strength. More important was the finding that when atrial systole was absent, the valve was 88% closed at the end of diastole when the ventricle was small, in contrast to only 28% closure when the ventricle was large. Thus, this suggests that 12 and 72% of mitral valve closure remains to be completed by ventricular systole in small and dilated hearts respectively. These observations not only provide support for previous views of mitral closure, but stress the added role of ventricular size on the pattern of mitral closure.

Further support for the role of the ventricular mechanism in final closure of the mitral valve, using an entirely different approach, comes from studies of transmitral flow by the group of Laniado and Yellin (92,95). They postulated that the inertia

of blood delivered into the ventricle by atrial contraction drives the leaflets apart and they remain open until adequate decelerative forces provided by ventricular pressure in early ventricular contraction are applied to the leaflets to halt further flow into the ventricles. This decelerative force must have finite duration before the pressure gradient across the mitral valve is reversed, and so must the reversed gradient have finite duration before flow is reduced and valve closure can occur. A phase delay of 20 to 40 msec was found to be created by the inertance properties of blood by these investigators⁽⁹⁵⁾. A similar delay was found to exist between echo and hemodynamic markers of mitral valve closure by Pohost and associates^(93,94) in their studies of the temporal relationships of mitral closure to hemodynamics.

The influence of the electrocardiographic PR interval on the relative contributions of atrial and ventricular systole in mitral valve closure were studied by Zaky et al⁽¹⁰²⁾, Shah⁽¹²⁶⁾, and Craige⁽¹²⁷⁾. In summary, they have shown that when the PR interval is less than about 180 msec atrial contraction does not cause adequate closure, and ventricular systole then completes the closure. On the other hand, when the PR interval exceeds about 180 msec, time permits the chamber to contract and relax fully and bring about a reversal of the pressure gradient, and closure. Under these conditions, there is apparent complete closure in presystole and ventricular systole merely seals the closed valve. When the PR interval exceeds 500 msec however, they suggested that the valve reopens and ventricular systole then initiates and completes final closure. Zaky, Steinmetz, and Feigenbaum⁽¹⁰²⁾ noted similar findings in complete heart block, but they also found incomplete and transient closure in presystole in advanced disease. The apparent contradictions in these observations are due to the fact that the distinction between the AB and BC portions of mitral closure was not clearly made.

The data in fact support the view that the AB portion relates to atrial relaxation, which is slow at first and accelerates near the end of atrial filling.⁽¹⁰²⁾ In contrast, the BC portion relates to ventricular systole.⁽¹²⁸⁾ It is probably better called BC_o ^(93,94), where C_o marks the end of the rapid posterior movement of the anterior mitral leaflet echo. The B (or B' in some cases) corresponds to the R wave of the QRS complex in the ECG. This latter definition takes into account the observation that a shoulder stretches the B point into a line B-B' in the presence of increased LVDP.⁽⁶⁹⁾ While the AB portion appears to be affected by the PR interval and heart rate^(102,126, 127), the BC portion is determined by ventricular contraction and may be influenced by ventricular volume.⁽¹¹³⁾

Two groups of independent investigators have commented briefly on the possible value of mitral valve closure velocity in assessing left ventricular function. Firstly, Yoshitoshi and associates⁽¹²⁹⁾ used frequency analysis of ultrasonic Doppler signals to derive peak mitral closure velocity in 1965. They obtained values ranging from 20 to 40 cm/sec in normal subjects, with a mean value of 27 cm/sec. High values were seen in mitral stenosis in the presence of sinus rhythm (range 30 to 80, mean 52 cm/sec), and in such a patient, the closure velocity was reduced from 65 to 30 cm/sec following mitral commisurotomy. In patients with mitral stenosis and atrial fibrillation, they found that the peak mitral closure velocity was high, with short preceding diastoles and low with long preceding diastoles. They also postulated a relationship between peak mitral closure velocity and left ventricular dynamics.

Thus:

$$M \times \frac{d^2s}{dt^2} + \left(\frac{1}{C_m} + \frac{1}{C_a} \right) s = \Delta P$$

where M = Mass of the whole system consisting mainly of blood,

C_m = Compliance of the mitral valve and chordae,

C_a = Compliance of the left atrial chamber,

S = Displacement of the mitral valve,

and ΔP = pressure gradient between the left ventricle and left atrium in early systole.

They also suggested that : (1) valve velocity and acceleration would increase as dp/dt increased, (2) the high velocity in mitral stenosis in the presence of elevated left atrial pressure was due to mitral valve closure occurring at a time when left ventricular pressure rose sharply, corresponding to the moment of high dp/dt , and (3) mitral velocity would reach a maximum at the certain value of $1/C_m$ and the velocity beyond that point would decline or there will be a resonance phenomenon. The formula, however, ignored viscous resistance of the valve, blood flow and tendon. Furthermore the formula should probably also be modified to include (dp/dt) since it influences early systolic events.

However, the observation made by Yoshitoshi et al⁽¹²⁸⁾ on the effect of preceding diastoles on mitral closure velocity suggests that an alternative explanation for the high values in mitral stenosis is that they related to the AB portion which exerted a dominant effect on the Doppler signal, so that the BC portion was not detected because of problems in resolution. Since in the normal situation AC velocity approximates both AB and BC velocities, and such

an error would not matter, the situation may be quite different in the presence of mitral stenosis.

In 1976, Kingsley⁽¹³⁰⁾ published a graph showing a linear correlation between mitral valve closure slope (BC) by echo and (dp/dt) in dogs. He also indicated that the BC slope was reduced in myocardial dysfunction (less than 20 cm/sec), and increased in hyperkinetic states (greater than 35 cm/sec), the normal range being 20 to 30 cm/sec. The detailed results were not revealed.

Other investigators have also measured mitral valve closing velocity by various methods which yielded similar results (Table I). Gordon et al⁽¹¹⁸⁾ followed the motion of radio-opaque markers using cineangiography in dogs and found peak closing velocity to be 33 ± 13 cm/sec. Buynkozturk, Kingsley and Segal¹³¹ found normal subjects had a range between 8 and 50.5 cm/sec with a mean of 22.1 ± 9.13 cm/sec. They also found that heart rates up to 130 beats/min and PR up to 190 msec had no effect on the closure slope. Emerson et al⁽¹³²⁾ measured instantaneous peak final closing velocity using a digital tracking system with a dynamic range gate locked to the mitral valve echogram and found that in normal subjects, they ranged from 23.0 to 46.7 cm/sec, with a higher mean (34.6 ± 7.8 cm/sec) than with manual Doppler methods. Recently Upton and his group⁽¹¹⁰⁾ in Britain reported results using manual digitization of echos recorded at high speeds of 100 mm/sec and found that in normal subjects the peak AC closure was 29.0 ± 8 cm/sec. Lalani and Lee⁽²³⁾ in this institution obtained values ranging from 13.7 cm/sec to 49.9 cm/sec in man (mean 27.4 ± 8.1 cm/sec) by the manual method and

41 ± 12 cm/sec in dogs⁽²²⁾ by electronic differentiation.

It is not always clear from these studies of the closure velocity whether AC or BC slopes were measured and this may explain the slight disparity between normal ranges.

From the information in this review, a unified concept of ventricular contraction can be formulated. Ventricular contraction can be visualized as a continuous sequence of events during ventricular systole, beginning with the progressive development of force (wall tension) and intraventricular pressure during isovolumic contraction, followed by abrupt fibre shortening and dissipation of energy sufficient to overcome the inertia of blood and eject it into the aorta under considerable velocity and acceleration. That a close relationship exists between parameters measured during isovolumic and ejection phases of contraction, has been demonstrated by Burns, Covell and Ross⁴⁴, and others^(28,45). Since the final BC portion of mitral valve closure is mediated by ventricular systole, it is logical to assume that a constant relationship exists between mitral valve closing velocity and acceleration, and aortic velocity and acceleration, and ventricular contractility (Figure 2). Since the AMVL closing velocity and acceleration are isovolumic phase measurements, like peak dp/dt , a close correlation between them can be expected. The exact relation between velocity of shortening of the ventricular muscle and maximum aortic and mitral acceleration is no doubt a complex one since (1) the magnitude and nature of the load in initial systole are not known, (2) the inertial properties of the mitral valve are not

known, and (3) the geometric coupling between muscle fibre shortening and blood movement are not known. That a close relationship exists between mitral valve motion and left ventricular function is further strengthened from studies of the ultrastructure and electromechanical properties of the mitral complex in dogs⁽¹³³⁻¹³⁵⁾. One group of researchers⁽¹³⁴⁾ found electrophysiological continuity between the mitral valve and the left ventricle but not the left atrium.

STATEMENT OF THE PROBLEM

Principal Problems

(a) To verify whether a relationship, suggested from the considerations of cardiac dynamics reviewed, exists between the echocardiographic measurement of anterior mitral valve leaflet closing velocity and peak aortic ejection velocity, and ventricular contractility.

(b) If so, to determine whether a relationship also exists between the derived anterior mitral valve leaflet closing acceleration and the derived peak aortic acceleration, and ventricular contractility.

(c) To verify the relationships in man.

Subsidiary Problems

(a) To determine whether the echocardiographic measurements of mitral valve closing velocity and acceleration can be easily obtained in man.

(b) To examine whether the method provides an equally effective or better means of assessing myocardial performance in man than conventional methods.

METHODS AND PROCEDURE

This study was conducted in two parts:

(I) Animal Study

(II) Human Study

(I) The Animal Study

This was carried out in three stages:

(a) A preliminary study was conducted in 3 dogs for two reasons:

Firstly, to compare the mitral valve closure slope derived from the AMVL echogram recorded on the strip chart of the echo machine and that derived from the record of its analog signal on the Electronics for Medicine recorder, model DR8, similar to that used in the human cardiac catheterization laboratory. Other aims were: (1) to verify the accuracy of the echocardiographic measurements in our hands, (2) to assess whether continuous recording of the mitral echo could be made simultaneous with pressure tracings and the ECG during routine cardiac catheterization in man, and (3) to assess the reliability of derived slopes.

Secondly, to examine the relation of the mitral valve closure slope to aortic ejection velocity measured by an electromagnetic catheter-tip velocity probe and to the first derivative of left ventricular pressure rise by on-line differentiation of left ventricular pressure measured by a catheter-tip transducer in the ventricle. All recordings were made on the Electronics for Medicine photographic recorder at paper speeds of 200 mm/sec.

(b) The second part of the animal study was carried out in three dogs, and it also related to methodology. Electronic differentiation of signals recorded on the magnetic tape were used to determine the relationship, on a beat to beat basis, between peak velocity and peak acceleration of the AMVL closure to peak aortic velocity and acceleration, as well as to the first and second derivatives of left ventricular pressure rise. In the dogs here, the validity of catheter-tip probe readings of aortic velocity

during interventions was assessed by comparing them with simultaneous recording using an electromagnetic cuff probe around the aortic root.

(c) The final part of the animal study was carried out in 12 dogs to further study the dynamics of mitral valve closure and ventricular ejection. Here, aortic velocity was measured by the cuff electromagnetic flow probe around the aortic root.

II The Human Study

This study was carried out in four parts:

(a) In 13 patients, the relation of the velocity of AMVL closure to angiographic left ventricular ejection fraction and cardiac output, obtained by Fick's method, was determined. The mitral echogram was recorded on the echo machine and its analog signal on the Electronics for Medicine recorder in use in the Cardiac Catheterization Laboratory.

(b) In 14 patients, the analog signal of the mitral echo and its first and second derivatives were recorded simultaneously on the Electronics for Medicine recorder. The relation between acceleration of the AMVL closure to ejection and cardiac output was thus studied.

(c) In 10 patients, the relationships between velocity and acceleration of AMVL closure to aortic ejection velocity and acceleration were determined.

(d) In 6 patients, the relationships between velocity and acceleration of AMVL closure to the first and second derivatives of left ventricular pressure rise obtained using an intracardiac catheter-tip pressure transducer, were determined.

ANIMAL STUDY

Preparation of the canine model

Eighteen mongrel dogs weighing between 18 and 34 kg. were anesthetized using sodium thiopental (10 mg/kg IV) and maintained with chloralose (80 mg/kg). A cuffed endotracheal tube was passed and the dogs were artificially ventilated with room air using a Bird ventilator. An intravenous infusion line with 5% Dextrose in saline was established in a brachial vein and run at the rate of 50 cc/hr. The chests were opened by a limited transverse thoracotomy at the sixth intercostal space with minimal bleeding. The heart was exposed and the pericardial sac opened. (Figure 2)

Ultrasound recording

Echograms of the mitral valve were obtained using a SKI Ekoline 20A Ultrasonoscope (Smith Kline Instruments Corporation) having a frequency output of 2.25 megahertz and a repetition rate of 1000 pulses per second and equipped with a 0.5 inch diameter transducer prefocused at 10 cm. The Ultrasonoscope was interfaced with a Honeywell 1865 strip chart recorder. Echo recordings were made directly on photosensitive Kodak linagraph paper (type 2167) at a speed of 50 mm/sec or 200 mm/sec. The echo signal was isolated by a time analog pre-amplifier module (SKI) with optimal adjustment of gate width.

The transducer was held in contact with epicardium of the anterior surface of the right ventricle to the right of the left anterior descending coronary artery. An adequate amount of coupling gel (Aquasonic) was used to form a cushion so as to overcome the problem of intermittent loss of direct contact between the tip of the transducer and the anterior cardiac surface. Care was taken to hold the transducer with minimal pressure, but rigidly enough so as to minimize relative motion between the transducer and the heart and to avoid lateral sliding of the transducer. The transducer tilt was also adjusted to maximize the amplitude of anterior mitral leaflet excursion^(93, 94), at which time the posterior mitral leaflet just comes into view. Anterior leaflet motion

was observed between a depth of 3 to 6 cm. in all preparations. The classical "M" shaped configuration of the AMVL was observed only when the heart rates were less than about 100 beats/min, but not at rates above this. This phenomenon is in agreement with observations by Taylor¹²³ who found in his animal experiments that at rapid heart rates (greater than 240 beats/min), the outlet area of the mitral valve is unchanged throughout the brief diastolic filling period, so that the early diastolic closure slope (EF) is absent.

The time delay in the ultrasound system was less than one millisecond, and the inherent frequency response limitation occurs above 500 Hertz (data provided by Smith Kline Instruments Corporation).

The analog signal of the AMVL echo was observed on a scope and optimal adjustments of gate width made before they were recorded on the Electronics for Medicine (Model DR8) multichannel recorder in the first 3 dogs, and on the 4 channel magnetic tape recorder (Hewlett-Packard Instrumentation Recorder 3960) in the other 15 dogs. Samples of the mitral echo were also recorded simultaneously on the strip chart and Electronics for Medicine recorder, the delay between signals on the two recorders being negligible. The height of the analog signal was calibrated by moving the gate by 1 cm.

Velocity recordings

An electromagnetic catheter-tip velocity probe (SE Medic) was used in the first 6 dogs. This was introduced via either the femoral or carotid artery which were isolated by prior cut-down. The tip of the catheter was positioned using fluoroscopy so that it was 3 cm. above the aortic valve in the aortic root. The catheter was connected to an SE Medic Flowmeter and readings of velocity were made directly on the flowmeter. The zero calibration was obtained with the catheter in saline prior to introduction into the blood stream. In addition, signals were recorded on the Electronics for Medicine photographic recorder at a paper speed of 200 mm/sec in the first 3 dogs, with Black box storage for later dark room processing.

In the 3 other dogs, the velocity from the Catheter probe was recorded on the magnetic tape as well. In addition, one of these dogs had both internal catheter tip and external cuff electromagnetic probes inserted for comparison of velocities. In the remaining 12 dogs, only external probes were used. They ranged in diameter from 1.0 to 1.6 cm and were placed around the aortic root to measure flow velocity. In each case the probe was connected to a pulsed logic flowmeter (Biotronex Laboratory, BL 610), the gain and frequency response modes being adjusted to give optimal signals. The output signals were recorded on both a pen recorder (Type R dynograph, Beckmann Instruments) at speeds of 25 to 100 mm/sec, as well as on the magnetic tape. Zero flow calibration for the cuff probe was obtained by placing the probe in saline initially, and later by instantaneous clamping of the aorta proximal to the cuff before terminating the experiments, and finally with the cuff in a beaker of blood. The frequency response for the stylus of the Beckmann recorder was 125 Hz at 1 cm deflection.

Linearity of response was checked for both catheter and cuff probes for velocities up to 300 cm/sec and flows up to 4 litres/min respectively. For the velocity catheter, the tip was placed in the middle of a long glass tube of even and known internal diameter (D_{cm}) and saline was injected into the distal end of the tube at a constant rate using an electric pump.

The volumes (Q ml) of saline flowing past the catheter tip in different timed intervals (t sec) in graduated steps, were collected in a graduated cylinder and measured. Laminar flow velocity (V cm/sec) was derived from the formula:

$$V = (Q/t)/(\pi D^2/4)$$

In the case of the cuff probes, the flow velocity of blood or saline through a section of the aortic root removed from each of the 12 dogs at the end of the individual experiments was measured at various flow rates (0 to 4 L/min) in graduated steps using a Travelol pump. Velocity was calculated from the cross-sectional area of each aorta.

Pressure recordings

Pressures were recorded using a high-fidelity transducer-tipped SF₁ pressure catheter (Statham Laboratories Inc) which was introduced into the left ventricle from the carotid or femoral artery isolated by previous cut-down. The catheter was guided with the help of fluoroscopy so that the tip lay free near the apex of the ventricular cavity. The signal from the intracardiac transducer was balanced against that of an external pressure transducer (Statham 23 Pdb) connected directly to the catheter on the Electronics for Medicine (DR-8 model) machine and recorded on photographic paper. The intracardiac signal was passed through a differentiator and the first derivative (dp/dt) recorded simultaneously at paper speeds of 100 to 200 mm/sec (with Dark box storage and later processing). The pressure signal was also recorded on magnetic tape for deriving first and second derivatives in 15 dogs.

Electrocardiogram

Lead 2 of the ECG was continuously monitored on the Electronics for Medicine recorder, the echo machine and the Beckmann recorder.

It was recorded simultaneously with other signals on tape.

Interventions and measurements

Simultaneous baseline recordings of the ECG, pressure, velocity and the mitral echo were made on the Electronics for Medicine recorder and the magnetic tape. They were then repeated sequentially after isoprenaline infusion ($1 \mu\text{g}/\text{min}$), after 3 boluses of propranolol ($0.05 \text{ mg}/\text{kg}$) given 5 minutes apart, after acute cross-clamping of the descending aorta, and finally after ligation of the left anterior descending coronary artery before sacrificing the dogs. In each case, sufficient time was allowed to achieve "steady state" conditions.

CALCULATIONS, SIGNAL PROCESSING AND PLAYBACK

(a) The closure slope of the anterior mitral valve leaflet

On all the 18 dogs, the AMVL closing velocity was derived manually from signals recorded on the strip chart of the echo machine, and in some cases on the photographic paper of the Electronics for Medicine machine. The measurement made is shown in Figure 3. The slope of the line joining points B and C on the final closing limb of the AMVL echo was measured. In cases where the B point was not clearly identified, the mean slope between A and C was measured provided AC was a smooth line. Otherwise B was identified from the R wave of the QRS complex of the ECG. The time and distance markers on the tracings were used to compute the slope in cm/sec . The arithmetic mean

of slopes from 5 consecutive, clearly recorded echoes, was designated the AMVL closure slope.

As suggested by Rubenstein and associates⁽⁹⁴⁾, the echo marker of closure was taken as the last rapid posterior movement in end-diastole to point C_0 , except when it was not obvious, in which case the hemodynamic marker was taken on the Electronics for Medicine tracings. The advantages of the $Q-C_0$ interval are that it does not change significantly with respiration or transducer angulation towards the valve ring⁽⁹⁴⁾. However, $Q-C_0$ was shown to be longer than the Q to left-ventricular systole-onset interval by 18 to 37 msec.

(b) Playback of native signals, and their first and second derivatives

The playback assembly is depicted in Figure 5.

Recordings stored on magnetic tape were replayed using a four-channel ultraviolet optical recorder (Brush Model 16-2300-00) at a paper speed of 2 in/sec (51 mm/sec). The native signals from the mitral echo, pressure and velocity were viewed on a scope (Hewlett-Packard Model 181A variable persistence oscilloscope) and were then differentiated electronically.

The frequency response of the recorders were well in excess of the maximal frequencies encountered in these experiments. Prior to electronic differentiation, the mitral echo signals were filtered through an electronic filter circuit (Krohn-Hite Filter model 3322, active "low-pass" filters) with zero Db gain and attenuation factor of 12 Db per octave and cut-off frequency of 40 Hz. In some cases, the aortic velocity signals recorded using the catheter-tip probe were similarly filtered with a cut-off frequency of 60Hz. Noble et al²⁷

have shown that this cut-off frequency exceeds the maximal frequencies of the upstroke of the aortic velocity signal.

Recorded signals were passed through "active" differentiators with a high cut-off frequency of between 40 to 60 Hz. These differentiators were built in the Medical Electronics Department at the University of Alberta Hospital using plug-in components on a Philbrick model MP operational manifold. First passage of the filtered mitral analog signal yielded a waveform corresponding to the first derivative of each portion of the mitral analog signal (Figure 5). The maximal deflection corresponding to the BC or AC slope of the mitral echogram was designated peak velocity of AMVL closure or ds/dt . Repassage of this first derivative through another "on-line" differentiator yielded the corresponding second derivative waveform. The peak deflection corresponding to peak velocity of AMVL closure was designated peak AMVL closure acceleration or d^2s/dt^2 (Figure 5).

The native ventricular pressure signals were similarly processed by sequential passage through on-line differentiators, but without prior filtering. The positive peak of the first derivative of isovolumic pressure rise was designated peak dp/dt , while the corresponding peak of the second derivative was designated d^2p/dt^2 . From simultaneous ECG, mitral echo and pressure playback, the point on the echo corresponding to the onset of left ventricular systole was defined as the hemodynamic marker of mitral valve closure^(93,94) in doubtful cases.

The aortic velocity signals were also processed by passage through an "on-line" differentiator without prior filtering. The peak deflection of the

velocity signal was taken as the peak aortic velocity or V . The first derivative of the upstroke portion of the velocity signal, corresponding to the ejection phase of contraction, was designated as the peak aortic acceleration of dV/dt .

The following parameters were compared:

1. Peak AMVL closing velocity and peak aortic velocity
2. Peak AMVL closing velocity and peak aortic acceleration
3. Peak AMVL closing acceleration and peak aortic velocity
4. Peak AMVL closing acceleration and peak aortic acceleration
5. Peak AMVL closing velocity and dp/dt
6. Peak AMVL closing velocity and d^2p/dt^2
7. Peak AMVL closing acceleration and dp/dt
8. Peak AMVL closing acceleration and d^2p/dt^2
9. Peak aortic velocity and peak aortic acceleration
10. Peak aortic velocity and peak dp/dt
11. Peak aortic acceleration and peak dp/dt
12. Peak dp/dt and peak d^2p/dt^2

The results were subjected to a statistical regression analysis program on a Hewlett Packard Calculator (9810A) and Plotter (9862A).

THE HUMAN STUDY

Echocardiograms were recorded on the echo machine and magnetic tape in 51 patients undergoing diagnostic cardiac catheterization as well as in 5 normal subjects. Echo recordings were made with the subjects recumbent and minimal left lateral tilt. The echo transducer was placed in the fourth or fifth left intercostal space, adjacent to the sternum using coupling gel (Aquasonic) over the skin in that area for optimal contact. The transducer was directed medially and posteriorly to capture the characteristic 'M' motion pattern of the AMVL echo and then adjusting the position so as to maximize this motion. Gain, damping and reject controls on the ultrasonoscope were adjusted for optimal resolution of echoes. The echo movement displayed in the M-mode on the echo machine was recorded on the stripchart. The analog signals were viewed on another scope, assembled on top of the echo machine scope by the Medical Electronics Department, so that only continuous analog signals were recorded on the Electronics for Medicine and the Magnetic tape recorders.

In 35 patients being catheterized, the mitral echo was recorded immediately before cardiac output measurements just prior to left ventricular angiography. The mitral echo was recorded on the Electronics for Medicine recorder in 14 patients after filtering the analog signal at 40 Hz.

In 6 patients, the left ventricular pressure signals were recorded, before angiography, using an SF₁ catheter-tip transducer introduced after informed consent was obtained. In these patients, peak dp/dt was obtained

by on-line differentiation of pressure on the Electronics for Medicine recorder, while the pressure was also recorded on magnetic tape. In 10 patients, aortic ejection velocity was measured using an electromagnetic catheter tip probe introduced with informed consent. Signals were recorded on the Electronics for Medicine recorder, as well as on magnetic tape. In the 45 patients who underwent left ventricular cineangiography the end-diastolic pressures before and after angiography were measured. Ejection fractions were obtained in 13 patients by replaying left ventricular cineangiograms and using the Sandler and Dodge equation for calculating major and minor diameters⁽¹³⁾. The volumes were digitized using a 9863A Hewlett-Packard digitizer interfaced with a calculator.

Peak AMVL closing velocity and acceleration were compared to indices of left ventricular function as cardiac output, left ventricular end-diastolic pressure, peak $(dp/dt)/P$ and peak $(d^2p/dt^2)/P$.

Peak AMVL closing velocity and acceleration were also compared with aortic ejection velocity and acceleration.

Peak aortic ejection velocity and acceleration were also compared to indices of left ventricular function.

Statistical analysis was done as in for the dog study.

RESULTS

I. Animal Study

The duration of these experiments was between three to five hours. Representative tracings of the anterior mitral valve leaflet (AMVL) from the strip chart of the ultrasonoscope and that from the photographic paper of the Electronics for Medicine (E for M) recorder is shown in Figure 3. The closure slope is also depicted in Figure 3. Although recording on the E for M recorder was possible, and this was done in the first three dogs, it required time consuming dark room photographic processing for a further 2 to 3 hours after the experiment, and recovery of data thus depended on the skill in processing. For this reason, simultaneous tape-recording of the echo signal was used in the subsequent 15 dogs. The ECG was helpful in timing closure events and differentiating the AMVL echo from that of the mitral valve ring (Figure 4).

The playback of signals from the tape, using the assembly shown in Figure 5, took between 2 to 4 hours per dog. Again the ECG facilitated the proper timing of the components of closure of the AMVL echo, although in unclear cases, simultaneous pressure playbacks were analyzed (Figure 6). Peak mitral closure velocity during the control phase was 26.96 ± 9.04 (SD) cm/sec ($n = 73$) in the 18 dogs. High values were seen in some cases, as in Dog 4 (mean $ds/dt = 53.4 \pm 6$ cm/sec) but the heart rate was also higher in that dog (148 beats/min). The high value was thus probably related to the masking effect of the faster, AB component, of closure over the slower, BC component. These components could be separated by further high speed recordings, and when this was done, a dimple or shoulder in the wave form corresponding to closure velocity became evident. The second peak was then read

as that corresponding to the BC component of AMVL closure. Similarly, the final mitral acceleration peak became notched, with two distinct negative peaks in such circumstances, and the second peak was taken to represent the acceleration corresponding to the BC component of AMVL closure.

The level of contractility in the control phase varied from dog to dog (Tables II,III). Thus, mean peak dp/dt for all 18 dogs was 1963 ± 632 (SD) mm Hg/sec. In Dog 4, only aortic dp/dt was measured and it was 932 mm Hg/sec in the control phase. In some dogs, contractility remained depressed for a prolonged length of time, and there was evidence of mechanical alternans despite a normal ECG (Figure 7). There was alternans in pressure, velocity, and the mitral echo. Alternans in velocity was also noted in anaesthetized dogs by Katz and Mills⁽⁷⁰⁾.

The heart rates during the control phase were within the physiological range in most of the 18 dogs. However, heart rate was elevated for a prolonged period of time in Dog 3 (mean 158 beats/min).

During the interventions, directional changes were produced in the peak dp/dt , peak mitral closure velocity and acceleration and peak aortic ejection velocity and acceleration. All parameters increased promptly following isoprenaline, decreased after propranolol, and decreased further after ligation of the left anterior descending coronary artery (LAD). The directional changes in all the parameters following isoprenaline or propranolol preceded changes in heart rate. When propranolol was given before isoprenaline, it was necessary to wait for up to one hour or administer more isoprenaline before measurable increases in the various parameters became apparent. The heart rate increased only marginally in these cases.

Two additional observations were made during the interventions: Firstly, the peak AMVL closing velocity did not change significantly with an acute afterload created by cross-clamping of the descending aorta. Secondly, following ligation of the coronary artery, the peak aortic velocity and acceleration decreased several seconds before the peak dp/dt on the simultaneous playbacks from the magnetic tape.

(1) Manual mitral closure slope and electronic peak mitral closing velocity (Figure 8).

The closure slopes obtained manually from the echo strip chart and from the E for M recordings were similar and nearly identical. Both recordings were made at speeds of 200 mm/sec. However, electronically derived peak closure velocities (Figure 6) of the AMVL were higher than manually derived values. The plot of paired readings from Dogs 3, 4, and 5 and those from 28 human subjects taken from Tables II, V, and VI is shown in Figure 8. The correlation coefficient was 0.93 ($N = 40, P < 0.001$).

(2) Peak aortic ejection velocity by electromagnetic cuff versus the catheter-tip probe (Figure 9).

Comparison of continuous recordings of aortic ejection velocity by these two probes were obtained in Dog 4 and revealed good correlation ($r = 0.993, N = 13, P < 0.0001$) for values within the physiological range, as shown in Figure 9.

At high velocities, after isoprenaline, the vigorous heart action caused displacement of the velocity catheter, so that while the cuff probe recorded values of 95.6 and 102.5 cm/sec, the corresponding catheter probe readings were 54.4

and 64.6 cm/sec respectively. Catheter displacement was confirmed by fluoroscopic examination and needed repositioning. For this reason, the cuff was used in 12 dogs (Dogs 7-18).

(3) Peak mitral closing velocity and peak aortic ejection velocity (Figure 10).

Because of catheter displacement, aortic velocity values in the first 6 dogs were not reliable at high values. However, aortic ejection velocity measured by the cuff in 12 dogs correlated closely with peak AMVL closing velocity. This is shown in Figure 10 and summarized below:

<u>Peak AMVL closing velocity (y)</u>		<u>Peak aortic ejection velocity (x)</u>	
Mean	28.4 cm/sec	65.6	cm/sec
SE	± 0.84	± 1.7	
$r = 0.824$		$N = 295$	
$y = 0.41 x + 1.45$		$P < 0.001$	
$SEE (y,x) = 8.21 \text{ cm/sec}$			

The deviation from the estimated line increased at higher aortic velocities.

A stronger correlation was seen in individual dogs (4 to 18) with r values ranging between 0.966 and 0.998 (Figure 11), and $P < 0.0001$.

(4) Peak mitral closing velocity and peak aortic acceleration (Figure 12).

Although a strong correlation was again present in individual dogs (4 to 18) with r values ranging between 0.957 to 0.987 ($P < 0.001$), a lesser r value was obtained for the composite line for all the points from the 3 dogs (4 to 6) using the catheter probe ($r = 0.61$, $N = 50$) or the 12 dogs (7 to 18) using the cuff probe

($r = 0.67$, $N = 288$). Thus, the data from 12 dogs with the cuff probe were:

<u>Peak mitral closing velocity (y)</u>			<u>Peak aortic acceleration (x)</u>	
Mean	27.7	cm/sec	1862.1	cm/sec ²
SE	± 0.7		± 80.1	
$r = 0.67$			$N = 288$	
$y = 0.0072 x + 14.2$			$P < 0.001$	
SEE (y,x) = 10.2 cm/sec				

The deviation from the estimated line was greater at higher aortic accelerations, and this may reflect an electronic amplification of the effect seen with high aortic velocities, especially marked in Dog 10. It is possible that such deviation at high velocities result from the relative motion of the cuff on the aortic root due to combined effects of rigorous heart action after isoprenaline and rather more than usual dissection of the aortic root so as to permit greater mobility of the cuff.

(5) Peak mitral closing acceleration and peak aortic ejection velocity

(Figures 13 and 14).

There was again strong correlation for individual dogs (4 to 18) with r values ranging between 0.959 and 0.996 ($P < 0.001$), and this is illustrated for 4 dogs using the cuff probe in Figure 13. However in the composite plot for the 12 dogs using the cuff probe (7 to 18), the correlation was slightly weaker than in individual dogs as shown in Figure 14. This is summarized below:

<u>Peak AMVL closing acceleration (y)</u>			<u>Peak aortic ejection velocity (x)</u>	
Mean	1536.7	cm/sec ²	65.6	cm/sec
SE	± 16.9		± 4.9	
$r = 0.83$			$N = 295$	
$y = 23.95 x - 34.8$			$P < 0.001$	
SEE (y,x) = 473.9 cm/sec ²				

(6) Peak mitral closing acceleration and peak aortic acceleration (Figure 15)

While good individual correlations between these parameters existed in all 15 dogs (4 to 18), with r values between 0.875 and 0.991, the correlation was again poor for Dog 10. The composite line for the 12 dogs using the cuff probe (7 to 18) was also affected in the same way as mitral closing velocity and aortic velocity.

The line is shown in Figure 15 while the results are summarized below:

	<u>Peak aortic acceleration (y)</u>	<u>Peak mitral closing acceleration (x)</u>
Mean	1863.7 cm/sec ²	1500.3 cm/sec ²
SE	± 47.2	± 73.9
$r = 0.66$	$N = 288$	$P < 0.001$
$y = 1.036 x + 309.1$		
SEE (y,x) = 942.5 cm/sec ²		

It is apparent from Figure 15 that if the upper points from Dog 10 were excluded, the r value would improve. Nevertheless, the trend of statistical correlation can be appreciated from the density of the points.

(7) Peak mitral closing velocity and the first and second derivatives of ventricular pressure rise (Figures 16-18).

Aortic pressure was monitored in Dog 4, and left ventricular pressure in the remaining 17 dogs.

There was a strong correlation between peak mitral closing velocity and peak dp/dt in all 18 dogs. In the first 3 dogs, where mitral closure slopes were measured manually, the r values were 0.81, 0.90 and 0.96 respectively. In all other dogs, peak mitral closure velocities were measured electronically. In Dog 4, peak aortic dp/dt correlated well with mitral closing velocity ($r = 0.99$). In the remaining

14 dogs (Dogs 5 to 18), the r values ranged between 0.942 to 0.997. The separate plots from 4 dogs are shown in Figure 16. The composite plot on all 17 dogs and excluding Dog 4 is shown in Figure 17, and the data summarized below:

<u>Peak mitral closure velocity (y)</u>			<u>Peak dp/dt (x)</u>
Mean	27.73	cm/sec	2057.1 mm Hg/sec
SE	± 0.57		± 71.2
$r = 0.734$			$P < 0.001$
$y = 0.0092 x + 8.72$			
SEE (y,x) = 9.44 cm/sec			
N = 380			

Similarly peak mitral closing velocity correlated with peak d^2p/dt^2 , with r values ranging from 0.923 to 0.989 in the 12 individual dogs (4 to 15). Although the composite plot, shown in Figure 18, gave a line with an r value of 0.621, it is apparent from the density of points that statistical dispersion occurs as contractility is increased, and that the dispersion is greater than in the mitral closing velocity versus dp/dt plot. The results are summarized below:

<u>Peak mitral closure velocity (y)</u>			<u>Peak d^2p/dt^2 (x)</u>
Mean	28.03	cm/sec	62790 mm Hg/sec ²
SE	± 0.25		± 2475
$r = 0.621$			$P < 0.001$
$y = 0.0002 x + 15.24$			
SEE (y,x) = 11.24 cm/sec			
N = 311			

(8) Peak mitral closing acceleration and the first and second derivatives of ventricular pressure rise (Figures 19,20).

In separate dogs, the peak mitral closing acceleration correlated closely to peak dp/dt (r from 0.910 to 0.997, $N = 15$ dogs) and peak d^2p/dt^2 ($r = 0.853$ to 0.984, $N = 12$ dogs). The composite plot, shown in Figure 19, also revealed good

correlation between mitral closing acceleration and peak dp/dt . There results are summarized below:

<u>Peak mitral closing acceleration (y)</u>		<u>Peak dp/dt (x)</u>	
Mean	1518.4 cm/sec ²	2096.5 mmHg/sec	
SE	± 62.7	± 46.1	
r	= 0.752	N = 330	P < 0.001
y	= 0.554 x + 357.3		
SEE (y,x)	= 553.3 cm/sec ²		

However, peak mitral closing acceleration did not correlate any closer to peak d^2p/dt^2 (Dog 4 and Dogs 7-18, $r = 0.626$, $N = 309$) than with peak dp/dt as shown in Figure 20.

(9) Peak aortic ejection velocity and peak dp/dt (Figure 21) .

The correlation coefficient ranged between 0.944 and 0.998 in the individual 12 dogs (Dog 7-18) and was reduced to 0.79 in the composite plot (Figure 21).

Data from the composite plot are summarized below:

<u>Peak aortic ejection velocity (y)</u>		<u>Peak dp/dt (x)</u>	
Mean	64.92 cm/sec	2025.0 mmHg/sec	
SE	± 1.67	± 62.2	
r	= 0.79	N = 302	P < 0.001
y	= 0.0212 x + 22.5		
SEE (y,x)	= 17.9 cm/sec		

(10) Peak aortic acceleration and peak dp/dt (Figure 22) .

The correlation coefficients for the individual 12 dogs (Dog 7-18) ranged from 0.94 to 0.99, except for Dog 10 whose r value as 0.849 . The composite plot, shown in Figure 22, gave an r value of 0.707. The data are summarized below:

<u>Peak aortic acceleration (y)</u>		<u>Peak dp/dt (x)</u>	
Mean	1840.0 cm/sec ²	2009.4 mmHg/sec	
SE	± 63.4	± 72.2	
r	= 0.707	N = 295	P < 0.001
y	= 0.81 x + 220.2		
SEE (y,x)	= 880.2 cm/sec ²		

(11) Peak aortic velocity and peak aortic acceleration (Figure 23) .

Individual correlation coefficients ranged between 0.957 and 0.996 in the 12 dogs with the cuff probe, except Dog 10 , where the r value was 0.867. The correlation coefficients for the dogs 4 to 6 , where the velocity catheter probe was used, were 0.988, 0.971 and 0.984 respectively. The composite plot for the 12 dogs with the cuff probes is shown in Figure 23 and the data are summarized below:

<u>Peak aortic acceleration (y)</u>		<u>Peak aortic ejection velocity (x)</u>	
Mean	1852.8 cm/sec ²	64.69 cm/sec	
SE	± 72.4	± 1.7	
r	= 0.829	N = 299	P < 0.001
y	= 35.7 x - 455.5		
SEE (y,x)	= 701.0 cm/sec ²		

For the 3 dogs using the catheter probe, the composite r value was 0.988 (N=50) and the line was given by $y = 18.4x - 200.5$, where y = aortic acceleration and x = aortic velocity, and SEE (y,x) was 72.9 cm/sec².

(12) Peak dp/dt and peak d²p/dt² in 12 dogs (Figure 24).

The individual correlation coefficients ranged between 0.954 and 0.989. The composite plot is shown in Figure 24, and the data are summarized below:

<u>Peak d^2p/dt^2 (y)</u>		<u>Peak dp/dt (x)</u>	
Mean	61,471 mmHg/sec ²	2019.6	mmHg/sec
SE	± 637	± 250.8	
r	= 0.947	N = 304	P<0.0001
y	= 37.3 x - 13859		
SEE (y,x)	= 14085 mmHg/sec ²		

(13) Peak mitral closing velocity and peak mitral closing acceleration in 15

dogs (Figure 25) .

The correlation coefficient for each individual dog (dogs 4-18) was excellent ($r = 0.99$) . The composite plot is shown in Figure 25 and the data summarized below:

<u>Peak mitral closing velocity (y)</u>		<u>Peak mitral closing acceleration (x)</u>	
Mean	29.4 cm/sec	1600.5	cm/sec ²
SE	± 0.83	± 48.5	
r	= 0.986	N = 348	P<0.0001
y	= 0.017 x + 2.28		
SEE (y,x)	= 2.62 cm/sec		

The correlation coefficients for the animal study are summarized in Table IV.

II. Human Study

The mitral echogram was easily recorded in human subjects over an average of 10 minutes. However, initial recordings on the E for M recorder were made on 14 patients only, because they proved to be more difficult, on account of "drop-off" of the analog mitral echo signals, and required an additional observer. Subsequent recordings were therefore made directly on the magnetic tape, while simultaneous strip chart records were obtained on the ultrasonoscope.

(1) Peak mitral closing and angiographic left ventricular ejection fraction (Figure 26).

The resting left ventricular ejection fractions from 13 patients (Table 4) did not correlate with peak mitral closing velocity ($r = 0.17$). The ejection fractions also correlated poorly with peak mitral closing acceleration ($r = 0.18$), as shown in Figure 26. However, the ejection fractions seemed to correlate better with resting end-diastolic pressures ($r = 0.64$). The apparent correlation with contractility cannot be considered significant in view of the few patients ($r = 0.5$, $N = 5$). The ejection fractions correlated poorly with aortic velocity ($r = 0.16$, $N = 8$) or aortic acceleration ($r = 0.68$, $N = 3$).

(2) Peak mitral closing velocity and acceleration and cardiac output (Figure 27).

Weak correlations were found between peak mitral closing velocity ($r = 0.387$, $N = 21$) or acceleration ($r = 0.295$, $N = 19$) and cardiac outputs obtained by Fick's method (Tables V and VI) in the heterogeneous group of 21 patients.

(3) Peak mitral closing velocity and acceleration and left ventricular end-diastolic pressure in man (Figures 28 and 29).

The peak mitral closing velocity in 6 normal subjects ranged from 23.6 to 28 cm/sec the mean value being 25.5 ± 1.62 (SD) cm/sec. Peak closing acceleration in one of

these patients was 1553 cm/sec^2 . These are illustrated in Figure 28.

In 36 patients with coronary artery disease, peak mitral closing velocity ranged from 11.0 to 47.7 cm/sec, while the acceleration in 18 of the patients ranged from 355 to 2250 cm/sec^2 . Neither resting left ventricular end-diastolic pressure (LVEDP), nor the post-left ventricular angiographic LVEDP adequately separated those with low peak mitral closing velocity and acceleration from those with values seen in the normal patients. Thus, mean peak mitral closing velocity was 26.0 ± 8.3 (SD) cm/sec (range 11.0 to 47.7 cm/sec) in those 24 patients with resting LVEDP < 14 mmHg, and 16.9 ± 4.3 (SD) cm/sec (range 12.0 to 24.0 cm/sec) in those 12 patients with resting LVEDP > 14 mmHg. The mean peak mitral closing velocity was 28.5 ± 4.6 (SD) cm/sec (range 22.4 to 38.5 cm/sec) in those 14 patients with post-angiographic LVEDP < 18 mmHg, and 18.9 ± 8.2 (SD) cm/sec (range 11.0 to 27.8 cm/sec) in those 22 patients with post-angiographic LVEDP > 18 mmHg.

In 7 patients with various cardiomyopathies (asymmetric septal hypertrophy in 4 patients, Syndrome X in 3 patients), the peak mitral closing velocity ranged from 21.0 to 55.5 cm/sec, the mean being 35.9 ± 13.8 (SD) cm/sec. Similar values were encountered in one patient with a ventricular septal defect (32.7 cm/sec) and 2 patients with aortic insufficiency (40.0 cm/sec and 33.4 cm/sec respectively). Very high values were encountered in 2 patients with mitral stenosis. In the first patient, the velocity was calculated from the mean manually derived slope (AC) of the echo recorded at 200 mm/sec paper speed, and was 77.9 cm/sec. In the other patient, the peak mitral closing velocity was calculated from the electronically differentiated signal; the peak corresponding to the rapid AB portion of the AMVL echo was 65.4 cm/sec, similar to the value from the strip chart manual slope.

Similar high values were obtained by Yoshitoshi et al for the AC slope⁽¹²⁹⁾.

However, when the electronic derivative was obtained by playbacks at a speed near 200 mm/sec, 2 distinct peaks became evident; the AB peak (65.4 cm/sec) as before and the smaller BC peak of 18.5 cm/sec. The corresponding accelerations were 2618 cm/sec² and 1332 cm/sec² respectively.

The relation between peak mitral valve closing velocity and acceleration and left ventricular end-diastolic pressure is shown in Figure 29.

The correlation coefficient for peak mitral closing velocity and LVEDP was 0.61 (N = 36). The correlation coefficient improved from $r = 0.31$ (N = 24) for all patients to $r = 0.44$ (N = 18) when considering only patients with coronary artery disease.

Subdivision of patients on the basis of resting LVEDP, or resting ejection fraction, or cardiac output is however not an accurate way of separating normal from diseased ventricle^(24, 61) and this fact probably explains the poor correlations.

(4) Peak mitral closing velocity and acceleration and peak dp/dt (Figure 30)

The peak dp/dt was measured using the catheter tip transducer in 6 patients. The correlation between mitral closing velocity and peak dp/dt ($r = 0.93$, $p < 0.01$) is shown in Figure 30 and the data are summarized below:

	<u>Peak mitral closing velocity (y)</u>	<u>Peak dp/dt (x)</u>
Mean	20.07 cm/sec	1371.7 mmHg/sec
SE	± 1.67	± 220.0
	$r = 0.93$	$N = 6$
	$y = 0.07 x + 10.4$	$P < 0.01$
	SEE (y,x) = 1.7 cm/sec	

This correlation is better than in dogs ($r = 0.734$ in 17 dogs) probably because of the effect of biological variation with the greater number of dogs, and possibly some translational echo transducer movement in the dogs.

The relation of mitral closure acceleration to peak dp/dt gave a lower r value of 0.79, and it can be seen from Figure 30 that the scatter of the points in the plot on the right is greater than for peak mitral closing velocity in the plot on the left. Again, this probably reflects the effect of the magnification and the electronic amplification during differentiation of the native signal. Nevertheless, the r value for peak mitral closing acceleration and peak dp/dt is better than for the 17 dogs ($r = 0.752$). The human data are summarized below:

	<u>Peak mitral closing acceleration (y)</u>	<u>Peak dp/dt (x)</u>
Mean	840.2 cm/sec	1372.0 mmHg/sec
SE	± 0.8	± 22
	$r = 0.79$	$N = 6$
	$y = 0.287 x + 446$	$P < 0.05$
SEE (y, x) =	134 cm/sec^2	

(5) Peak mitral closing velocity and acceleration, and aortic ejection velocity
(Figure 31).

In 10 patients, a good correlation ($r = 0.81$) was present between peak mitral closure velocity and aortic ejection velocity (Figure 31), similar to that in the 12 cuff-probe dogs ($r = 0.82$). The data are summarized below:

	<u>Peak mitral closing velocity (y)</u>	<u>Peak aortic ejection velocity (x)</u>
Mean	23.6 cm/sec	36.7 cm/sec
SE	± 2.76	± 4.38

$$\begin{aligned}
 r &= 0.81, & N &= 10 & P < 0.005 \\
 y &= 0.51x + 4.9 \\
 \text{SEE}(y, x) &= 5.42 \text{ cm/sec}
 \end{aligned}$$

Similarly, in 8 patients, peak mitral closing acceleration correlated closely ($r = 0.91$) to peak aortic ejection velocity as shown in Figure 31. This is similar to the 12 cuff-probe dogs ($r = 0.83$). The data are summarized below:

	<u>Peak mitral closing acceleration (y)</u>	<u>Peak aortic ejection velocity (x)</u>
Mean	1017.4 cm/sec ²	33.5 cm/sec
SE	<u>+176</u>	<u>+ 4.85</u>
$ \begin{aligned} r &= 0.91 & N &= 8 & P < 0.005 \\ y &= 33.0x - 88.75 \\ \text{SEE}(y, x) &= 222 \text{ cm/sec}^2 \end{aligned} $		

There were only four patients in whom aortic acceleration was measured. The correlation coefficients with mitral closing velocity and acceleration were 0.24 and 0.44 respectively, but the number of patients is too small for meaningful analysis.

DISCUSSION

The task of the physician in making a complete cardiac diagnosis is not only to assess the degree of functional impairment produced by various diseases but to develop a rational plan of treatment and to evaluate the effectiveness of his treatment. Physiologic techniques are essential for the precise and objective assessment of cardiac function in order to support and provide quantifiable equivalents of clinical examination.

It is generally accepted that the clinical value of echocardiography lies in its non-invasive methodology, providing an opportunity to repeat measurements in a serial fashion⁽¹⁾. However, the use of diagnostic ultrasound for quantitative analysis of ventricular function requires experienced and meticulous technique to obtain the high quality echocardiograms needed for such analysis^(12, 21, 88). Furthermore, the value in coronary artery disease, which plagues the adult population of the western world is limited by geometric assumptions made in deriving estimates of function from the quantitative data.

Thus, all the conventional echo methods for calculating left ventricular volumes, stroke volume, ejection fraction and cardiac output⁽²⁻¹²⁾ are limited by assumptions of ellipsoid shape of the heart, constant relationships between the axes, and uniformity of contraction. Improved quantitative methods^(11, 17, 136-138) have been proposed but they also suffer from the same drawbacks, albeit to a lesser degree. In addition, loading conditions affect all these derived indices to lesser or greater degree. A new approach suggested by Lalani and Lee^(22, 23) assumes a direct relation between the final closure slope of the mitral valve echogram and the aortic ejection velocity and acceleration. This assumption was based on suggestions of cardiac mechanics by Rushmer⁽⁶³⁾ and investigations using the Doppler method by Yoshitoshi et al⁽¹²⁹⁾. While it is generally agreed that left ventricular function is probably better characterized by contractility⁽⁴⁴⁻⁵¹⁾, aortic velocity has also been shown to be a sensitive index of pump function⁽²⁴⁾. Furthermore Noble⁽²⁷⁾ proposed aortic acceleration as a more

sensitive index of contractile function than dp/dt . However, like dp/dt ⁽²⁵⁾, aortic acceleration appears to be influenced by preload and afterload⁽³¹⁾.

In the animal studies described in this thesis, close correlation was found between peak AMVL closing velocity and (1) peak aortic velocity and acceleration, and (2) peak dp/dt . A similar close correlation was demonstrated between the peak AMVL acceleration and these parameters, but the correlation was no better than with peak AMVL velocity. This may reflect a limitation of the methodology employed. A significant correlation was also demonstrated between dp/dt and (1) peak aortic velocity and (2) peak aortic acceleration. Again aortic acceleration did not seem to correlate better than aortic velocity to the peak dp/dt . Moreover, following coronary artery ligation, or propranolol, reductions in both peak aortic ejection velocity and peak aortic acceleration preceded that of the dp/dt by several seconds, in support of Noble's findings⁽²⁷⁾.

In the human studies, similar strong correlations were found between peak mitral closing velocity and acceleration and (1) peak dp/dt , and (2) peak aortic velocity. Weaker correlations were found between these parameters and, in decreasing order, resting LVEDP, cardiac output and ejection fraction. Similarly peak aortic velocity correlated poorly with resting LVEDP, or ejection fraction. These findings are similar to those of Kolettis and his associates⁽³³⁾ who measured peak aortic velocity and acceleration by means of a catheter probe in 40 patients. Correlation coefficients in their study, between peak aortic velocity and acceleration to ejection fraction were 0.272 and 0.279 respectively. The r values for the relation of the same parameters to peak dp/dt were 0.318 and 0.289 respectively. They concluded that peak aortic velocity and acceleration failed to discriminate between good, moderate and poor left ventricular function and suggested various ways to normalize the values in order to increase the discriminant value.

The peak mitral closing velocity and acceleration in our hands provided some separation of patients with various diseased states, although more patients need to be studied. One might argue that the mitral valve closing velocity is more likely to be affected by preload and contractility rather than afterload, since mitral closure is completed prior to aortic ejection. It follows from that, since the final or BC portion of mitral closure is influenced by forces generated in the early isovolumic period, the initial impulse causing the final closure may be different from that contributing to aortic acceleration. Noble and associates^(27, 67) have suggested that inertiance dominates the opposition to left ventricular ejection at the time of maximum acceleration. Thus, although mitral closing velocity or acceleration correlates well with aortic ejection velocity, it does not follow that it either should correlate better with aortic acceleration. In our animal experiments, acute changes in afterload did produce significant changes in mitral closing velocity or acceleration.

Thus, the peak mitral closing velocity and acceleration can be used in patients without mitral and aortic valvular heart disease as an index of peak aortic ejection velocity and peak aortic acceleration, and left ventricular contractile function. Although the results also suggest that these indices may reflect contractile properties of the left ventricle in the presence of aortic and mitral valve disease, the numbers of these patients were too few, and more patients with these conditions need to be studied. Also, it is not suggested that these indices are superior than peak dp/dt in providing an estimate of contractile function of the heart.

This method of assessing left ventricular function does not depend on the assumptions made in conventional methods and the results seem to be unaffected

by contraction abnormalities. Although it is a technically easier methods, there are several limitations in its present form:

- (1) Further studies need to be done with controlled preload, afterload and heart rate.
- (2) Further studies are needed in patients with mitral and aortic valve disease.
- (3) Further studies need to be done in the presence of arrhythmias.
- (4) The electronic system needs to be further developed for on-line digitization and digital display of the results.

CONCLUSIONS

- (1) The manually drawn final AMVL closure slope corresponding to the BC portion of the echogram is related to peak aortic ejection velocity, peak aortic acceleration, and the first and second derivatives of left ventricular pressure rise in dogs and man.
- (2) The electronically derived peak AMVL closing velocity and acceleration in dogs significantly correlate with peak aortic ejection velocity, peak aortic acceleration, and dp/dt and reflect the directional changes in contractility produced by interventions.
- (3) The electronically derived peak AMVL closing velocity and acceleration was easily obtained in man, and correlated significantly with peak aortic velocity and peak dp/dt , suggesting that they can provide reliable and non-invasive estimates of left ventricular contractile function in man.
- (4) The electronically derived peak AMVL closing velocity and acceleration may be useful in estimating left ventricular contractile function in various disease states in man.

TABLE I

SUMMARY OF VALUES OF LATE CLOSURE OF THE ANTERIOR MITRAL VALVE LEAFLET FROM THE LITERATURE

Year	Group	Reference	Method	Subject	AMVL Closing Velocity (cm/sec)		
					Definition	Range	Mean \pm SD
1965	Yoshitoshi et al	129	Doppler	Man	? AC	20-40	27
1972	Buynkozturk et al	131	Echo: Manual	Man	AC or BC	8-50.5	22.1 \pm 9.13
1974	Gordon et al	118	Cineangio Opaque markers	Dog	? BC	-	33 \pm 13
1974	Emerson et al	132	Echo: Computer Tracking	Man	? BC	23-46.7	34.6 \pm 7.8
1974	Upton et al	110	Echo: Manual Digitization	Man	? AC	-	29.0 \pm 8
1976	Kingsley et al	130	Echo: ? Manual	Man	BC	20-30	-
1976	Lalani and Lee	22,23	Echo: Electronic	Dogs Man	AC (? BC)	25.7-60.0 13.7-49.9	41 \pm 12 27.4 \pm 8.1
1977	Jugdutt and Lee	Present Thesis	Echo: Electronic	Dogs Man	BC	15.6-57.3 23.6-28.0	26.96 \pm 9.04 25.5 \pm 1.6

TABLE II

HEMODYNAMIC AND ECHO DATA ON 18 DOGS

(a) Dogs 1-3

	Heart Rate Beats/Min	Peak SP/EDP mmHg	Peak dp/dt mmHg/sec	PI mmHg	Ratio Peak $\frac{dp_1}{dt}/PI$ sec	Peak $\frac{ds}{dt}$ cm/sec	VCE ₅₀ ML/sec	V _{max} ML/sec
<u>Dog 1 (23.4 kg)</u>								
<u>Control</u>								
1	141	136/3	2540	90.2	28.2	27.0		
<u>Isoprenaline</u>								
1	154	130/4	3208	78.7	40.7	35.4		
2	154	130/4	3056	78.7	38.9	34.1		
3	154	146/0	2739	69.3	39.6	33.7		
4	154	146/0	2620	80.3	32.6	33.6		
5	154	146/0	2481	78.7	31.5	27.2		

(Continued Over)

TABLE II (a) (Contd.)

	Heart Rate Beats/Min	Peak SP/EDP mmHg	Peak dp/dt mmHg/sec	PI mmHg	Ratio Peak dp/dt/PI sec ⁻¹	Peak ds/dt cm/sec	VCE ₅₀ ML/sec	V _{max} ML/sec
<u>Propranolol</u>								
1	154	136/3	2357	75.2	31.4	20.5		
2	151	148/8	2270	85.9	26.4	26.5		
3	151	148/8	2381	87.9	27.1	28.7		
4	144	145/5	2024	78.7	25.7	25.4		
5	148	145/0	1969	76.2	25.8	24.9		
<u>Dog 2 (33.8 kg)</u>								
<u>Control</u>								
1	131	140/0	1808	78.4	23.1	18.6	1.28	1.86
2	129	145/4	2246	79.2	28.4	22.5	1.34	1.63
3	127	123/4	1431	72.6	19.7	15.6	0.96	1.26
4	129	114/4	1961	70.2	27.9	19.5	1.36	1.75

(Continued Over)

TABLE II (a) (Contd.)

	Heart Rate Beats/Min	Peak SP/EDP mmHg	Peak dp/dt mmHg/sec	PI mmHg	Ratio Peak $\frac{dp}{dt}/PI$ sec	Peak ds/dt cm/sec	VCE ₅₀ ML/sec	V _{max} ML/sec
<u>Isoprenaline</u>								
1	115	121/5	1567	76.7	20.4	27.3	0.87	0.90
2	114	153/4	2130	80.8	26.4	-	1.08	1.19
3	114	131/3	1824	73.6	24.8	30.5	1.16	1.51
4	133	120/3	2001	53.4	37.6	35.5	1.66	2.40
5	109	115/4	1744	72	24.2	30.0	1.31	2.25
6	122	113/3	1879	75	23.0	29.8	1.40	2.13
7	113	126/4	1937	71	27.5	30.5	1.32	2.31
8	115	224/13	3134	133.5	17.5	38.1	1.48	1.77
9	103	123/3	1406	78.5	17.9	25.0	0.95	1.36
10	113	176/3	2230	96	23.0	25.0	1.24	1.54
11	122	230/3	4079	202	20.2	53.0	1.15	1.26
12	127	230/3	3777	190	19.9	48.3	0.81	0.81

(Continued Over)

TABLE II (a) (Contd.)

	Heart Rate Beats/Min	Peak SP/EDP mmHg	Peak dp/dt mmHg/sec	PI mmHg	Ratio Peak dp/dt/PI sec ⁻¹	Peak ds/dt cm/sec	VCE ₅₀ ML/sec	V _{max} ML/sec
<u>Propranolol</u>								
1	71	94/5	1109	48.6	22.8	18.4	0.95	0.96
2	76	84/5	804	46.5	17.3	16.8	0.53	1.51
3	73	92/5	1065	54.0	19.7	9.7	0.83	0.82
4	67	115/8	1206	60.0	20.1	9.1	-	-
5	75	67/6	563	24.0	23.3	9.1	0.67	1.23
6	72	101/8	1165	57.6	20.2	11.0	0.74	0.76
<u>LAD Ligation</u>								
1	72	80/4	820	62	13.3	5.9	0.57	0.88
<u>Dog 3 (19.4 kg)</u>								
<u>Control</u>								
1	157	96/2	1502	57	26.2	22.4	1.22	2.34

TABLE II (a) (Contd.)

	Heart Rate Beats/Min	Peak SP/EDP mmHg	Peak dp/dt mmHg/sec	PI mmHg	Ratio Peak dp/dt/PI sec ⁻¹	Peak ds/dt cm/sec	VCE ₅₀ ML/sec	V _{max} ML/sec
2	157	96/2	1540	59	26.0	23.8	1.03	2.23
3	162	90/2	1631	60	26.9	25.9	1.32	2.34
4	156	101/2	1407	62	22.7	22.4	1.12	1.94
5	158	94/2	1789	59	30.4	28.2	1.47	2.57
<u>Isoprenaline</u>								
1	157	101/4	2256	58	39.8	43.1		
2	154	96/4	2031	57	35.5	40.5		
3	157	104/4	2001	58	34.7	39.6		
4	158	103/4	2041	56	36.5	40.5		
5	150	111/3	1885	52	27.5	37.4		
6	156	111/3	2412	68	33.6	44.4		
7	150	101/6	1583	62	25.5	32.1		

(Continued Over)

TABLE II (a) (Contd.)

	Heart Rate Beats/Min	Peak SP/EDP mmHg	Peak dp/dt mmHg/sec	PI mmHg	Ratio Peak dp/dt/PI sec ⁻¹	Peak ds/dt cm/sec	VCE ₅₀ ML/sec	V _{max} ML/sec
<u>Propranolol</u>								
1	129	84/13	809	39	20.9	12.3		
2	123	96/13	711	38	18.6	12.8		
3	114	96/14	887	48	18.4	18.5		
4	112	96/14	819	51	16.2	17.2		
5	112	85/6	739	42	17.5	13.2		
<u>LAD Ligation</u>								
1	103	68/10	397	22	17.9	10.7		

(Continued Over)

TABLE II

(b) Dogs 4-6

	Heart Rate Beats/Min	Peak SP mmHg	Peak dp/dt mmHg/sec	Peak d^2p/dt^2 mmHg/sec ² $\times 10^3$	Peak V^* cm/sec ²	Peak dV/dt cm/sec	Peak ds/dt cm/sec	Peak d^2s/dt^2 cm/sec ²
<u>Dog 4 ** (27 kg)</u>								
<u>Control</u>								
1	150	117	938	35.8	60.0	908	49.4	2920
2	145	117	1006	41.7	66.3	1031	57.3	3245
<u>Propranolol</u>								
1	143	153	693	29.8	45.0	663	39.0	2271
2	143	143	658	23.2	43.0	644	37.8	2076
3	143	143	508	22.3	30.0	426	26.0	1622
4	143	143	538	23.2	38.0	530	31.3	1622
5	143	143	748	35.8	47.0	691	40.3	2466
6	143	143	875	34.3	53.0	781	45.5	2596

TABLE II (b) (Contd.)

	Heart Rate Beats/Min	Peak SP mmHg	Peak dp/dt mmHg/sec	Peak d^2p/dt^2 mmHg/sec ² x 10 ³	Peak V* cm/sec	Peak dV/dt cm/sec ²	Peak ds/dt cm/sec	Peak d^2s/dt^2 cm/sec ²
7	143	143	945	37.2	55.0	880	46.8	2725
8	143	143	963	38.7	61.4	804	52.0	3115
9	143	153	1016	43.2	66.3	1038	58.5	3310
10	143	143	1063	44.4	72.0	1159	62.4	3245
<u>Isoprenaline</u>								
1	143	141	1188	49.2	76.1	1230	65.0	3440
2	143	141	1284	50.1	81.9	1313	68.9	3635
3	143	141	1313	50.6	87.2	1383	71.5	3764
4	160	148	1438	56.6	92.5	1500	78.0	4413
5	160	148	1494	59.6	101.5	1750	84.5	4549
6	136	131	1218	46.2	81.5	1281	67.6	3569
7	133	127	1001	41.7	66.3	870	55.9	3115

(Continued Over)

TABLE II (b) (Contd.)

	Heart Rate Beats/Min	Peak SP mmHg	Peak dp/dt mmHg/sec	Peak d^2p/dt^2 mmHg/sec ² x 10 ³	Peak V* cm/sec	Peak dV/dt cm/sec ²	Peak ds/dt cm/sec	Peak d^2s/dt^2 cm/sec ²
<u>Dog 5 (16 kg)</u>								
<u>Control</u>								
1	122	128	1733		68.5	1064	21.3	1136
2	122	128	1650		66.0	1030	20.0	1039
3	122	128	1575		61.1	983	18.8	973
<u>Isoprenaline</u>								
1	133	138	2265		92.5	1480	28.8	1482
2	133	144	2625		98.5	1498	33.1	1888
3	133	141	2756		108.0	1696	33.8	1947
4	133	152	3265		130.0	1973	41.3	2262
<u>Propranolol</u>								
1	92	128	1773		58	800	17.5	941
2	92	120	1444		51	738	16.3	913

(Continued Over)

TABLE II (b) (Contd.)

	Heart Rate Beats/Min	Peak SP/EDP mmHg	Peak dp/dt mmHg/sec	Peak d^2p/dt^2 mmHg/sec ² x 10 ³	Peak V* cm/sec	Peak dV/dt cm/sec ²	Peak ds/dt cm/sec	Peak d^2s/dt^2 cm/sec ²
3	92	110	1138				15	714
4	88	105	1050		40.7	638	13.8	649
5	88	84	953		37	600	11.3	624
6	85	84	663		22	338	8.8	324
7	85	126	1969		80	1269	25	1250
8	88	128	2035		82	1269	26.3	1321
<u>Dog 6 (17.8 kg)</u>								
Control								
1	104	234/25	2979	86.7	31.0	342	24.5	1351
2	104	224/19	3104	88.8	31.4	351	26	1427
3	104	228/19	2896	82.6	29.9	310	23	1299

(Continued Over)

TABLE II (b) (Contd.)

	Heart Rate Beats/Min	Peak SP/EDP mmHg	Peak dp/dt mmHg/sec	Peak d^2p/dt^2 mmHg/sec ² $\times 10^3$	Peak V^* cm/sec	Peak dV/dt cm/sec ²	Peak ds/dt cm/sec	Peak d^2s/dt^2 cm/sec ²
<u>Propranolol</u>								
1	100	225/17	2400		27.4	251	20.8	934
2	90	185/20	2156	62.0	26.3	228	18.6	827
3	80	159/17	1655	43.4	21.3	160	15.6	778
4	77	156/17	1490	43.4	18.3	137	12.4	519
5	73	93/17	1035	30.9	11.5	91	9.0	324
6	63	85/20	828	23.8			7.9	296
<u>Isoprenaline</u>								
1	101	225/17	2896	78.5	32.9	356	26.0	1558
2	101	225/16	3041	82.6	31.4	351	24.5	1427
3	102	235/17	3351	103.3	36.5	422	28.1	1532

(Continued Over)

TABLE II (b) (Contd.)

	Heart Rate Beats/Min	Peak SP/EDP mmHg	Peak dp/dt mmHg/sec	Peak d^2p/dt^2 mmHg/sec ² x 10 ³	Peak V* cm/sec	Peak dV/dt cm/sec ²	Peak ds/dt cm/sec	Peak d^2s/dt^2 cm/sec ²
4	104	245/14	3724	115.7	40.2	493	32.3	1817
5	109	248/17	4974	123.9	50.4	639	37.5	2441
6	114	265/13	4873		49.8	650	41.6	2652
7	125	270/10	5250		52.9	708	43.7	2727
8	130	270/10	5500		54.8	799	48.7	3117
9	140	272/10	6250		59.5	855	51.9	3276

(Continued Over)

TABLE II

(c) Dogs 7 - 18

	Heart Rate beats/min	Peak SP mm Hg	Peak dp/dt mmHg/sec	Peak d^2p/dt^2 mmHg/sec ² $\times 10^3$	Peak V^{***} cm/sec	Peak dV/dt cm ³ /sec ²	Peak ds/dt cm/sec	Peak d^2s/dt^2 cm/sec ²
<u>Control</u>								
		<u>D o g 7 (20 kg)</u>						
1	120	145	3033	98.3	50.7	995	16.9	936
2	120	145	3118	106.9	51.4	1068	17.3	959
3	120	145	3160	113.3	52.5	1166	17.5	983
<u>Isoprenaline</u>								
1	140	148	3314	115.4	54.3	1175	18.1	1014
2	140	153	3454	128.2	55.4	1194	18.5	1092
3	140	156	3581	138.9	56.1	1195	19.0	1131
4	145	145	3708	145.3	58.6	1286	20.6	1232
5	150	138	4213	149.1	68.8	1538	23.8	1404
6	150	133	4424	158.2	73.2	1630	26.9	1482
7	150	140	4845	193.8	79.6	1810	27.5	1560

(Continued over)

TABLE II (c) (Contd.)

	Heart Rate beats/min	Peak SP mmHg	Peak dp/dt mmHg/sec	Peak d^2p/dt^2 mmHg/sec ² $\times 10^3$	Peak V^{***} cm/sec	Peak dV/dt cm/sec ²	Peak ds/dt cm/sec	Peak d^2s/dt^2 cm/sec ²
8	155	146	5476	206.4	86.9	1935	30.0	1638
9	155	139	5898	277.9	95.6	2198	33.8	1872
10	155	138	6319	294.8	102.5	2565	35.6	2028
<u>Propranolol</u>								
1	120	149	3496	145.3	55.7	1178	18.8	1092
2	120	147	2949	97.3	48.9	1063	16.3	936
3	115	144	2696	96.2	47.1	1029	15.6	905
4	115	141	1769	52.7	29.0	680	9.4	593
5	100	150	1601	42.1	25.3	543	8.8	546
6	100	125	1264	33.7	21.7	471	8.1	468
7	100	140	2190	85.5	32.9	815	12.8	655

(Continued over)

TABLE II (c) (Contd.)

	Heart Rate beats/min	Peak SP mmHg	Peak dp/dt mmHg/sec	Peak d^2p/dt^2 mmHg/sec ² x10 ³	Peak V*** cm/sec	Peak dV/dt cm/sec ²	Peak ds/dt cm/sec	Peak d^2s/dt^2 cm/sec ²
<u>Control</u>								
<u>D o g 8 (18 kg)</u>								
1	125	145	2813	73.7	64.3	1921	32.8	1775
2	125	145	3094	79.6	68.3	2055	34.6	1920
3	125	145	2700	70.2	61.6	1759	28.9	1680
<u>Isoprenaline</u>								
4	140	140	3938	158.7	90.0	3724	46.1	2640
5	145	140	4388	185.3	103.5	4204	50.1	2880
6	145	140	5175	188.1	113.0	4729	59.7	3360
7	165	138	5456	196.6	119.0	5193	65.5	3600
8	160	140	3150	119.3	73.7	2513	35.6	2161
9	155	145	3000	76.4	66.1	2105	33.6	1872
10	150	145	4613	182.5	104.5	4171	52.0	2976
11	150	140	3544	105.3	81.7	2948	42.3	2448

(Continued over)

Table II (c) (Contd.)

	Heart Rate beats/min	Peak SP mmHg	Peak dp/dt mmHg/sec	Peak d^2p/dt^2 mmHg/sec ² x10 ³	Peak V*** cm/sec	Peak dV/dt cm/sec ²	Peak ds/dt cm/sec	Peak d^2s/dt^2 cm/sec ²
12	145	142	4275	165.7	96.7	3769	48.1	2736
13	145	142	3825	154.4	87.1	3518	43.4	2593
<u>Propranolol</u>								
1	145	135	3206	126.4	75.7	2596	36.6	2304
2	125	130	2531	98.3	55.6	1123	28.9	1680
3	92	130	2250	63.2	51.6	1005	26.9	1440
4	92	128	1800	39.3	41.5	804	21.2	1151
5	86	125	1575	35.1	36.9	754	19.3	959
6	86	120	1350	30.9	33.5	636	17.4	864
7	80	115	1069	21.1	28.1	586	13.5	768
8	75	110	900	18.3	23.5	403	9.8	624
<u>Cross-Clamping Descending Aorta</u>								
Before	75	110	731	14.0	20.1	339	8.6	480
During	75	120	535	9.9	13.4	251	7.6	432
During	75	120	394	8.4	8.0	166	6.8	384
After	80	122	1575	32.3	34.8	686	20.3	1056

(Continued over)

TABLE II (c) (Contd.)

	Heart Rate beats/min	Peak SP mmHg	Peak dp/dt mmHg/sec	Peak d^2p/dt^2 mmHg/sec ² $\times 10^3$	Peak V^{***} cm/sec	Peak dV/dt cm/sec ²	Peak ds/dt cm/sec	Peak d^2s/dt^2 cm/sec ²
<u>Control</u>								
			<u>D o g 9 (24 kg)</u>					
1	120	134	1398	33.2	52.0	1168	23.1	1143
2	120	130	1466	31.9	53.4	1253	25.1	1299
3	120	115	1536	29.7	56.7	1335	27.1	1454
4	120	115	1816	38.4	68.4	1503	30.3	1663
5	120	110	1643	34.9	61.2	1390	29.3	1558
<u>Isoprenaline</u>								
1	120	117	2166	55.5	86.7	2403	37.6	2078
2	120	110	2235	64.6	92.7	2669	41.8	2390
3	120	125	2655	75.4	100.0	2919	45.9	2649
4	125	138	3074	91.4	111.7	3069	46.9	2714
5	125	123	2688	75.1	103.4	3003	46.3	2668
6	125	140	3354	104.8	123.0	3328	51.5	2649
7	125	150	3843	108.3	133.4	3745	54.3	3117

(Continued over)

TABLE II (c) (Contd.)

	Heart Rate beats/min	Peak SP mmHg	Peak dp/dt mmHg/sec	Peak d^2p/dt^2 mmHg/sec ² x10 ³	Peak V*** cm/sec	Peak dV/dt cm/sec ²	Peak ds/dt cm/sec	Peak d^2s/dt^2 cm/sec ²
8	125	118	2515	69.9	96.7	2836	43.8	2338
9	125	115	2096	61.2	83.4	2168	36.5	2078
10	120	116	2026	57.7	76.9	1744	35.5	1922
Propranolol								
1	118	110	1695	52.4	73.4	1669	31.3	1817
2	118	110	1650	50.7	65.1	1503	28.9	1699
3	115	115	1559	48.9	58.4	1350	26.1	1299
4	115	110	1083	22.7	45.3	934	20.3	1193
5	100	110	1014	19.2	40.7	874	18.8	1039
6	95	110	909	17.5	36.7	668	16.8	883
7	95	100	629	16.8	26.7	534	12.3	663
8	90	100	489	13.9	21.7	469	10.4	624
9	90	90	419	10.5	18.0	389	8.4	468
10	80	90	349	7.8	13.3	334	6.3	390

(Continued over)

TABLE II (c)(Contd.)

	Heart Rate beats/min	Peak SP mmHg	Peak dp/dt mmHg/sec	Peak d^2p/dt^2 mmHg/sec ² x10 ³	Peak V*** cm/sec	Peak dV/dt cm/sec ²	Peak ds/dt cm/sec	Peak d^2s/dt^2 cm/sec ²
<u>Isoprenaline</u>								
1	109	131	3179	52.0	67.0	3278	42.5	2338
2	140	139	4104	129.9	126.0	2875	76.1	4210
3	140	135	3788	126.1	114.8	2588	71.6	3898
4	135	134	2999	98.5	98.8	2444	58.1	3342
5	140	129	4261	141.8	136.0	3019	80.5	4455
6	133	135	2904	94.5	91.8	2386	53.6	3118
7	133	131	2683	74.8	86.1	2329	51.5	3008
8	133	117	3156	102.4	111.9	2530	66.9	3675
<u>D o g 11 (21 kg)</u>								
<u>Control</u>								
1	130	104	1154	27.2	38.8	945	18.6	1251
2	130	101	1108	24.9	34.3	850	16.6	913
3	130	105	1579	45.4	57.3	1715	26.9	1677
4	134	102	1320	31.0	49.7	1398	22.9	1345
5	130	115	1549	43.9	56.1	1460	26.0	1641

(Continued over)

TABLE II (c) (Contd.)

	Heart Rate beats/min	Peak SP mmHg	Peak dp/dt mmHg/sec	Peak d^2p/dt^2 mmHg/sec ² $\times 10^3$	Peak V^{***} cm/sec	Peak dV/dt cm/sec ²	Peak ds/dt cm/sec	Peak d^2s/dt^2 cm/sec ²
<u>Propranolol</u>								
1	120	110	1640	46.9	59.2	1588	27.1	1563
2	110	110	1428	31.8	50.9	1294	23.0	1346
3	109	109	1215	25.7	38.2	763	18.6	991
4	90	101	971	22.7	31.9	794	15.6	782
5	80	92	850	19.7	21.3	480	11.5	704
6	80	92	623	18.2	20.4	440	10.4	521
7	85	92	1001	24.2	31.9	794	16.1	931
8	90	109	1215	28.8	41.4	1033	20.3	1120
9	100	108	1275	30.3	44.6	1111	21.9	1198
<u>Isoprenaline</u>								
1	110	118	1519	41.6	52.7	1310	24.0	1434
2	110	108	1549	43.9	56.1	1460	26.0	1563
3	140	118	2369	64.3	74.9	1951	36.5	1955
4	140	112	2430	68.1	79.6	2033	40.0	1997

(Continued Over)

TABLE II (c) (Contd.)

	Heart Rate beats/min	Peak SP mmHg	Peak dp/dt mmHg/sec	Peak d^2p/dt^2 mmHg/sec ² x10 ³	Peak V*** cm/sec	Peak dV/dt cm/sec ²	Peak ds/dt cm/sec	Peak $\frac{d^2s}{dt^2}$ cm/sec ²
5	140	116	2551	70.4	82.8	2095	41.6	2033
6	150	114	2673	72.4	89.2	2144	43.8	2345
7	150	118	2976	79.4	103.2	2779	49.4	2739
8	180	116	3190	81.7	117.9	3175	53.0	2861
9	150	118	2886	75.7	98.7	2381	48.1	2605
10	130	130	2080	58.7	60.5	1794	29.1	1694
Control				<u>D o g 12 (22 kg)</u>				
1	110	106	2139	54.7	52.8	1420	33.8	1791
2	110	106	1891	53.4	51.4	1403	32.1	1769
3	110	106	1851	51.3	50.7	1385	30.4	1685
4	110	106	2221	58.5	56.5	1598	37.1	2000
5	110	106	2180	57.5	53.5	1438	35.5	1895
Propranolol								
1	103	130	1728	44.1	47.9	1243	28.6	1601
2	103	125	1645	42.1	47.2	1100	27.0	1580
3	100	119	1570	39.0	45.8	1065	25.4	1390

(Continued over)

TABLE II (c) (Contd)

	Heart Rate beats/min	Peak SP mmHg	Peak dp/dt mmHg/sec	Peak d^2p/dt^2 mmHg/sec ² x10 ³	Peak V*** cm/sec	Peak dV/dt cm/sec ²	Peak ds/dt cm/sec	Peak d^2s/dt^2 cm/sec ²
4	100	140	1480	29.8	38.7	941	23.6	1264
5	100	145	1234	20.6	36.8	821	20.3	1179
6	95	145	1069	21.6	31.7	693	18.5	1137
7	95	132	1029	20.5	30.3	675	16.9	758
8	100	119	1769	46.2	49.3	1278	29.5	1668
<u>Isoprenaline</u>								
1	142	112	2303	63.6	63.4	1704	42.3	2106
2	150	106	3908	156.0	112.6	-	67.5	3707
3	150	165	3701	133.4	107.0	-	65.9	3580
4	158	185	4441	184.8	119.7	-	77.6	4212
5	150	119	2796	78.0	77.4	2929	50.6	2738
6	145	133	2961	98.5	78.1	2983	54.0	2864
7	145	172	3290	110.7	95.0	-	57.4	2948
8	145	130	3208	100.6	91.5	-	58.1	3033
9	140	172	3455	118.0	100.7	-	60.8	3159
10	130	169	2714	88.3	75.3	2894	47.3	2569

(Continued over)

TABLE II (c) (Contd.)

	Heart Rate beats/min	Peak SP mmHg	Peak dp/dt mmHg/sec	Peak d^2p/dt^2 mmHg/sec ² x10 ³	Peak V*** cm/sec	Peak dV/dt cm/sec ²	Peak ds/dt cm/sec	Peak d^2s/dt^2 cm/sec ²
11	125	145	2674	87.3	71.1	2698	45.6	2401
12	120	139	2385	73.9	66.9	2396	43.4	2317
13	110	139	1809	56.5	59.8	1651	-	-
Control				<u>D o g 13 (19 kg)</u>				
1	142	152	1769	32.8	47.6	1364	19.8	1329
2	133	148	1728	32.3	46.3	1288	19.3	1303
3	133	143	1728	32.3	50.2	1299	20.8	1512
4	133	152	1851	33.9	47.6	1299	20.3	1407
5	133	152	1810	33.9	48.5	1320	19.8	1368
<u>Isoprenaline</u>								
1	135	158	2468	56.5	80.6	1818	33.4	1875
2	138	166	2674	61.6	96.9	2813	37.1	1955
3	138	201	3085	85.2	108.3	2921	39.6	2084
4	138	201	3208	87.3	111.2	3409	41.6	2214
5	140	214	3496	88.3	121.2	3618	44.8	2917

(Continued over)

TABLE II (c) (Contd.)

	Heart Rate beats/min	Peak SP mmHg	Peak dp/dt mmHg/sec	Peak d^2p/dt^2 mmHg/sec ² x10 ³	Peak V*** cm/sec	Peak dV/dt cm/sec ²	Peak ds/dt cm/sec	Peak d^2s/dt^2 cm/sec ²
6	150	214	3701	93.3	134.2	3786	46.9	3075
7	150	290	3825	94.4	142.9	4111	52.1	3178
8	150	166	4441	100.6	149.4	4688	54.6	3231
9	160	158	4811	107.8	158.1	5301	57.3	3396
10	125	110	2056	43.1	72.8	1536	31.2	1772
<u>Propranolol</u>								
1	125	118	1933	40.0	63.7	1751	26.0	1512
2	125	99	1645	35.9	60.6	974	22.9	1433
3	113	99	1480	30.8	54.9	974	21.9	1276
4	103	79	1151	18.8	38.9	693	18.7	1225
5	100	59	905	12.3	36.4	639	15.6	782
6	66	40	740	10.3	32.9	541	12.5	626
7	38	30	411	5.1	26.9	498	10.4	599

(Continued over)

TABLE II (c) (Contd.)

	Heart Rate beats/min	Peak SP mmHg	Peak dp/dt mmHg/sec	Peak: d^2p/dt^2 mmHg/sec ² $\times 10^3$	Peak V^{***} cm/sec	Peak dV/dt cm/sec ²	Peak ds/dt cm/sec	Peak d^2s/dt^2 cm/sec ²
<u>Dog 14 (19 kg)</u>								
<u>Control</u>								
1	120	135	3118	103.7	82.3	4623	28.1	1435
2	115	134	2910	100.6	80.1	4241	26.9	1373
3	113	132	3243	113.1	83.2	4745	28.8	1498
4	113	131	3075	98.6	81.5	4369	27.5	1404
5	113	121	2910	91.3	80.1	4186	28.8	1404
<u>Isoprenaline</u>								
1	120	117	2910	67.6	81.3	4369	29.4	1404
2	122	108	2910	71.0	83.6	4441	30.0	1454
3	128	106	2910	99.6	85.4	4914	30.6	1498
4	130	110	3049	101.8	86.6	5460	31.3	1552
5	133	116	3408	112.0	104.3	5824	35.0	1724

TABLE II (c) (Contd.)

	Heart Rate beats/min	Peak SP mmHg	Peak dp/dt mmHg/sec	Peak d^2p/dt^2 mmHg/sec ² x 10 ³	Peak V*** cm/sec	Peak dV/dt cm/sec ²	Peak ds/dt cm/sec	Peak d^2s/dt^2 cm/sec ²
6	143	105	3533	119.3	122.4	6188	40.0	2340
7	150	108	4285	131.5	135.1	6843	45.0	2808
8	160	114	3159	103.7	93.0	5642	32.5	1622
<u>Propranolol</u>								
1	113	98	2494	88.2	78.6	4914	28.8	1404
2	113	115	2701	90.3	74.3	4278	27.5	1404
3	113	124	2723	85.1	71.3	3823	26.3	1466
4	107	118	2494	57.1	69.9	3276	25.0	1310
5	105	110	2218	51.5	65.5	3130	23.8	1279
6	100	102	1958	50.6	62.6	3568	22.5	1154
7	98	96	1809	48.2	61.2	2913	21.9	1123
8	98	101	1684	36.3	59.7	2730	21.3	1061
9	92	94	1496	32.7	58.2	2184	20.0	998

(Continued Over)

TABLE II (c) (Contd.)

	Heart Rate beats/min	Peak SP mmHg	Peak dp/dt mmHg/sec	Peak d^2p/dt^2 mmHg/sec ² x 10 ³	Peak V*** cm/sec	Peak dV/dt cm/sec ²	Peak ds/dt cm/sec	Peak d^2s/dt^2 cm/sec ²
10	92	82	1248	23.9	56.8	3021	18.8	967
11	92	101	1455	25.9	49.5	2549	17.5	983
12	60	83	1081	22.4	43.7	1893	16.3	874
13	50	73	915	21.8	42.2	2258	15.6	780
14	75	64	749	12.4	39.8	1893	14.4	686
15	40	50	624	11.4	38.3	-	13.1	499
Control				Dog 15 (17.5 kg)				
1	110	114	1344	41.9	60.9	1320	21.3	885
2	100	114	1344	41.9	66.0	1396	22.1	944
3	75	114	1386	43.9	73.1	1599	24.8	1238
4	75	114	1408	45.0	76.1	1611	25.1	1356
5	70	114	1428	46.1	77.1	1675	26.0	1386

(Continued over)

TABLE II (c) (Contd.)

	Heart Rate beats/min	Peak SP mmHg	Peak dp/dt mmHg/sec	Peak d^2p/dt^2 mmHg/sec ² x 10 ³	Peak V*** cm/sec	Peak dV/dt cm/sec ²	Peak ds/dt cm/sec	Peak d^2s/dt^2 cm/sec ²
<u>Isoprenaline</u>								
1	150	185	2814	85.3	139.9	4695	49.5	2948
2	150	154	2751	71.2	116.7	4188	42.4	2506
3	145	150	2520	64.9	109.6	3934	42.4	2359
4	136	141	2310	54.4	106.6	3680	41.3	2359
5	133	127	2100	50.0	102.5	3553	35.4	2064
6	125	120	1890	46.1	101.5	3501	33.0	1857
7	120	117	1596	39.8	81.2	2030	31.9	1799
8	130	107	1470	36.6	76.6	1941	29.5	1530
9	100	100	1260	36.7	71.1	1650	27.1	1538
10	146	140	2730	73.3	113.7	3934	42.4	2359

(Continued Over)

TABLE II (c) (Contd.)

	Heart Rate beats/min	Peak SP mmHg	Peak dp/dt mmHg/sec	Peak $\frac{d^2p}{dt^2}$ mmHg/sec ² x 10 ³	Peak V*** cm/sec	Peak dV/dt ² cm/sec ²	Peak ds/dt cm/sec	Peak $\frac{d^2s}{dt^2}$ cm/sec ²
<u>Propranolol</u>								
1	103	68	1225	26.4	63.2	1396	18.9	708
2	100	60	756	13.6	55.8	1143	15.1	826
3	96	47	504	10.5	50.8	889	9.4	550
4	71	54	630	11.5	30.5	508	11.8	339
5	70	60	546	9.4	20.3	381	7.1	284
6	100	64	798	14.1	58.5	1260	15.4	885
<u>LAD Ligation</u>								
1	100	70	840	15.7	25.4	381	13.3	560
2	100	74	924	16.7	30.5	508	14.1	590
(Continued Over)								

TABLE II (c) (Contd.)

	Heart Rate beats/min	Peak SP mmHg	Peak dp/dt mmHg/sec	Peak d^2p/dt^2 mmHg/sec ² $\times 10^3$	Peak V^{***} cm/sec	Peak dV/dt cm/sec ²	Peak ds/dt cm/sec	Peak $\frac{d^2s}{dt^2}$ cm/sec ²
<u>Cross Clamped Descending Aorta</u>								
Before	100	75	966	17.8	40.1	761	17.8	737
During	100	54	420	8.4	18.3	355	7.1	226
After	100	91	1260	36.7	55.8	889	18.9	924
<u>Control</u>								
				<u>D o g 16 (17.6 kg)</u>				
1	140	90	1200	45.0	42.3	950	19.0	789
2	140	90	1200	48.0	45.6	1071	20.1	866
3	140	95	1240	45.9	43.4	1016	19.0	838
4	140	102	1160	42.0	43.1	988	18.9	799
5	140	102	1094	38.0	41.5	923	17.9	714
<u>Propranolol</u>								
1	135	83	984	35.7	40.2	873	17.3	558
2	125	81	969	32.0	37.6	816	16.8	686
3	120	77	960	30.0	35.9	698	15.6	782
4	115	64	920	28.0	31.1	658	14.6	643
5	110	60	880	25.0	28.7	598	14.5	491

(Continued over)

TABLE II (c) (Contd.)

	Heart Rate beats/min	Peak SP mmHg	Peak dp/dt mmHg/sec	Peak d^2p/dt^2 mmHg/sec ² $\times 10^3$	Peak V^{***} cm/sec	Peak dV/dt cm/sec ²	Peak ds/dt cm/sec	Peak d^2s/dt^2 cm/sec ²
6	105	54	809	24.0	27.9	578	13.4	439
7	100	50	720	20.0	23.9	419	12.3	406
<u>Isoprenaline</u>								
1	150	90	1800	58.0	79.9	1750	28.5	1292
2	160	83	1656	56.0	64.2	1373	26.9	1117
3	140	81	1563	54.0	58.3	1295	24.6	1061
4	130	64	1280	47.0	54.3	1236	23.1	1014
5	115	51	1120	38.0	50.2	1133	22.4	914
6	109	50	1040	36.0	45.6	1071	20.3	866
7	103	42	1006	35.7	40.1	863	17.4	663
<u>Cross-Clamped Descending Aorta</u>								
Before	103	41	994	35.0	40.0	888	17.3	590
After	102	45	1640	54.2	63.5	1313	25.3	1055
<u>LAD Ligation</u>								
1	100	41	920	27.9	28.2	613	13.5	494
2	133	45	760	24.0	23.9	419	10.9	387

(Continued Over)

TABLE II (c) (Contd.)

	Heart Rate beats/min	Peak SP mmHg	Peak dp/dt mmHg/sec	Peak d^2p/dt^2 mmHg/sec ² x 10 ³	Peak V*** cm/sec	Peak dV/dt cm/sec ²	Peak ds/dt cm/sec	Peak d^2s/dt^2 cm/sec ²
3	133	45	640	23.0	19.9	359	8.9	346
4	133	45	560	12.0	15.9	239	6.2	279
<u>Dog 17 (21 kg)</u>								
<u>Control</u>								
1	142	150	2249	77.9	89.1	2064	22.4	1257
2	142	145	2166	72.8	86.0	1841	21.8	1173
3	141	145	2084	70.7	84.5	1693	20.6	1123
4	141	140	2000	68.6	79.6	1668	20.1	1014
5	140	140	1916	63.4	75.5	1628	19.0	1061
<u>Propranolol</u>								
1	133	122	1854	58.2	73.6	1556	18.1	977
2	125	115	1666	52.5	72.3	1429	16.9	921
3	120	115	1639	47.8	71.3	1419	16.8	894

(Continued Over)

TABLE II (c) (Contd.)

	Heart Rate beats/min	Peak SP mmHg	Peak dp/dt mmHg/sec	Peak d^2p/dt^2 mmHg/sec ² $\times 10^3$	Peak V^{***} cm/sec	Peak dV/dt cm/sec ²	Peak ds/dt cm/sec	Peak d^2s/dt^2 cm/sec ²
4	115	113	1625	45.7	70.7	1318	16.5	858
5	109	110	1500	43.7	69.6	1311	15.6	782
6	105	110	1413	38.6	64.7	1223	15.1	698
7	100	100	1209	36.4	54.2	1239	13.4	614
8	95	100	1125	31.2	48.0	1191	11.2	391
9	90	90	1041	22.3	43.3	1198	10.6	335
<u>Isoprenaline</u>								
1	139	120	2043	67.6	81.1	1640	20.0	978
2	142	115	2216	72.8	86.0	1905	21.9	1201
3	145	108	2209	74.9	87.8	1985	20.6	1256
4	145	112	2166	70.7	85.9	1841	21.3	1201

(Continued Over)

TABLE II (c) (Contd.)

	Heart Rate beats/min	Peak SP mmHg	Peak dp/dt mmHg/sec	Peak d^2p/dt^2 mmHg/sec ² x 10 ³	Peak V*** cm/sec	Peak dV/dt cm/sec ²	Peak ds/dt cm/sec	Peak d^2s/dt^2 cm/sec ²
5	150	112	2750	90.5	105.0	2375	24.3	1368
6	155	112	2833	93.6	110.0	2571	26.9	1457
7	155	110	3083	114.4	111.4	2625	27.9	1675
8	140	108	2500	84.2	92.4	2223	22.9	1313
9	130	112	1000	68.6	82.8	1715	19.0	1117
10	120	100	1395	45.4	64.7	1285	14.9	744
<u>LAD Ligation</u>								
1	100	67	1168	33.8	58.9	1215	13.4	697
2	100	57	916	26.0	43.3	1111	10.6	382
3	90	37	375	11.4	35.0	825	8.5	304
4	80	30	209	7.3			5.6	209

(Continued Over)

TABLE II (c) (Contd.)

	Heart Rate beats/min	Peak SP mmHg	Peak dp/dt mmHg/sec	Peak d^2p/dt^2 mmHg/sec ² $\times 10^3$	Peak V^{***} cm/sec	Peak dV/dt cm/sec ²	Peak ds/dt cm/sec	Peak d^2s/dt^2 cm/sec ²
<u>Control</u>								
Dog 18 (19.5 kg)								
1	158	117	2320	74.9	92.4	2303	43.9	2730
2	158	117	2600	80.0	93.6	2395	45.5	2867
3	150	115	2206	64.6	89.2	2223	42.8	2594
4	150	115	2000	60.0	84.4	2080	41.7	2048
5	145	115	1800	57.4	79.6	1936	38.4	2129
<u>Propranolol</u>								
1	131	109	1600	55.7	73.3	1866	35.9	1911
2	125	103	1464	53.7	66.9	1668	30.7	1720
3	120	95	1400	42.0	62.0	1433	28.5	1693
4	114	85	1040	32.7	54.5	1310	24.1	1583
5	110	70	1000	28.0	47.8	1159	23.0	1502
6	102	65	1140	35.9	46.2	1098	22.0	1420
7	95	51	1040	32.7	41.1	1000	20.8	1010
8	81	45	1000	27.9	39.6	884	19.7	983

(Continued over)

TABLE II (c) (Contd.)

	Heart Rate beats/min	Peak SP mmHg	Peak dp/dt mmHg/sec	Peak d^2p/dt^2 mmHg/sec ² $\times 10^3$	Peak V*** cm/sec	Peak dV/dt cm/sec ²	Peak ds/dt cm/sec	Peak d^2s/dt^2 cm/sec ²
9	75	38	706	21.9	26.7	654	13.5	669
10	65	33	560	21.5	19.1	445	10.9	491
<u>Isoprenaline</u>								
1	81	64	720	23.6	24.9	531	14.3	764
2	95	70	760	25.9	31.9	715	15.4	874
3	110	83	1280	34.9	50.9	1080	24.1	1092
4	120	95	1520	47.9	60.5	1429	30.7	1502
5	125	102	1750	54.9	66.9	1668	31.8	1638
6	130	95	1840	73.4	73.3	1866	32.9	1747
7	135	95	2030	79.9	86.6	2286	39.5	2184
8	140	90	2460	90.5	98.7	2730	44.4	2239
9	145	90	2600	98.6	101.9	2773	49.3	2321
10	150	90	2625	99.8	102.3	2794	52.6	2457
<u>Gross Clamped Ascending Aorta</u>								
Before	115	58**	800	26.0	35.5	794	-	-
During	110	0	0	0	0	0	-	-
After	100	60**	1400	59.9	47.8	1064	-	-

TABLE II (c) (Contd.)

Heart Rate beats/min	Peak SP mmHg	Peak dp/dt mmHg/sec	Peak d^2p/dt^2 mmHg/sec ² x 10 ²	Peak V*** cm/sec	Peak dV/dt cm/sec ²	Peak ds/dt cm/sec	Peak d^2s/dt^2 cm/sec ²
<u>Cross Clamped Descending Aorta</u>							
Before	115	60	850	25.9	38.2	873	-
After	115	60	1000	39.9	98.7	2666	300
<u>LAD Ligation</u>							
1	75	64	1040	28.0	43.3	921	-
2	71	75	800	27.6	36.9	874	-
3	83	59	840	34.9	31.9	604	-
4	Heart	70	800	41.8	35.1	730	655
5	Block	64	720	30.0	38.2	825	-

* Velocity by catheter probe

** Aortic pressure

*** Velocity by cuff probe

Abbreviations LAD = left anterior descending coronary artery;

PI = Instantaneous pressure; SP = systolic pressure;

EDP = End-diastolic pressure;

V = aortic ejection velocity

TABLE III - Summary of hemodynamic and echo data in 18 dogs

	Heart Rate beats/min	Systolic Pressure mm Hg	Peak dp/dt mm Hg/sec	Peak ds/dt cm/sec	Peak d^2s/dt^2 cm/sec ²	Peak V cm/sec	Peak dV/dt cm/sec ²
CONTROL (18 dogs)							
Mean	127	127	1963	26.96	1526	61.8	1634
\pm SD	19	28	632	9.04	582	16.4	935
N	73	71	73	73	63	63	63
ISOPRENALINE (18 dogs)							
Mean	136	137	2883	39.7	2244	86.4	2454
\pm SD	17	45	1122	14.66	890	27.2	1333
N	157	157	153	158	134	136	129

(Continued Over)

TABLE III.- Summary of hemodynamic and echo data in 18 dogs (Contd.)

	Heart rate beats/min	Systolic pressure mm Hg	Peak dp/dt mm Hg/sec	Peak ds/dt cm/sec	Peak d^2s/dt^2 cm/sec ²	Peak V cm/sec	Peak dV/dt cm/sec ²
PROPRANOLOL (18 dogs)							
Mean	102	107	1344	20.87	1140	45.6	1131
± SD	22	33	614	10.17	624	16.6	828
N	132	129	141	142	125	123	123
LAD LIGATION (6 dogs)							
Mean	91	57	780	11.3	470	33.8	626
± SD	31	15	242	3.6	176	10.7	294
N	16	16	16	12	12	15	15

(Continued Over)

TABLE III.- Summary of hemodynamic and echo data in 18 dogs (Contd.)

Heart rate beats/min		Systolic pressure mm Hg	Peak dp/dt mm Hg/sec	Peak ds/dt cm/sec	Peak d^2s/dt^2 cm/sec ²	Peak V cm/sec	Peak dV/dt cm/sec ²
CROSS-CLAMPED DESCENDING AORTA 3 dogs (N = 3)							
BEFORE:	Mean	96	81	849	13.2	609	32.8
	± SD	20	26	118	7	182	11.0
DURING:	Mean	96	98	449	7.2	347	13.2
	± SD	38	75	75	0.4	108	5
AFTER:	Mean	98	91	1278	14.9	760	63.1
	± SD	18	31	288	8.2	404	33
							1089

(Continued Over)

TABLE III - Summary of hemodynamic and echo data in 18 dogs (Contd.)

	Heart Rate beats/min	Systolic pressure mmHg	Peak dp/dt mm Hg/sec	Peak ds/dt cm/sec	Peak $\frac{d^2s}{dt^2}$ cm/sec ²	Peak V cm/sec	Peak $\frac{dV}{dt^2}$ cm/sec
CROSS-CLAMPED ASCENDING AORTA: 1 dog (N = 1)							
BEFORE	115	58*	800	-	-	35.5	794
DURING	110	0*	0	-	-	0	0
AFTER	100	60*	1400	-	-	47.8	1064

* Aortic Pressure

Abbreviations: LAD = left anterior descending coronary artery; V = aortic ejection velocity

TABLE IV
SUMMARY OF CORRELATION COEFFICIENTS IN THE ANIMAL STUDY

	Peak V	Peak dV/dt	Peak dp/dt	Peak d^2p/dt^2	Peak d^2s/dt^2	Manual BC Slope
Peak Mitral Closing Velocity (ds/dt)	0.824 P<0.001 N=295	0.67 P<0.001 N=288	0.734 P<0.001 N=380	0.621 P<0.001 N=311	0.986 P<0.0001 N=348	0.93 P<0.001 N=40
Peak Mitral Closing Acceleration (d^2s/dt^2)	0.83 P<0.001 N=295	0.66 P<0.001 N=288	0.752 P<0.001 N=330	0.626 P<0.001 N=309		
Peak Aortic Ejection Velocity (V)	0.993 (Probe vs Cuff) P<0.0001 N=13	0.829 P<0.001 N=299	0.79 P<0.001 N=302	Not Plotted		
Peak Aortic Acceleration (dV/dt)	0.829 P<0.001 N=229		0.707 P<0.001 N=295	Not Plotted		
Peak dp/dt				0.947 P<0.0001 N=304		

TABLE V

HEMODYNAMIC AND ECHO DATA IN 42 HUMAN SUBJECTS

No.	ID	Sex	Age Yr.	Dx	HR Beats/Min	CO L/min	EDP (mmHg) $\frac{a}{b}$	Manual BC slope $\frac{\text{cm/sec}}{\text{cm/sec}}$	ds/dt $\frac{\text{cm/sec}}{\text{cm/sec}}$	d2s/dt2 $\frac{\text{cm/sec}^2}{\text{cm/sec}^2}$
1	CB	M	55	CAD	70	7.6	5 12	32.5	33.0	2250
2	GW	M	63	CAD	67	3.0	24 28	12.2	8.8	355
3	JK	M	60	CAD	70	-	15 20	14.4	18.3	-
4	JL	M	52	CAD	74	5.2	12 29	-	22.6	560
5	DC	M	35	ASD	62	4.7	10 72	13.8	21.9	1125
*6	ERB	F	40	MS	65	4.3	5 -	65.4	18.5	1332
7	HD	F	58	CAD	70	-	18 29	19.2	24.0	975
8	ES	M	47	CAD	66	4.9	16 27	45.9	33.4	1664
9	JRC	M	52	CAD	68	-	9 14	23.2	32.2	1285
10	RG	M	40	CAD	72	-	17 25	20.0	25.0	2500
11	JV	F	49	MR	80	4.2	9 -	-	15.3	445
12	GB	M	60	CAD	76	-	8 15	31.0	32.9	1578

(Continued Over)

TABLE V (Contd.)

No. ID	Sex	Age Yr.	Dx	HR Beats/Min	CO L/min	EDP (mmHg) $\frac{a}{b}$	Manual BC slope cm/sec	ds/dt cm/sec	d^2s/dt^2 cm/sec ²
13 RG	M	33	AS	60	-	-	23.9	31.0	1040
14 RG	M	67	CAD	72	-	12	25.0	30.3	1179
15 JL	M	41	CAD	85	4.3	7	38.5	-	-
16 JOB	M	43	CAD	78	5.9	12	13.0	15.5	520
17 ED	F	50	N	72	-	-	24.0	24.8	1553
18 GM	M	50	CAD	76	-	11	28.8		
19 WM	M	56	CAD	84	7.7	7	29.9		
20 DM	M	43	CM	72	-	9	25.7		
21 HK	M	49	CAD	78	-	13	25.0		
22 SR	F	68	CAD 1	80	-	12	27.8		
23 GW	F	46	CAD	54	-	-	50.1		
24 RY	M	47	ASH	79	6.6	8	55.5		

(Continued Over)

TABLE V (Contd.)

No. ID	Sex	Age Yr.	Dx	HR Beats/Min	CO L/min	EDP (mmHg) $\frac{a}{b}$	Manual BC slope cm/sec	ds/dt cm/sec	d^2s/dt^2 cm/sec ²
25 IS	F	57	CM SX	76	6.2	9 12	29.5	—	
26 FT	M	64	CAD	72	6.1	25 29	12.0	—	
27 GW	M	29	ASH	70	5.8	10 3	44.7	—	
*28 EW	F	33	MS	58	2.2	5 8	77.9	—	
29 FM	M	45	CAD	62	2.7	15 20	20.6	—	
30 NB	F	49	CAD	80	3.5	19 20	18	—	
31 MS	M	54	CAD	108	—	31 39	12	—	
32 LO	F	51	CAD	70	—	14 23	13.5	—	
33 WL	M	59	CAD	72	4.5	7 17	22.4	—	
34 OV	F	48	CAD	78	5.3	12 13	23.2	—	
35 JC	M	51	CAD	100	5.1	11 20	10.8	14.5	
36 JB	M	57	CAD	91	10.5	10 12	24.5	—	

TABLE V (Contd.)

No.	ID	Sex	Age Yr.	Dx	HR Beats/min	CO L/min	$\frac{\text{EDP (mmHg)}}{a}$	$\frac{\text{Manual BC slope}}{\text{cm/sec}}$	$\frac{ds}{dt}$ cm/sec	$\frac{d^2s}{dt^2}$ cm/sec ²
37	DE	M	50	N	72	-	-	21.8	25.2	-
38	BJ	M	32	N	70	-	-	28.0	-	-
39	PM	M	32	N	72	-	-	26.8	-	-
40	BVM	M	40	N	80	-	-	24.5	-	-
41	AB	M	39	CAD	66	-	12 22	16.7	-	-
42	DMF	M	38	N	70	-	-	23.6	-	-

* Atrial fibrillation

Abbreviations: ASD = Atrial Septal Defect; ASH = Asymmetric septal hypertrophy;
a = resting; b = post-angiography; CAD = coronary artery disease;

CO = cardiac output; CM = Cardiomyopathy; Dx = Diagnosis; MS = Mitral stenosis;
MR = Mitral regurgitation; N = Normal; SX = Syndrome X

TABLE VI : Mitral echo , Aortic Velocity , High Fidelity Ventricular Pressure and Ejection Fraction in 15 Human patients .

No.	ID	Age Yr.	Sex	Dx	HR Beats/min	CI L/min	EDP(mm Hg)			EF %	ds/dt cm/sec	d^2s/dt^2 cm/sec ²	V (cm/sec)		dV/dt cm/sec ²	dp/dt mmHg/sec
							a	b					Asc	Arch	Desc	
1	GD	26	M	AR	96	14.6	6	9		51.0	40.0	-	49	88	92	-
2	HS	55	M	CAD	55	7.6	8	11		68.5	30.7	2214	65	73	65	-
3	ELB	57	M	CAD	68	4.4	8	11		46.5	26.9	932	32	30	29	-
4	SB	61	M	CAD	48	4.8	14	20		62.4	21	870	34	68	48	-
5	PD	43	F	CAD	65	4.3	12	20		70.9	14	600	24	48	66	444
6	TH	58	F	CM	75	3.8	5	20		-	20	893	25	42	48	1380
7	BR	65	M	CAD	97	6.9	32	39		19.2	12.4	973	21	29	23	-
8	TM	55	M	CAD	65	8.7	22	38		53.3	20	893	35	40	48	1620
9	JS	65	M	CAD	70	-	16	22		65.1	18.7	764	32	82	84	1120
10	BL	56	F	CAD	72	4.5	5	17		59.2	26.7	1170	-	-	-	1690

(Continued over)

TABLE VI. (Contd.)

No.	ID	Age Yr.	Sex	Dx	HR Beats/min	CI L/min	EDP(mm Hg)		EF %	ds/dt cm/sec	d^2s/dt^2 cm/sec ²	V(cm/sec)			dV/dt cm/sec ²	dp/dt mm Hg/sec
							a	b				Asc	Arch	Desc		
11	VT	27	M	CM	65	6.5	16	24	47.1	21	721	-	-	-	-	1690
12	MM	26	F	VSD	80	5.3	10	17	-	32.7	-	50	58	92	-	-
13	DG	55	M	CAD	70	6.9	8	12	67.7	24.4	1034	-	-	-	-	-
14	RB	58	M	CAD	85	4.1	6	22	57.0	48.0	-	-	-	-	-	-
15	RW	59	M	CAD	78	5.7	8	22	55.1	26.0	1200	-	-	-	-	-

Abbreviations: a = before angiography and resting ; b = after angiography ; CI = Cardiac Index ; EDP = End-diastolic pressure ;

EF = Ejection Fraction ; Asc = Ascending ; Desc = Descending Aorta.

TABLE VII
SUMMARY OF CORRELATION COEFFICIENTS IN THE HUMAN STUDY

	Cardiac Output	Left Ventricular End-diastolic Pressure	Ejection Fraction	Peak dp/dt	Peak V	Peak dV/dt
Peak ds/dt	0.387	0.61	0.17	0.93	0.81	r=0.24
	N=21	N=36	N=13	N=6	N=10	N=4
	NS	P<0.02	NS	P<0.005	P<0.005	NS
Peak d ² _s /dt ²	0.295	0.44	0.18	0.79	0.91	r=0.44
	N=19	N=18	N=11	N=6	N=8	N=4
	NS	P<0.02	NS	P<0.05	P<0.005	NS

Figure 1: Relation Between Aortic Acceleration to Aortic Velocity and Peak dp/dt . Computer Plots of Data from Noble et al (27)

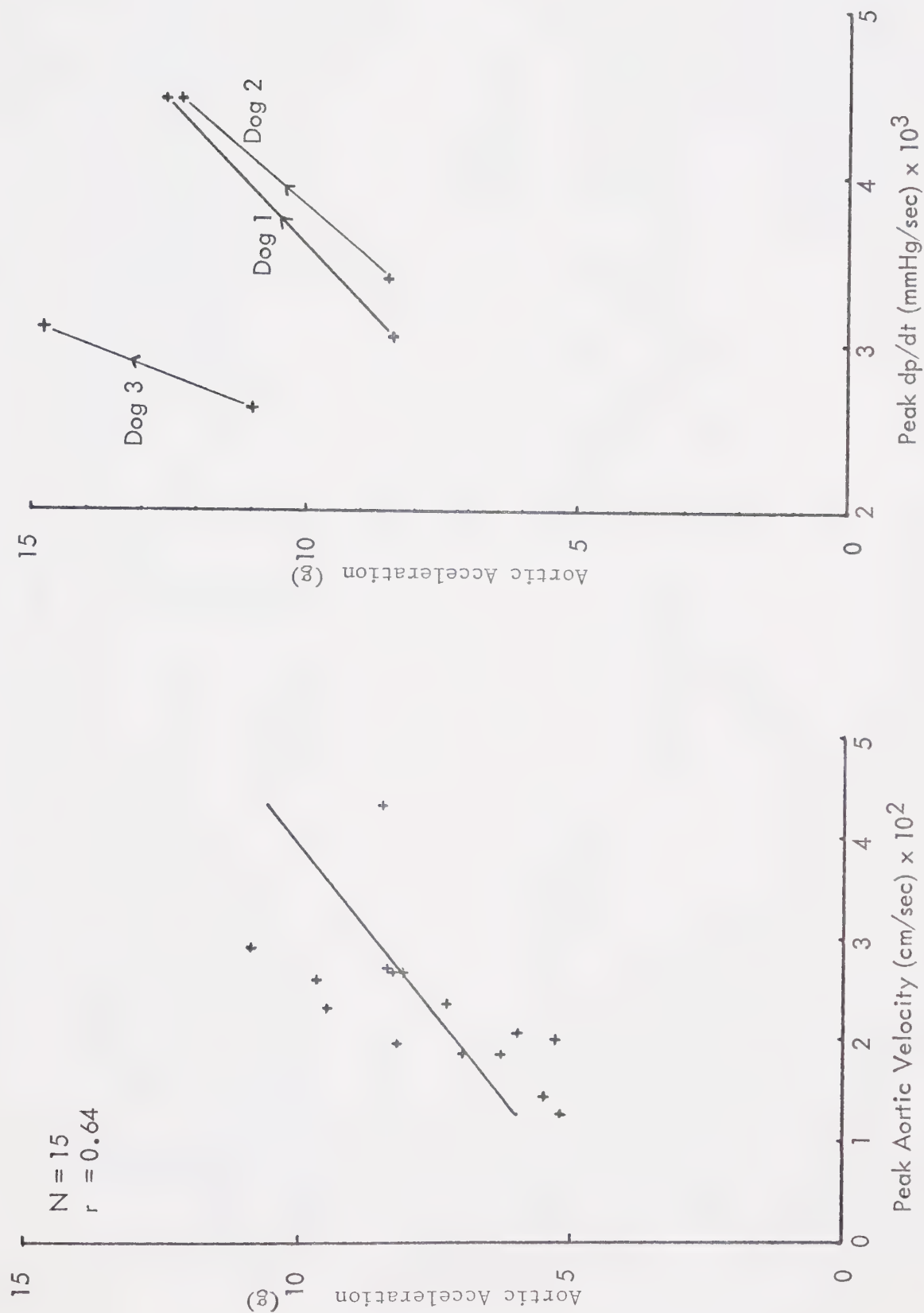


Figure 2: The Animal Model and Assembly of Instruments

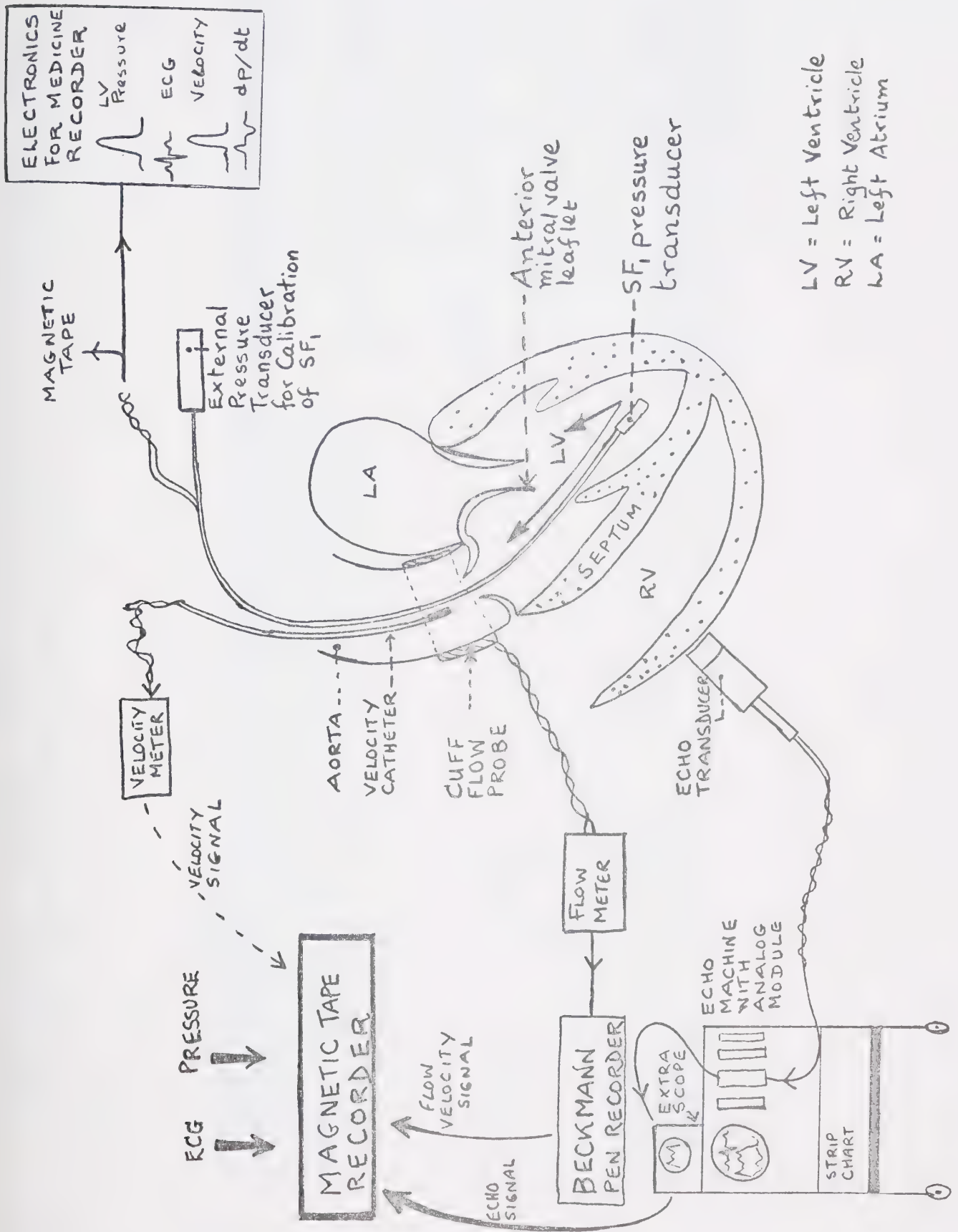


Figure 3 MEASUREMENT OF CLOSURE SLOPE FROM STRIP CHART RECORDINGS MANUAL
METHOD (SLOW AND RAPID HEART RATES)

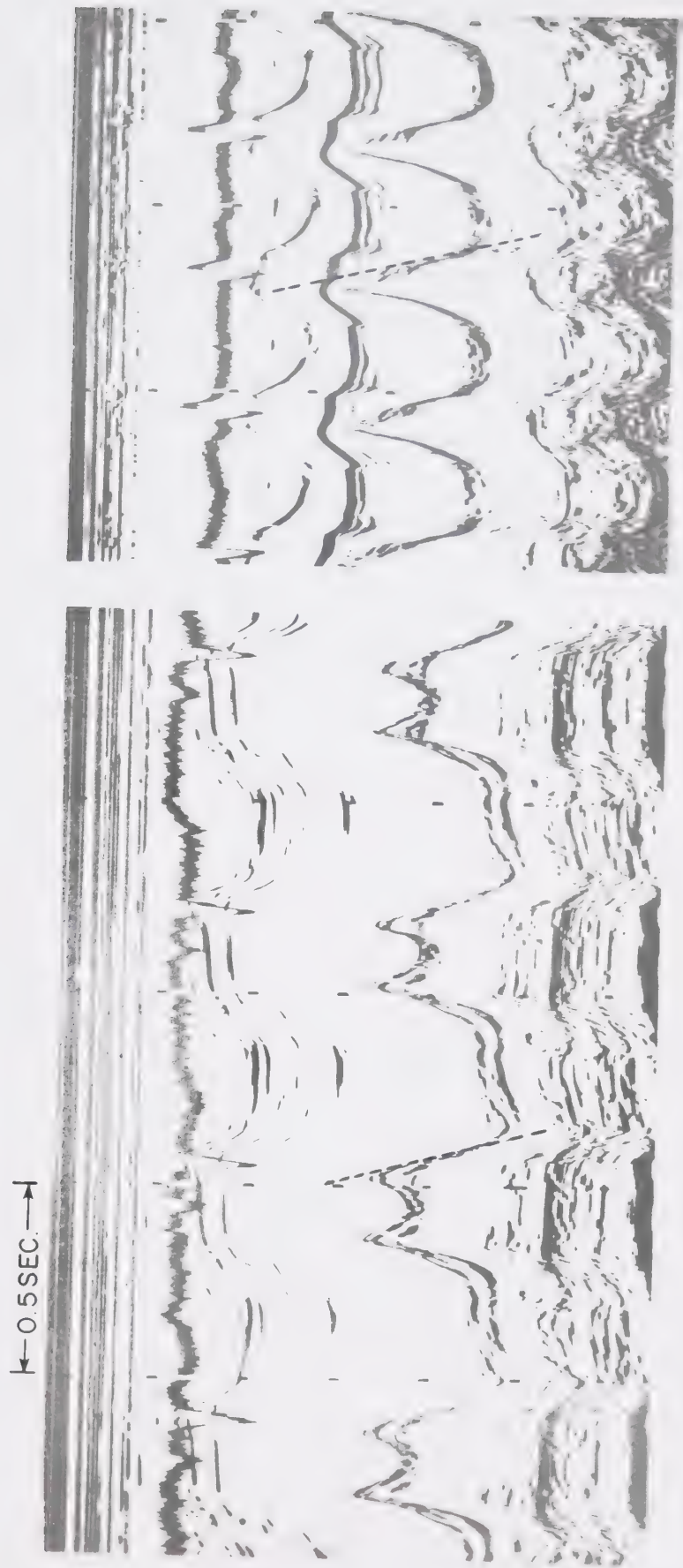


Figure 4 ANALOG MITRAL ECHO RECORDING OF ELECTRONICS FOR MEDICINE RECORDER

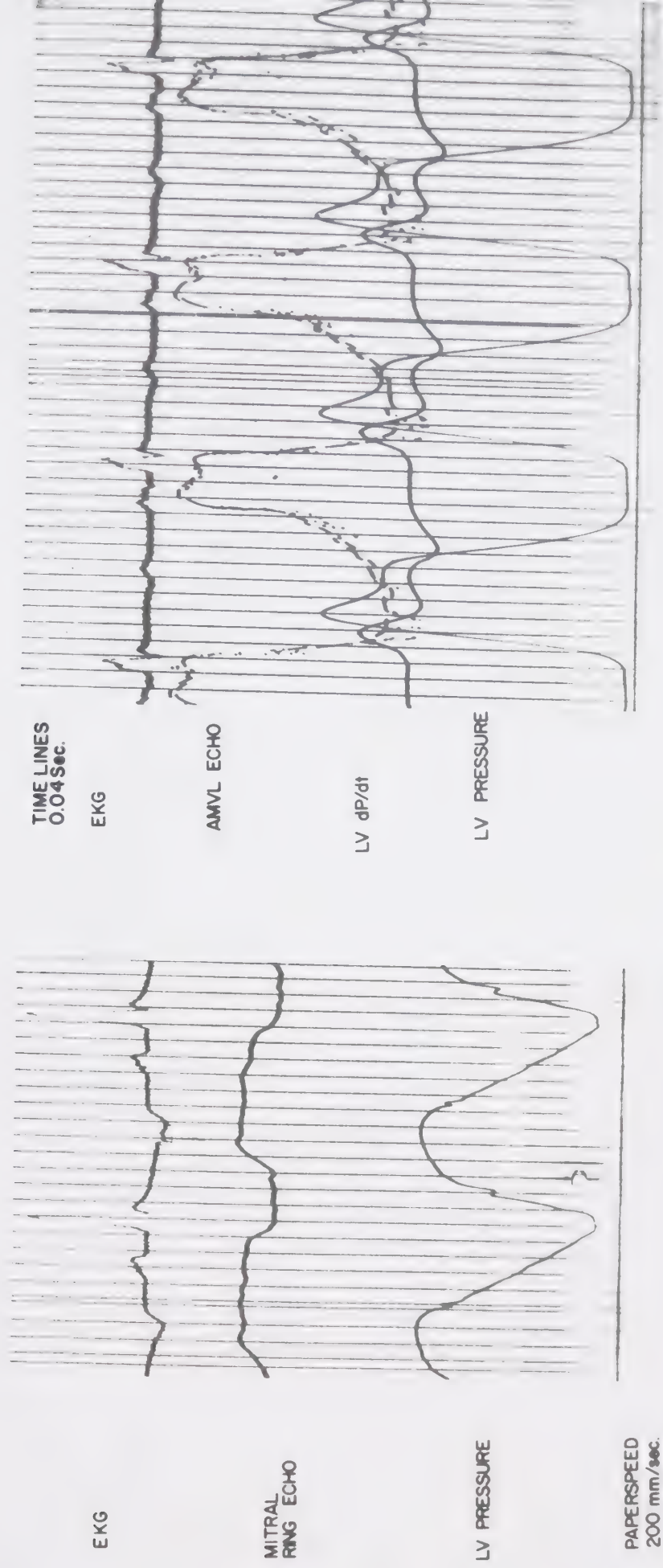


Figure 5: The Playback Assembly for Pressure, Echo and Velocity From the Magnetic Tape

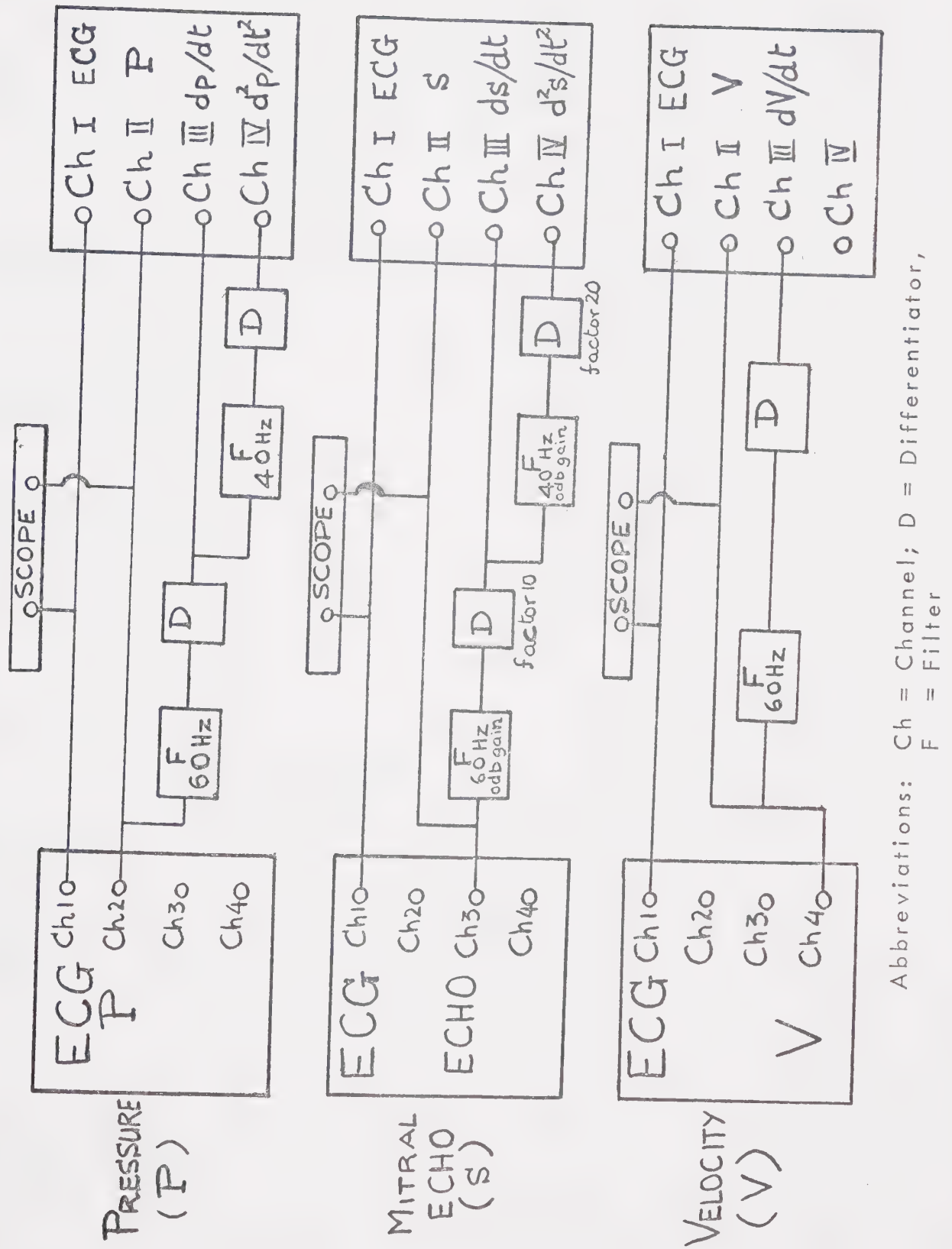


Figure 6 FIRST AND SECOND DERIVATIVES OF AMVL ECHO
AND TIMING WITH PRESSURE AND VELOCITY SIGNALS

EKG

FILTERED MITRAL
ECHO SIGNAL

LEFT VENTRICULAR
PRESSURE (mmHg)

AORTIC
VELOCITY cm/sec

EKG

UNFILTERED
MITRAL ECHO
SIGNAL

FIRST
DERIVATIVE
OF ECHO

SECOND
DERIVATIVE
OF ECHO

100
(cm)
0

25
cm/sec
0

0
cm/sec²
1000

PEAK AMVL
CLOSING VELOCITY

PEAK AMVL
CLOSING ACCELERATION

ARTIFACT

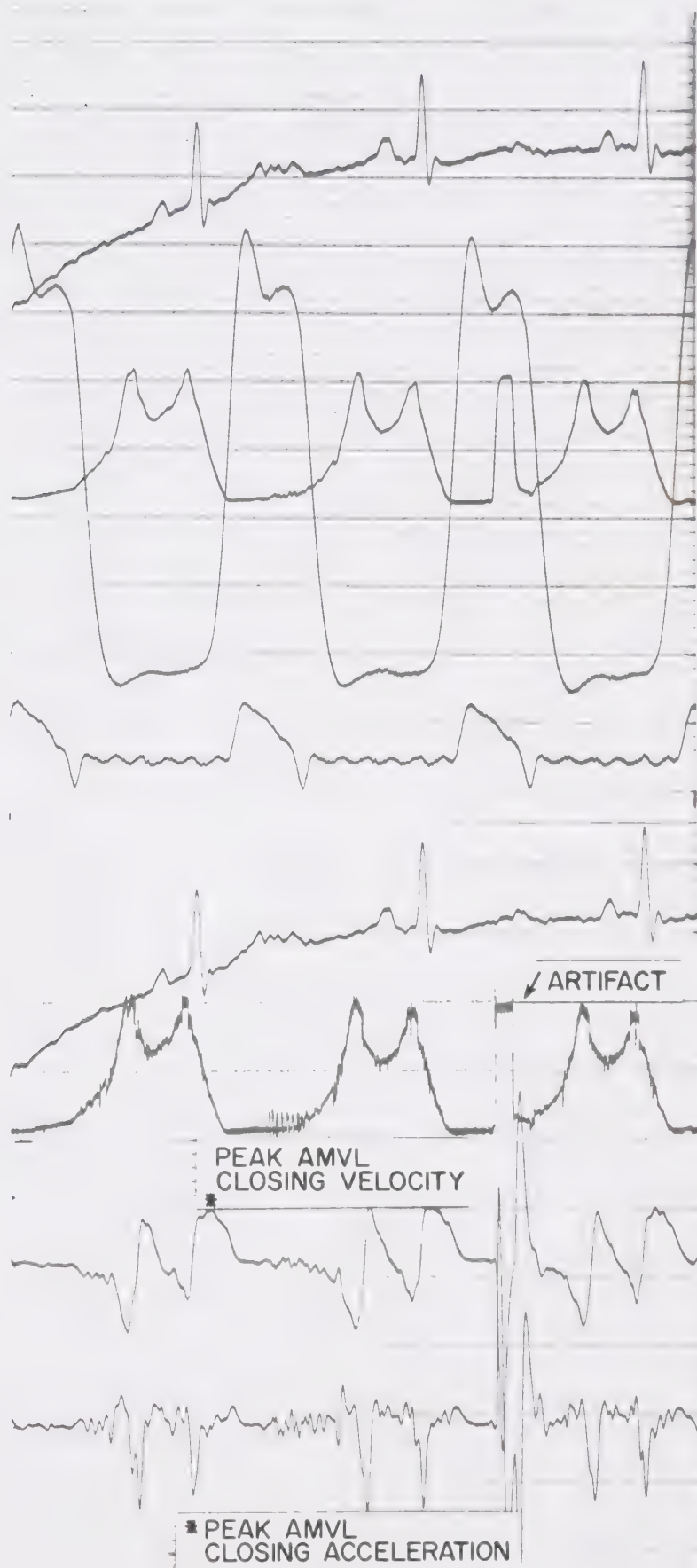


Figure 7 MECHANICAL ALTERNANS IN THE ANAESTHETISED DOG

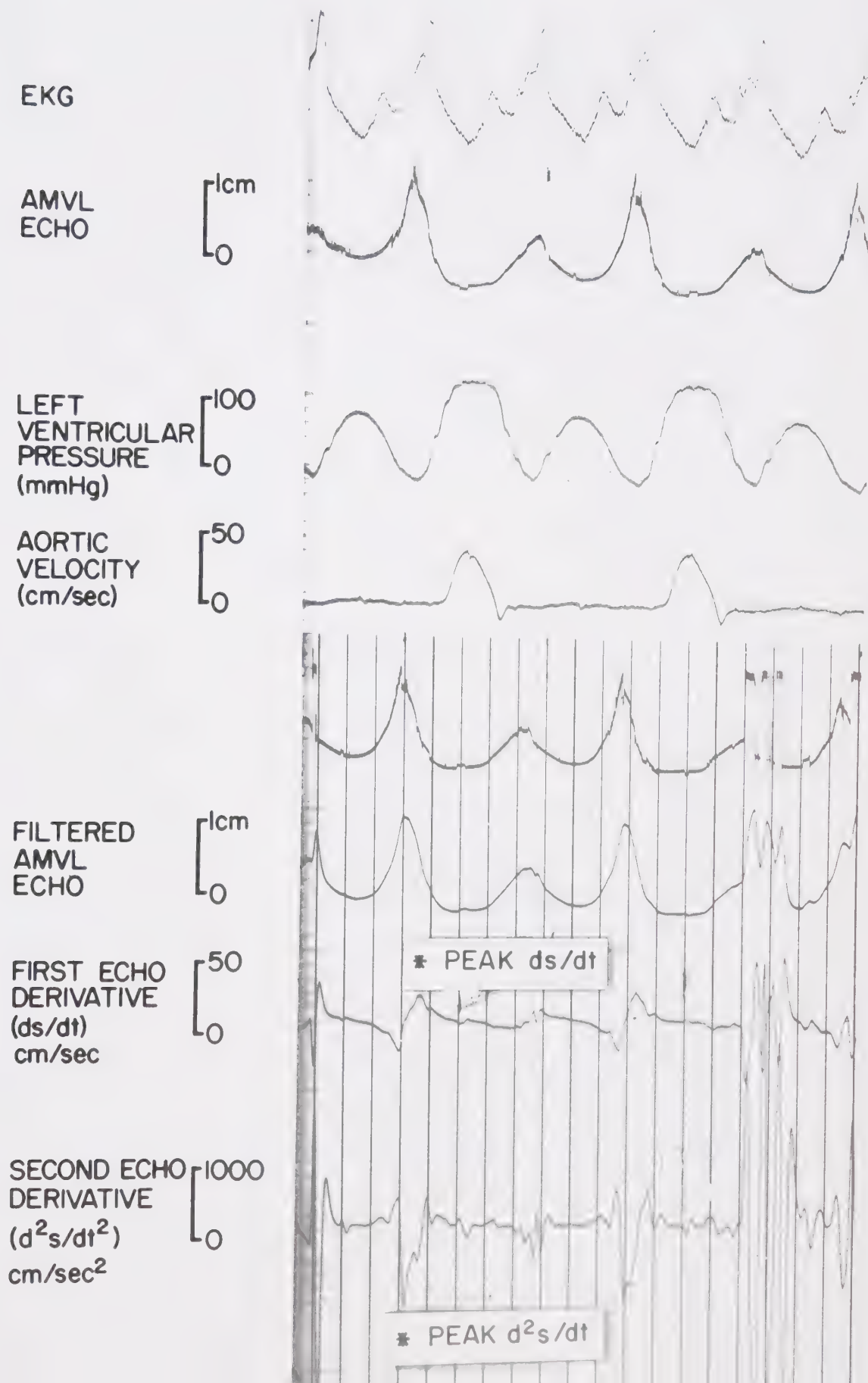


Figure 8: Comparison of AMVL Closure Velocity Obtained
By Manual and Electronic Methods

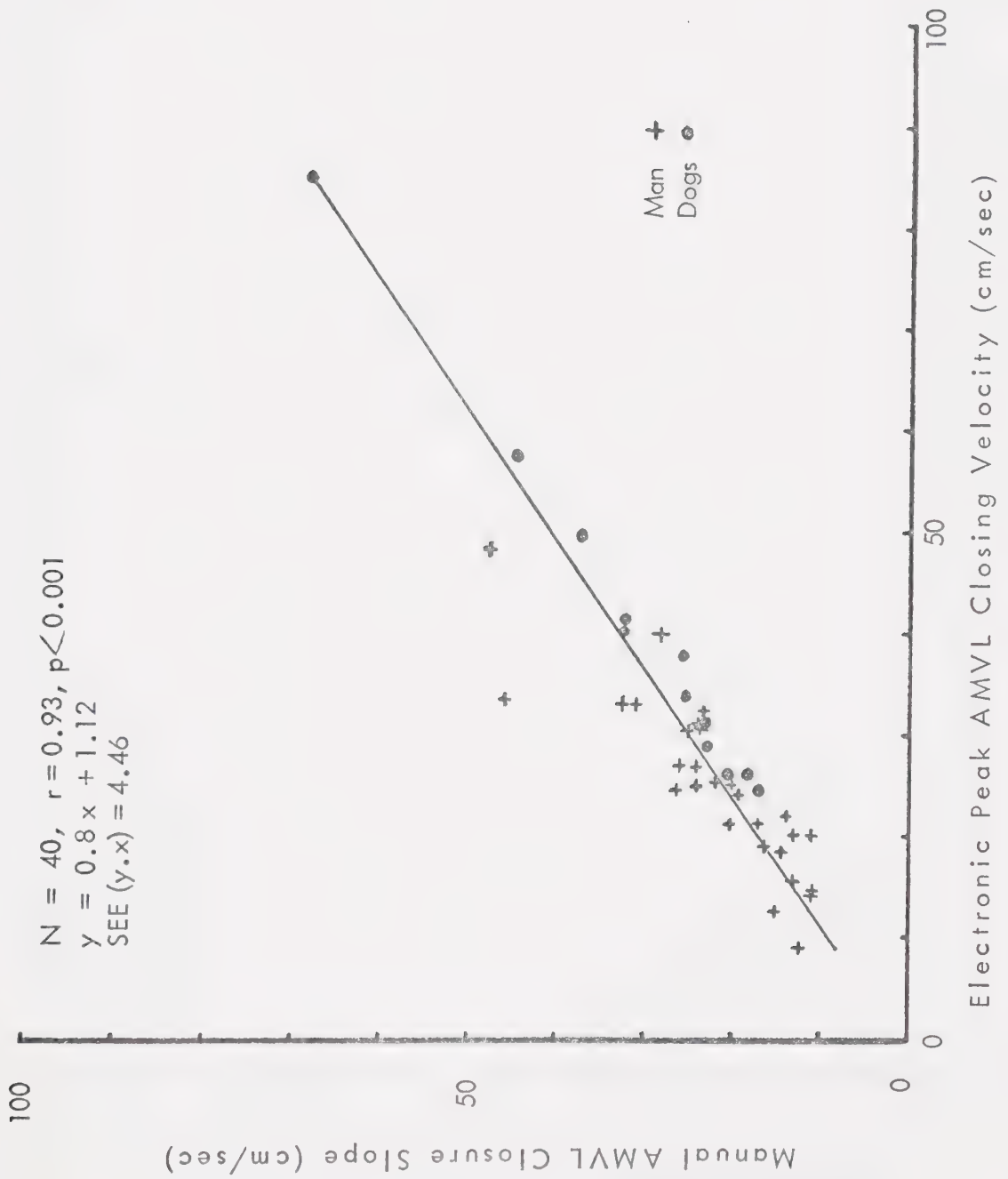


Figure 9: Comparison of Peak Aortic Ejection Velocity Recorded by the Electromagnetic Cuff Versus the Catheter-tip Probes

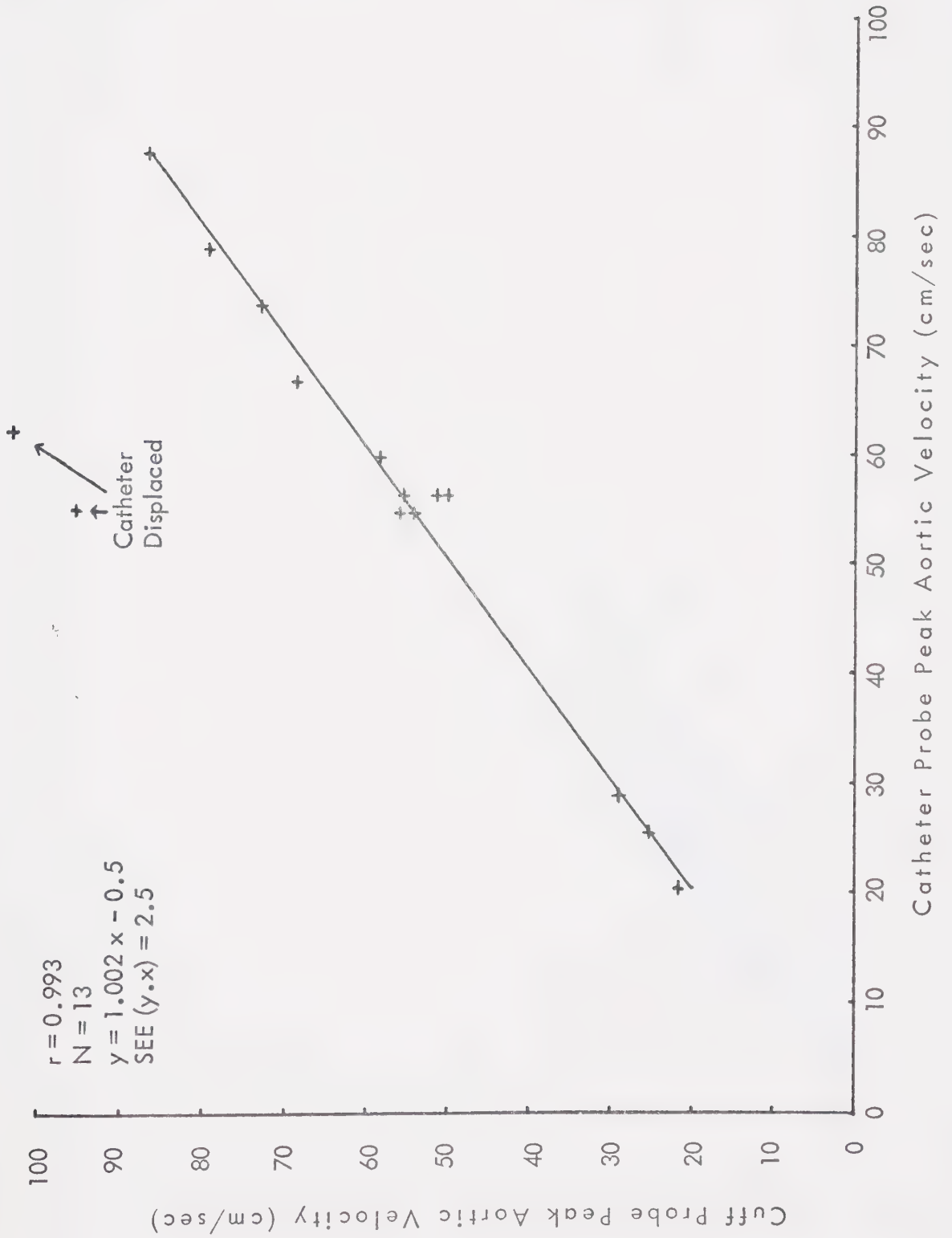


Figure 10: Relation Between Mitral Closing Velocity and Aortic Ejection Velocity in 12 Dogs
(Cuff Probe)

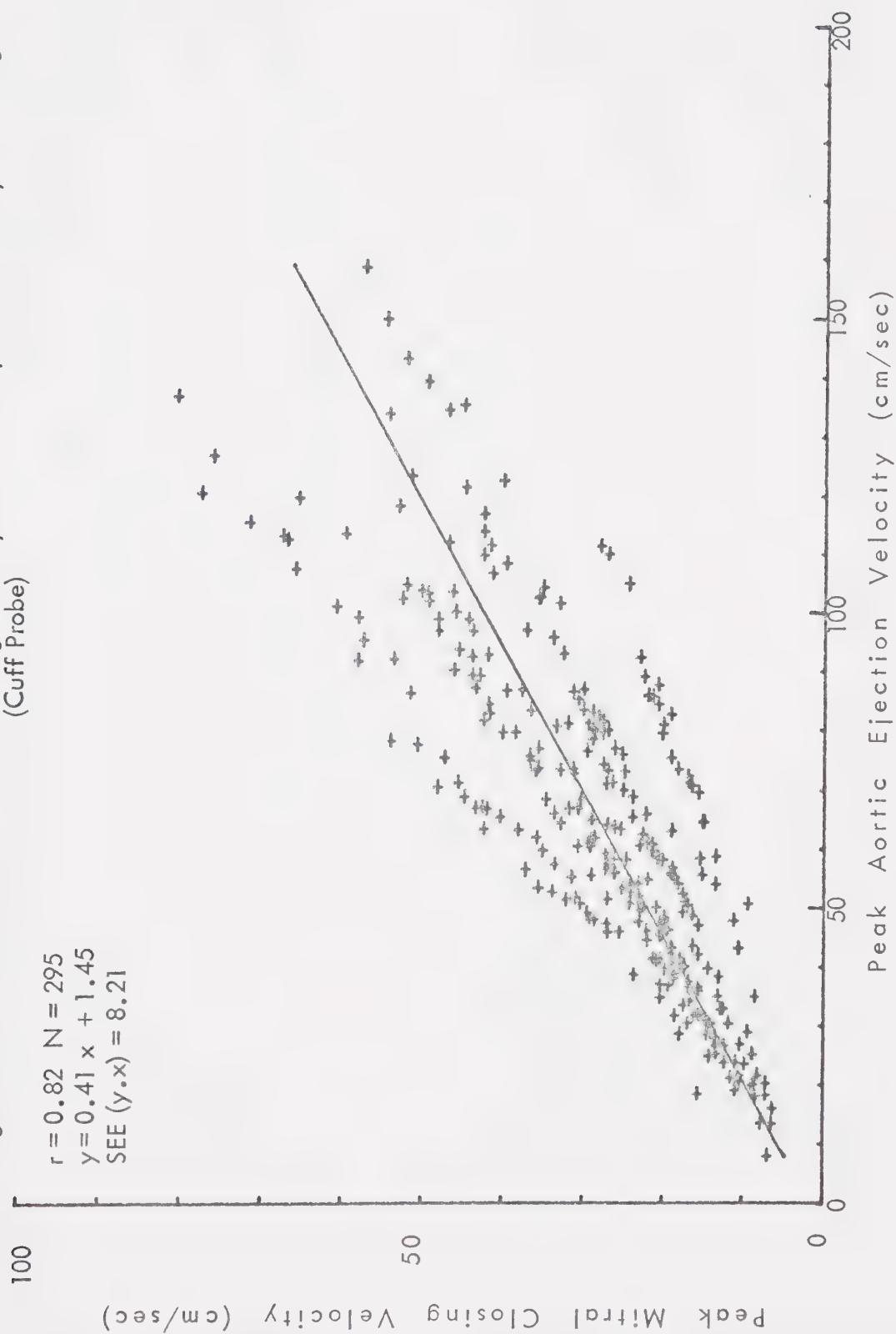


Figure 11: Individual Relationships Between Peak Mitral Closing Velocity and Peak Aortic Ejection Velocity by Cuff Probe in 4 Dogs

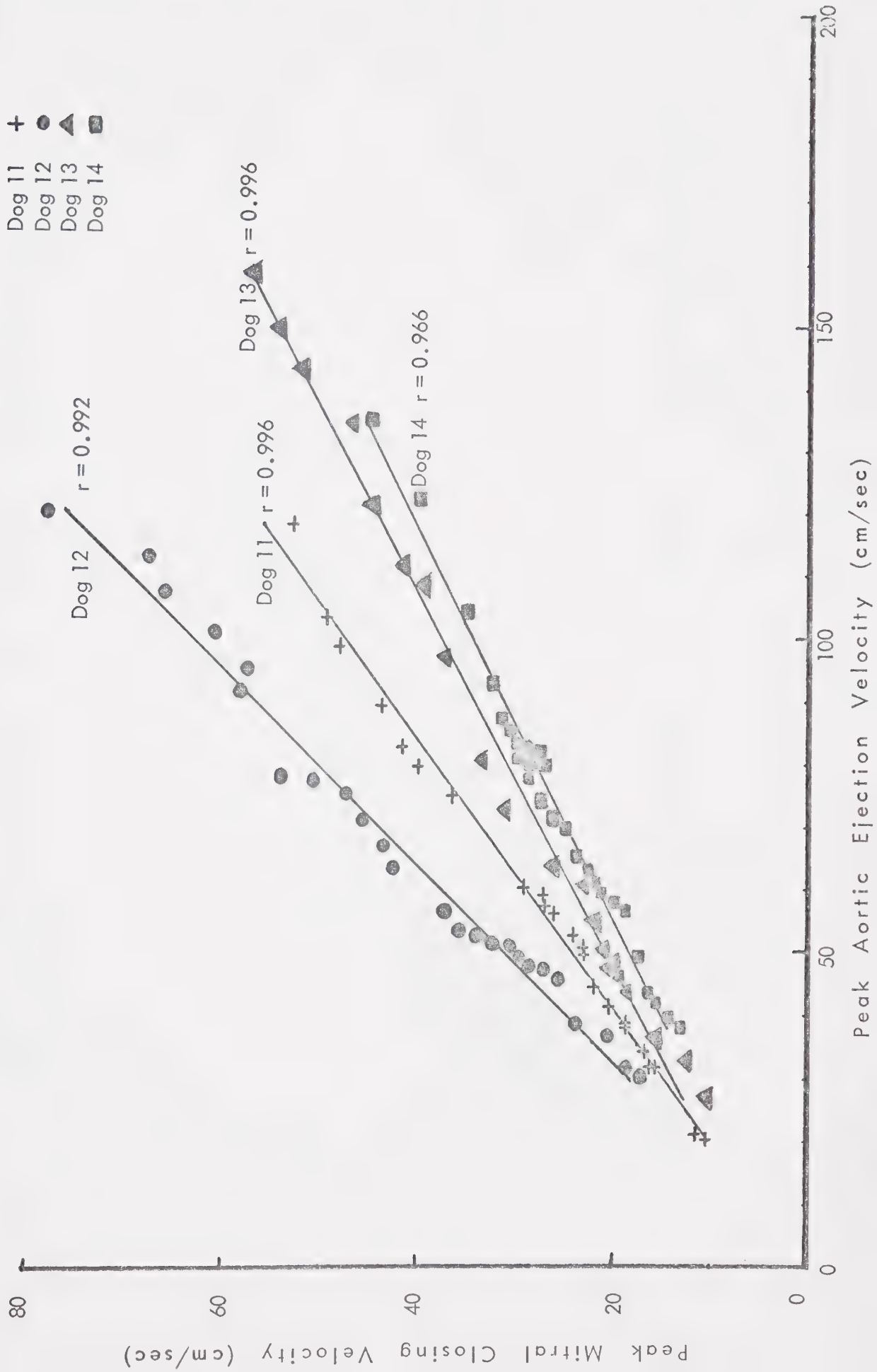


Figure 12: Relation of Peak Mitral Closing Velocity to Peak Aortic Acceleration in 12 Dogs

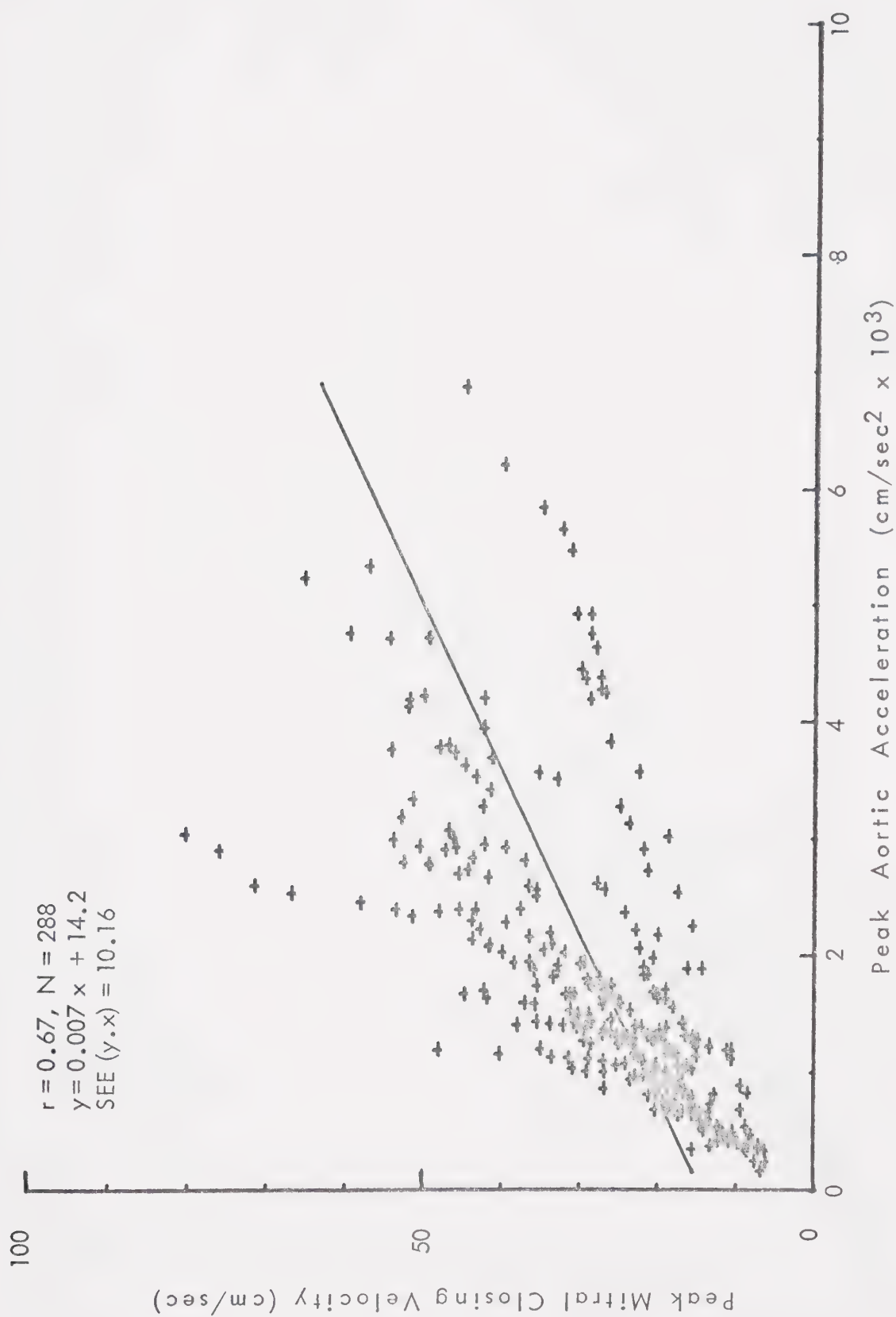


Figure 13: Individual Relationships Between Peak Mitral Closing Acceleration and Peak Aortic Velocity by Cuff Probe in 4 Dogs

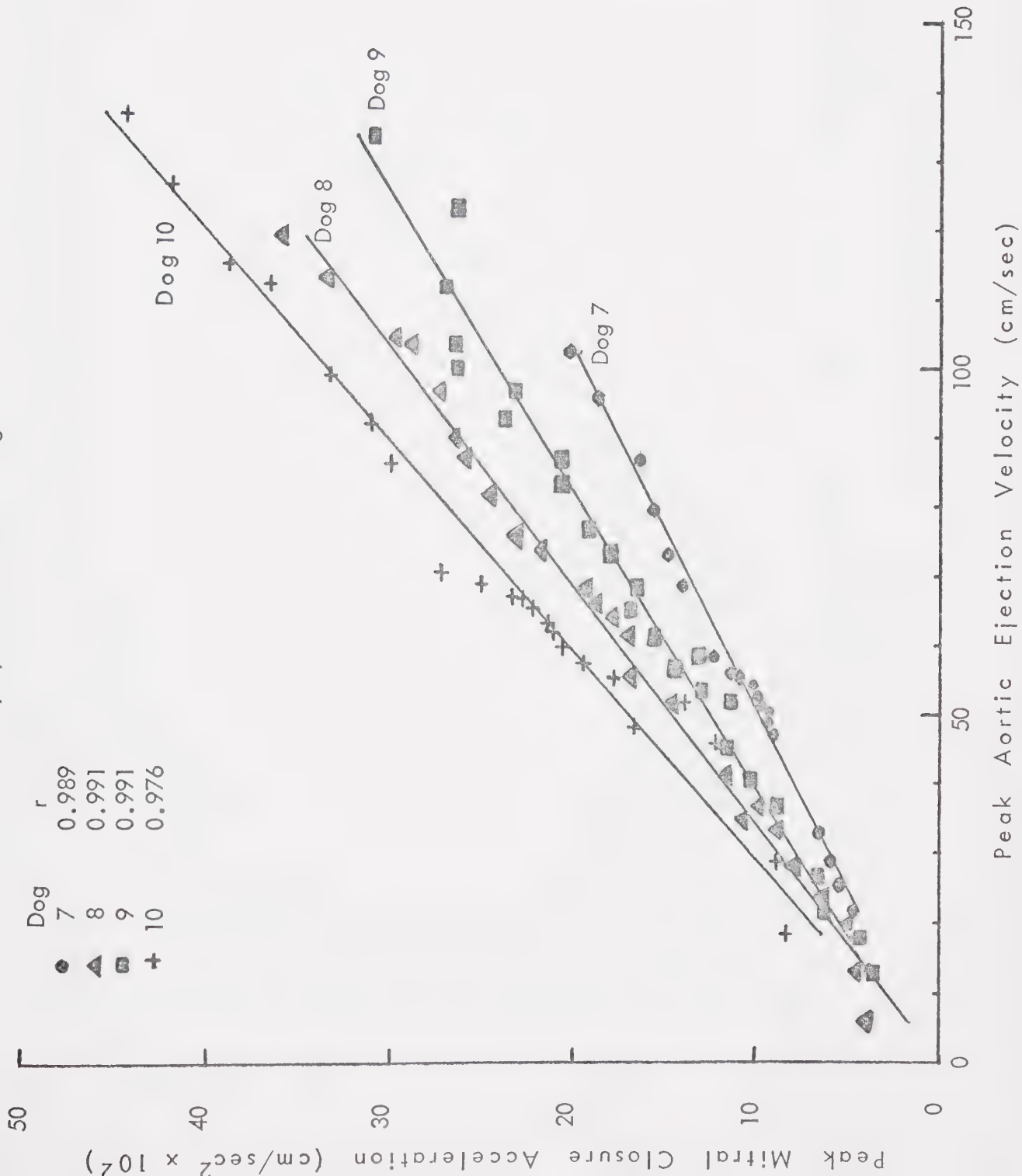


Figure 14: Relation of Peak Mitral Closing Acceleration to Peak Aortic Ejection Velocity by Cuff Probe in 12 Dogs

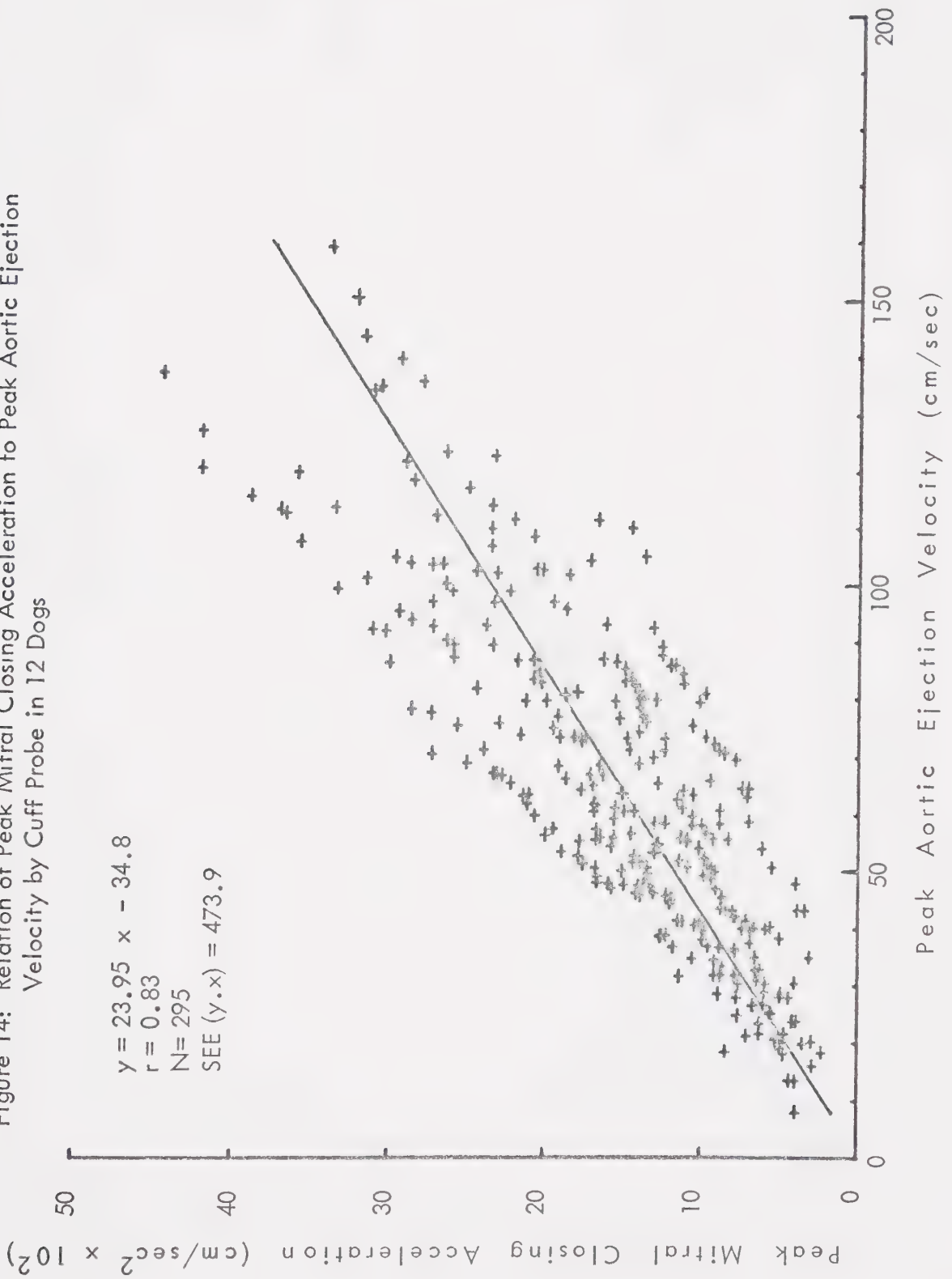


Figure 15: Relation of Peak Mitral Closing Acceleration to Peak Aortic Acceleration in 12 Dogs
With Cuff Probes

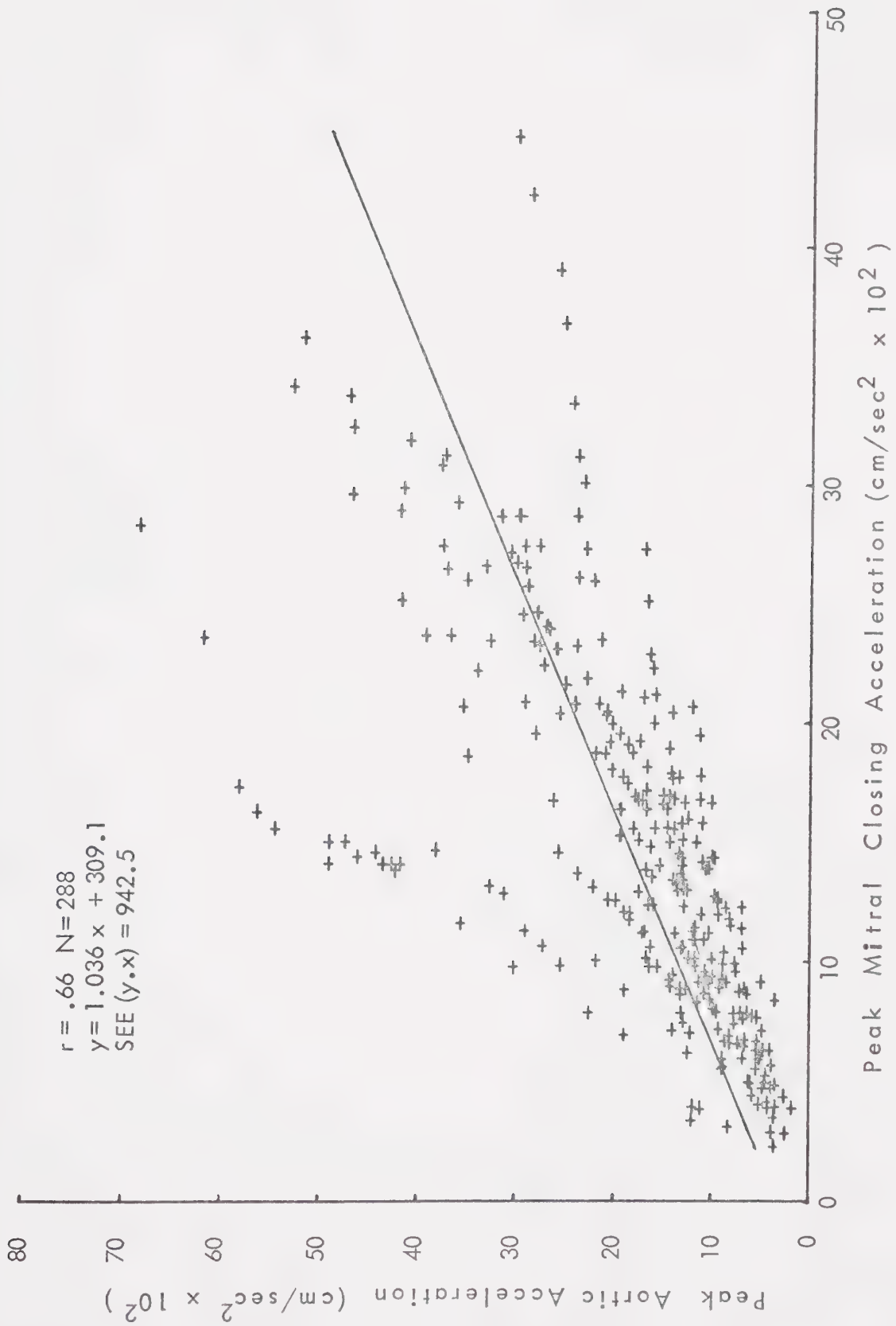


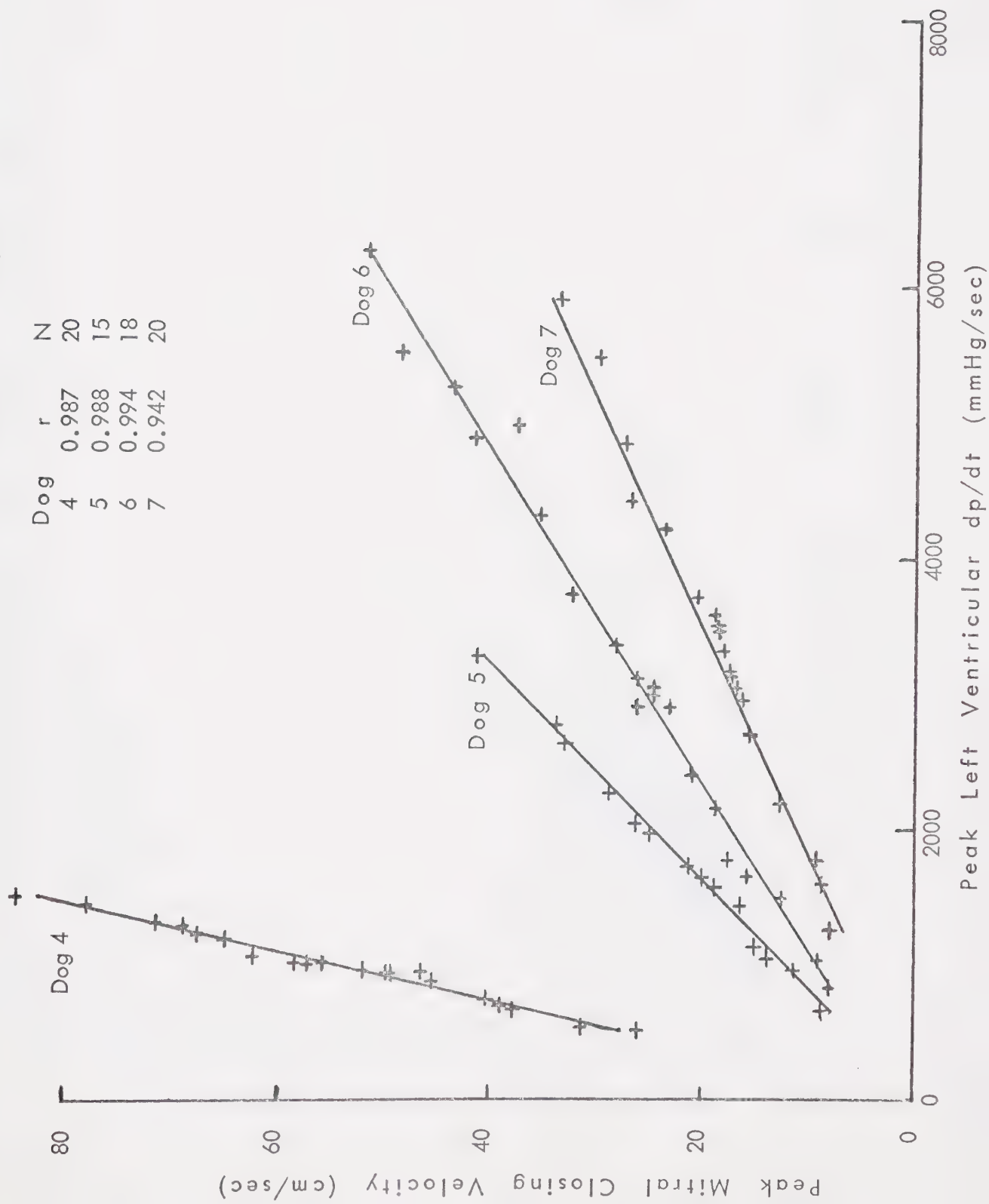
Figure 16: Relation of Peak Mitral Closing Velocity to Peak dp/dt in 4 Separate Dogs

Figure 17: Relation of Peak Mitral Closing Velocity to Peak Left Ventricular dp/dt in 17 Dogs

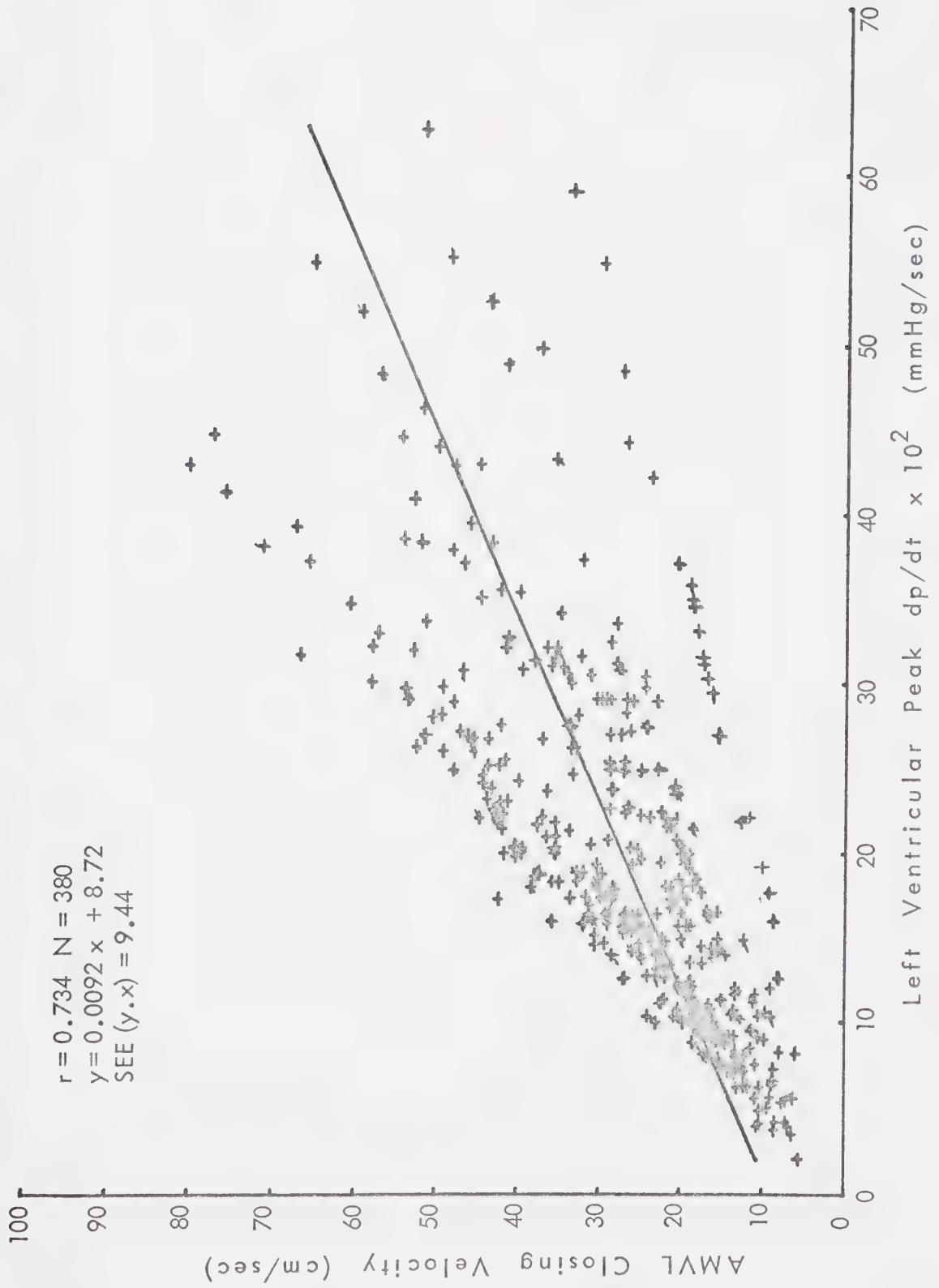


Figure 18: Relation Between Peak Mitral Closing Velocity and Peak d^2p/dt^2 in 12 Dogs

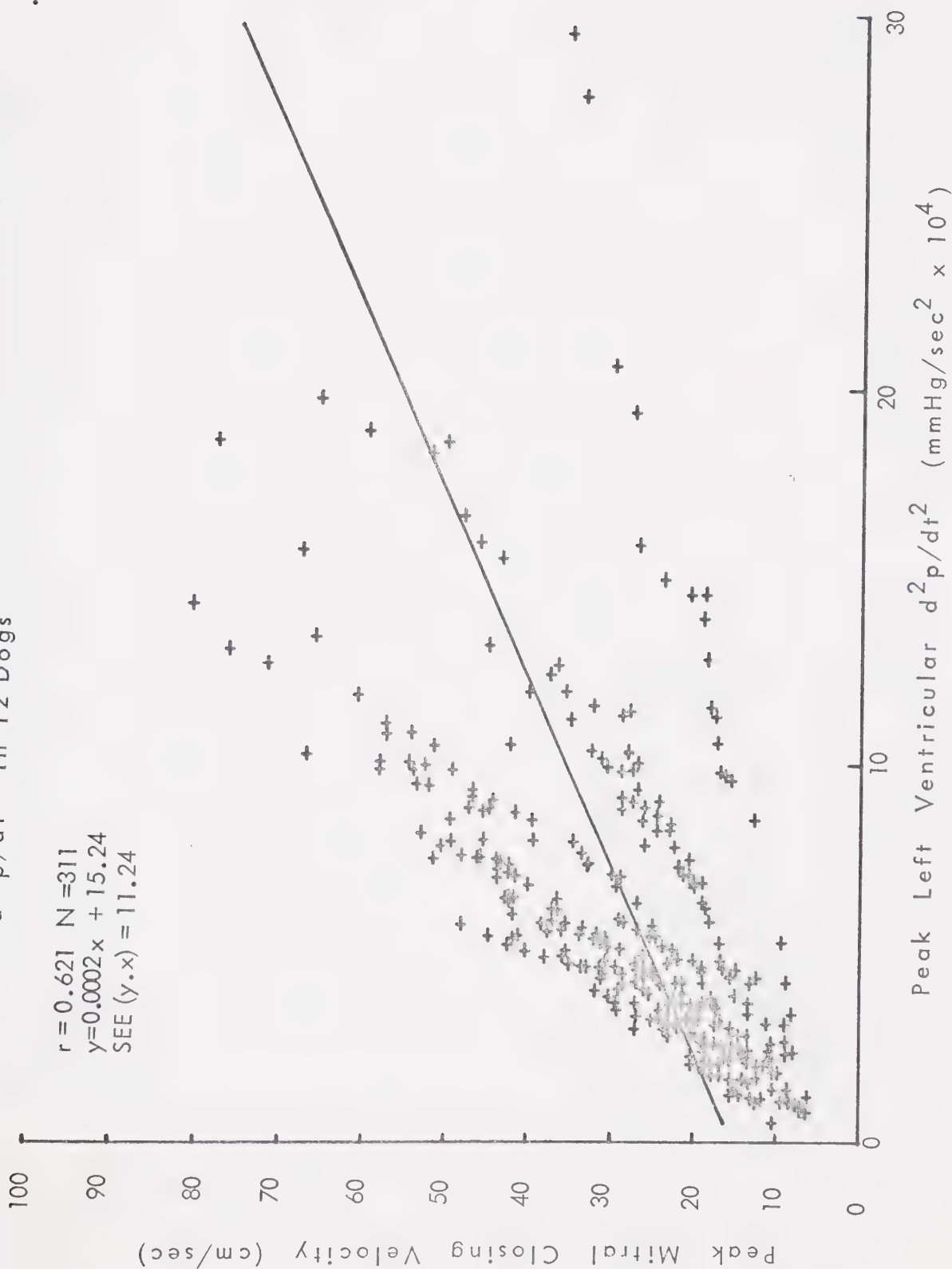


Figure 19: Relation Between Peak Mitral Closing Acceleration and Peak dp/dt in 15 Dogs

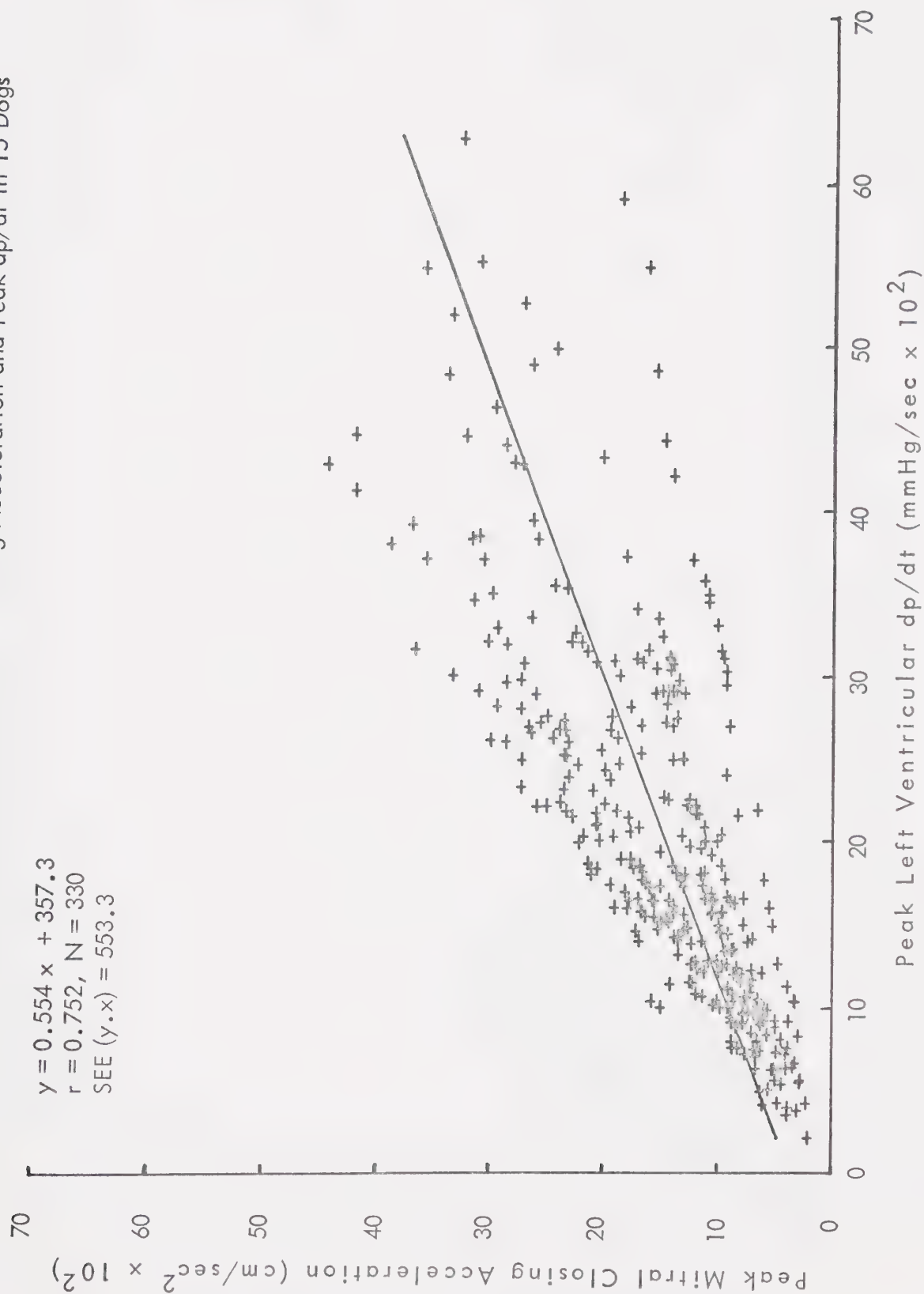


Figure 20: Relation Between Peak Mitral Closing Acceleration and Peak d^2p/dt^2 in 13 Dogs

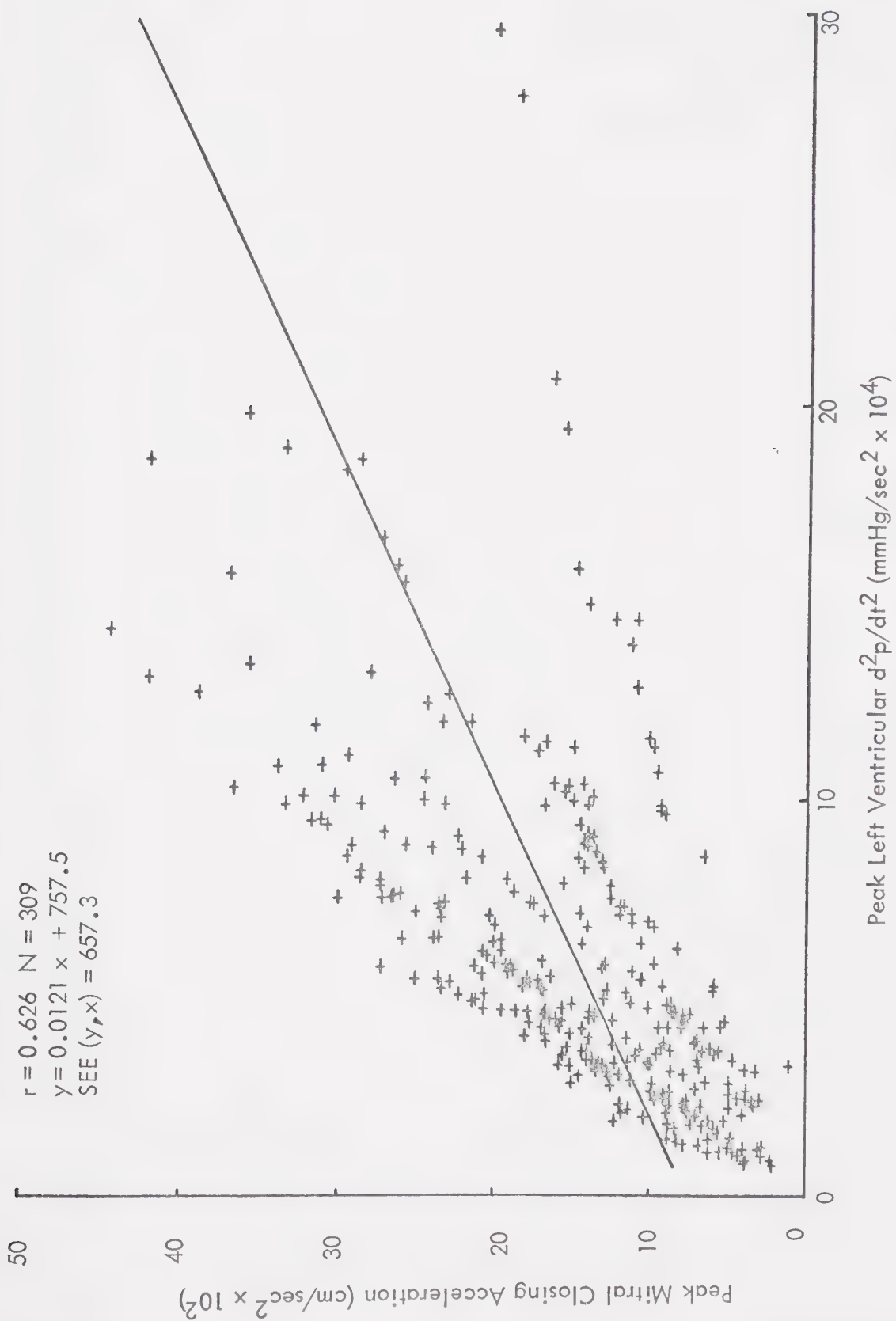


Figure 21: Relation Between Peak Aortic Ejection Velocity and Peak dp/dt in 12 Dogs

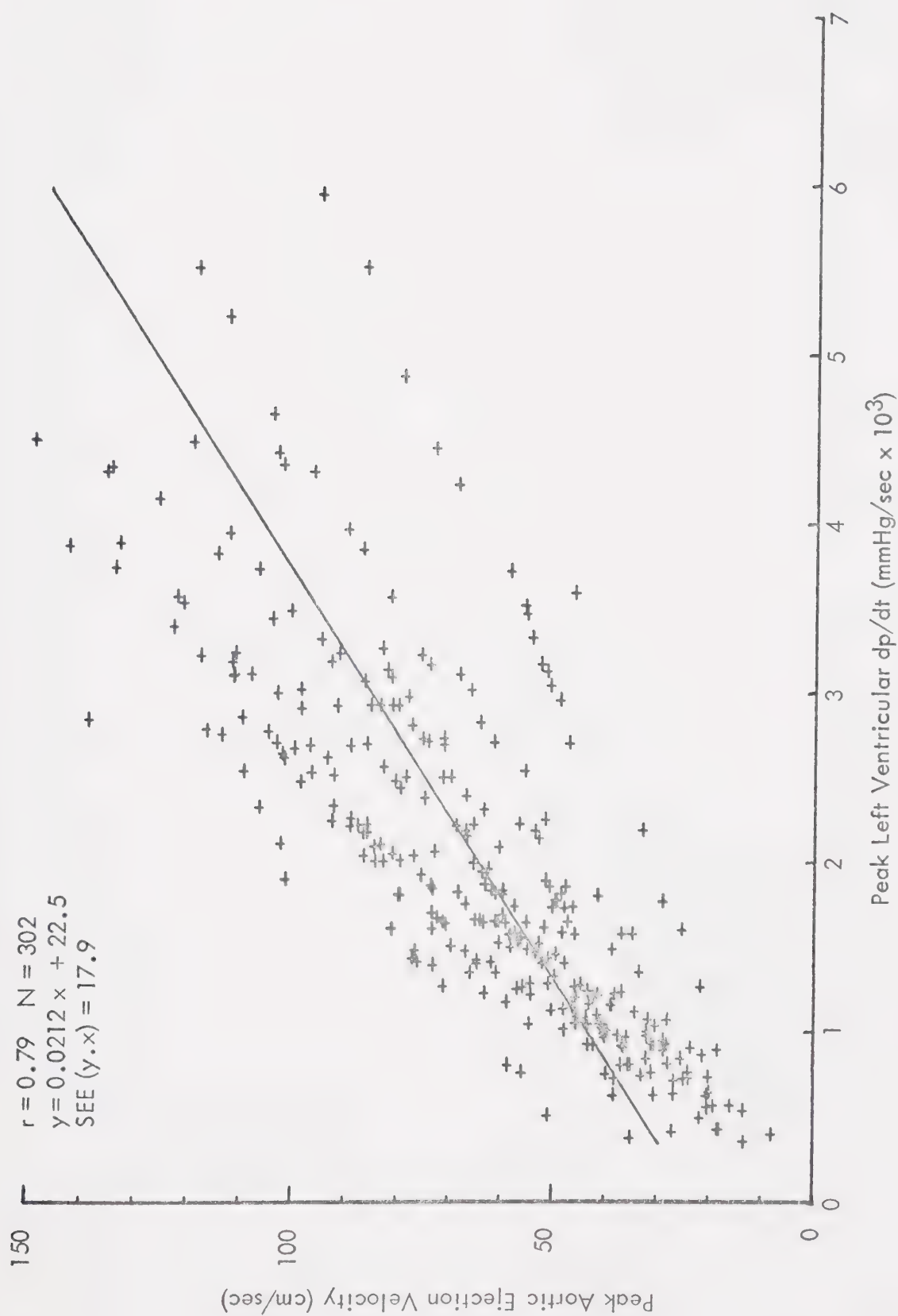


Figure 22: Relation of Peak Aortic Acceleration and Peak dp/dt in 12 Dogs

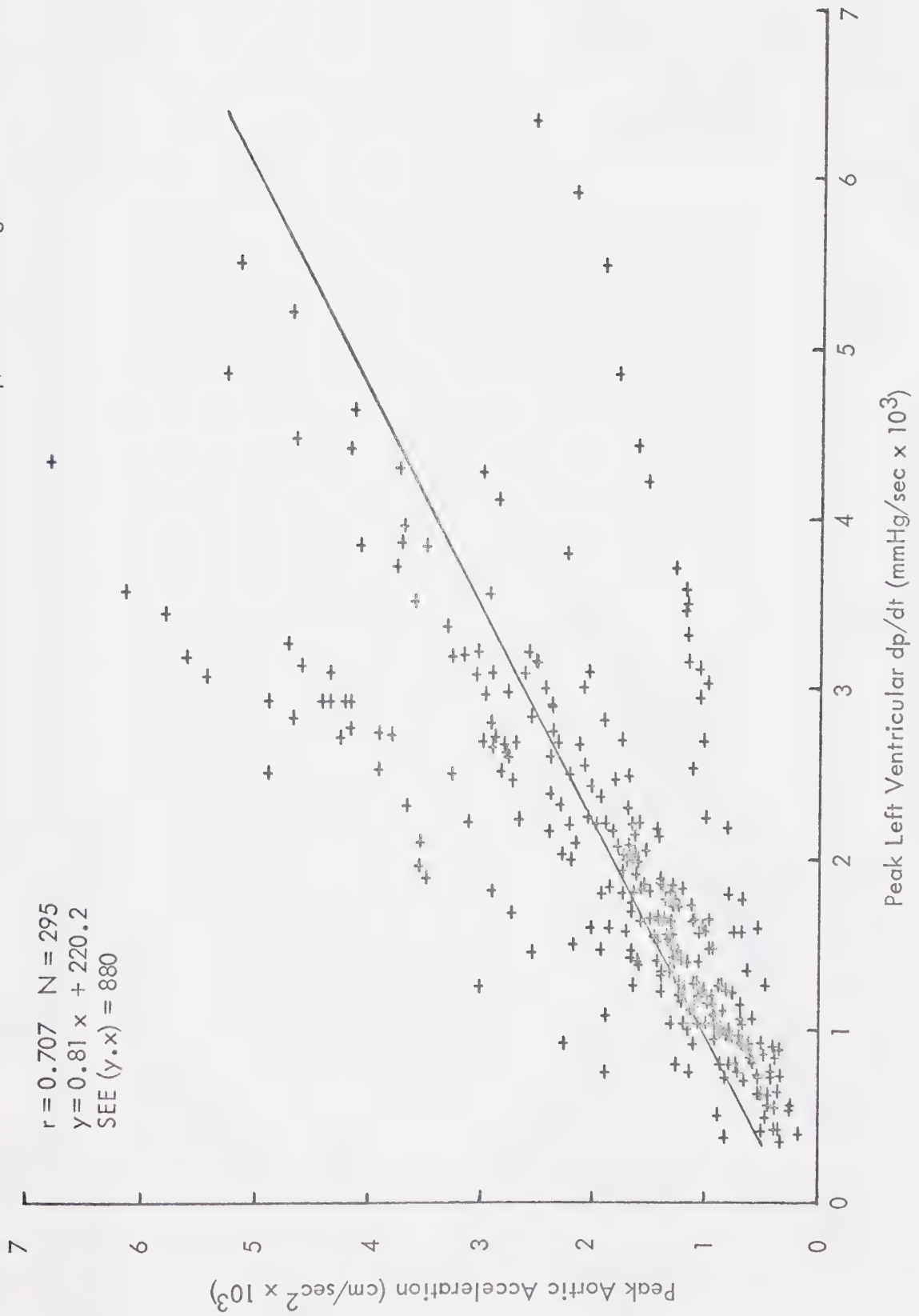


Figure 23: Relation Between Peak Aortic Velocity and Peak Aortic Acceleration in 12 Dogs

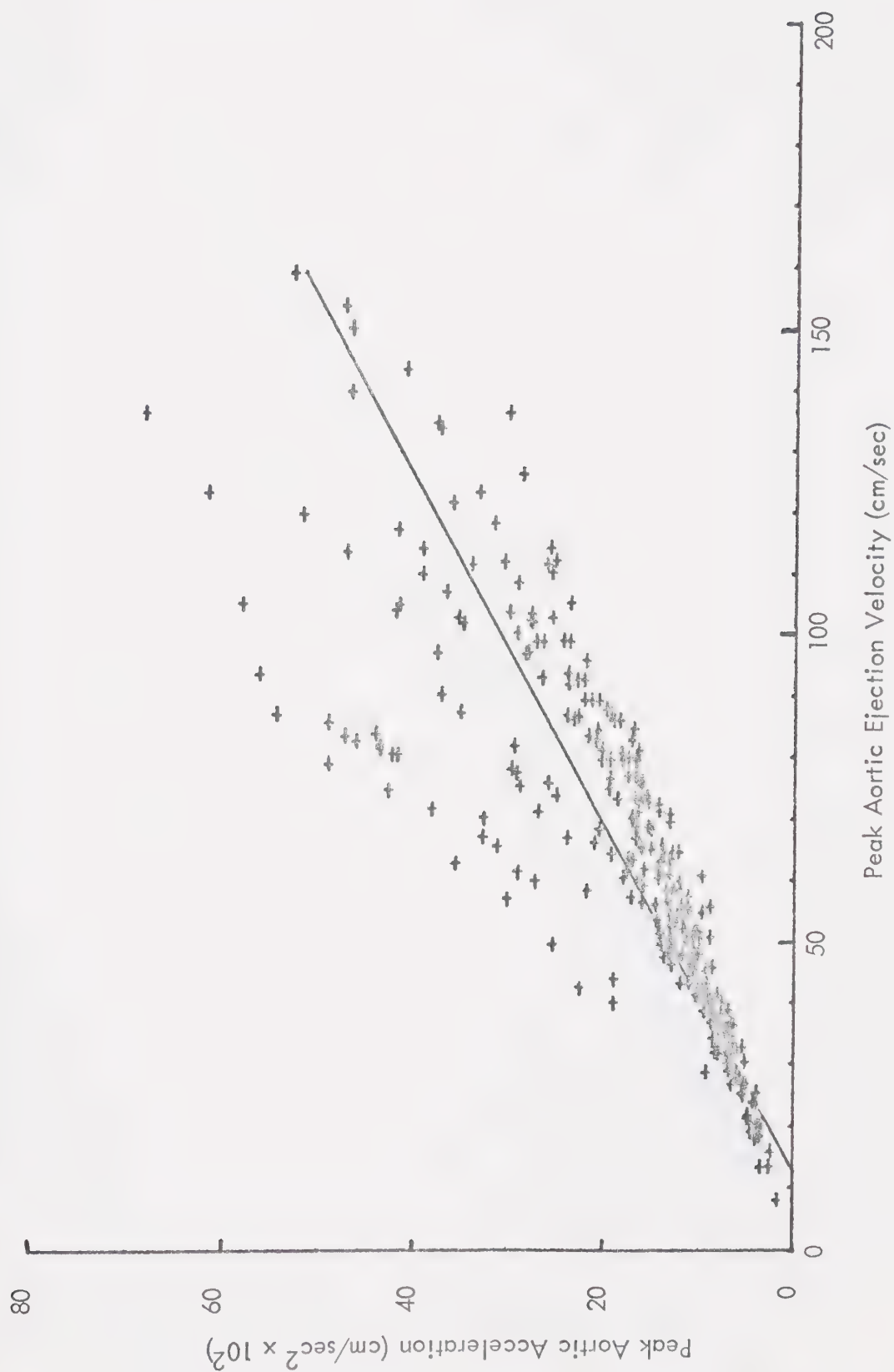


Figure 24: Relation Between Peak dp/dt and Peak d^2p/dt^2 in 12 Dogs

$r = 0.947$ $N = 304$

$y = 37.3 \times - 13859$

$SEE(y.x) = 14085$

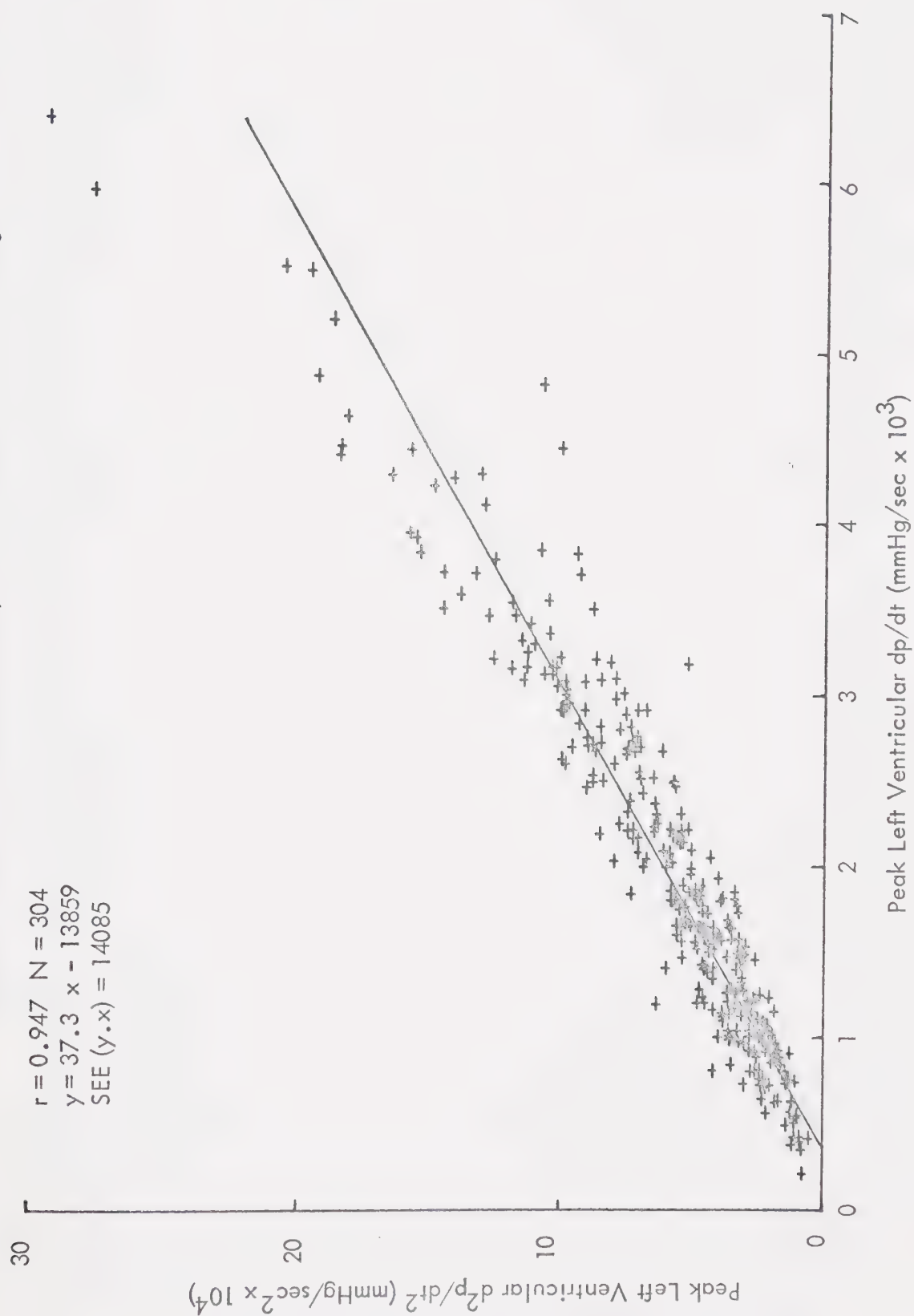


Figure 25: Relation Between Peak Mitral Closing Velocity and Peak Mitral Closing Acceleration in 15 Dogs

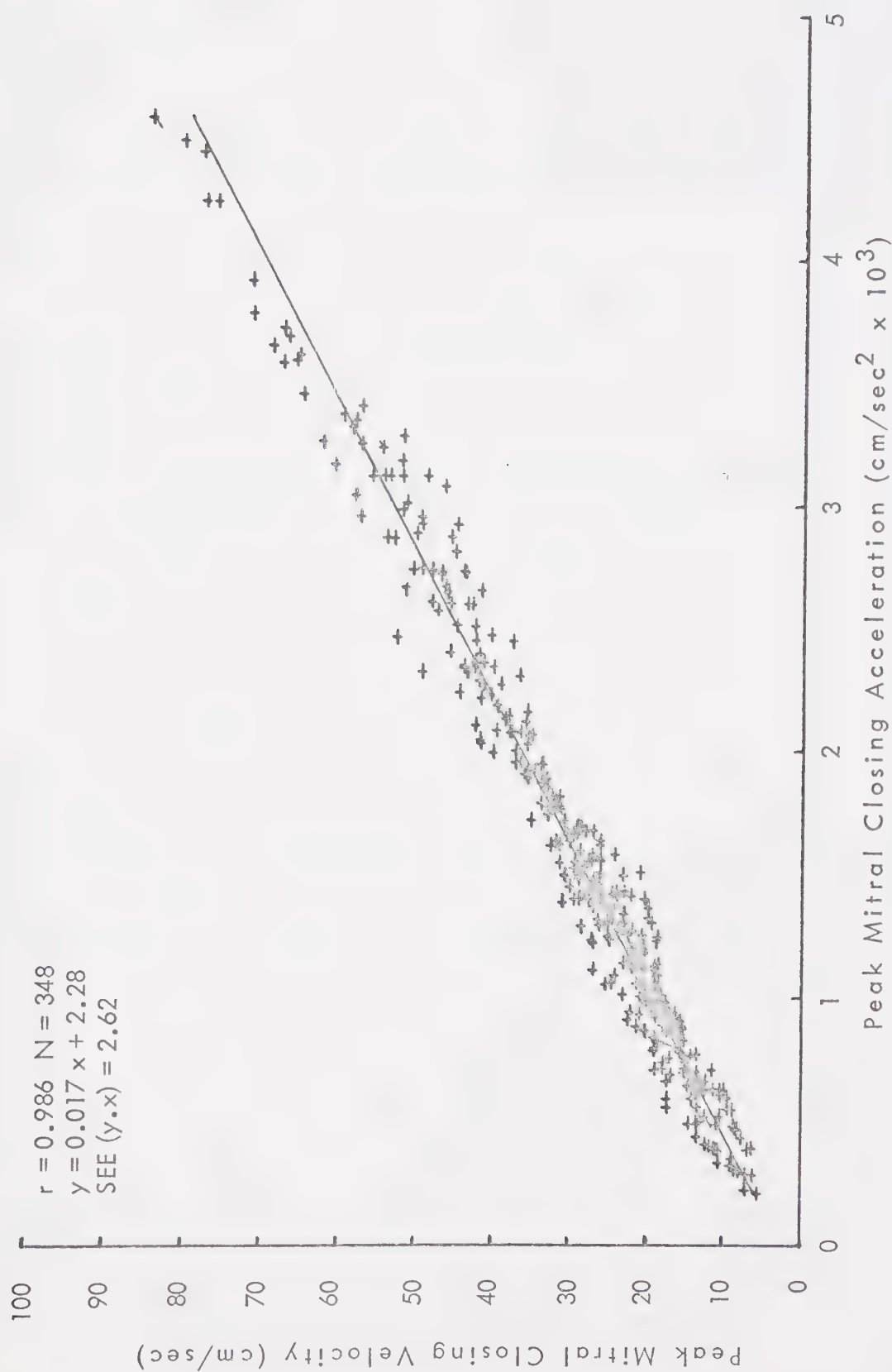


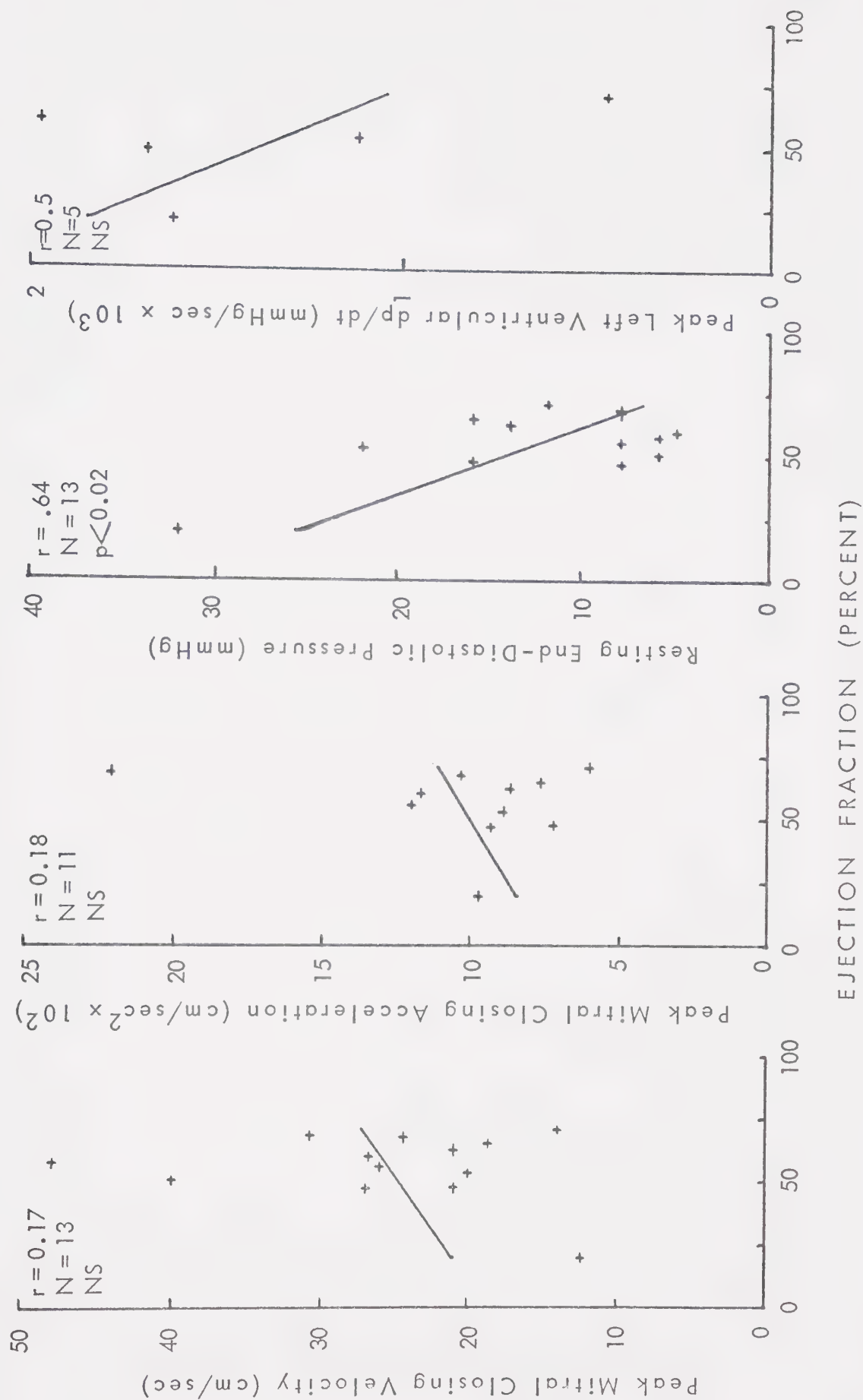
Figure 26: Left Ventricular Ejection Fraction and the Mitral Echo, End-Diastolic Pressure and Peak dp/dt in Man

Figure 27: Relation Between Peak Mitral Closing Velocity and Acceleration to Cardiac Output in Patients With Various Disease States Except Valvular Disease

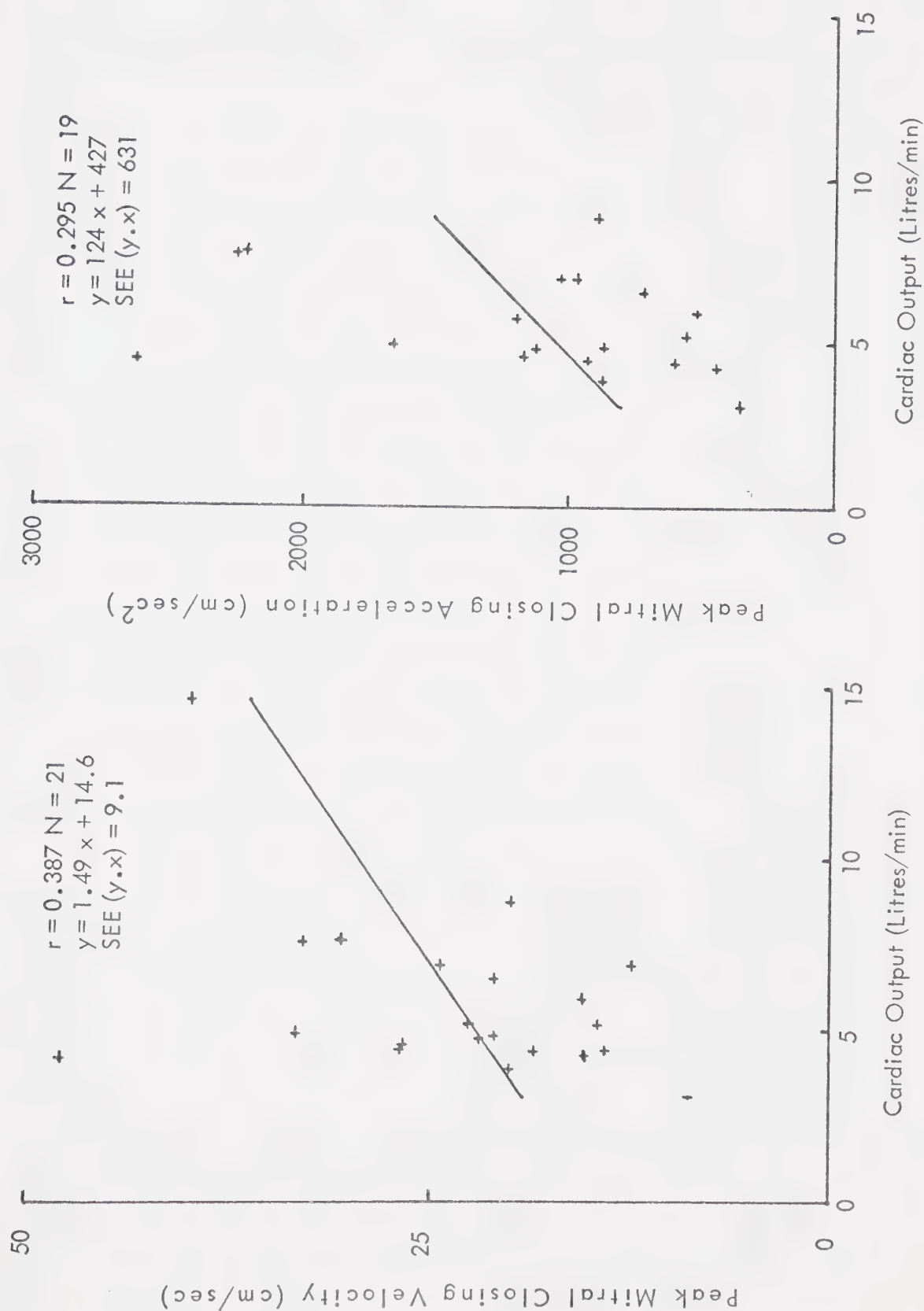
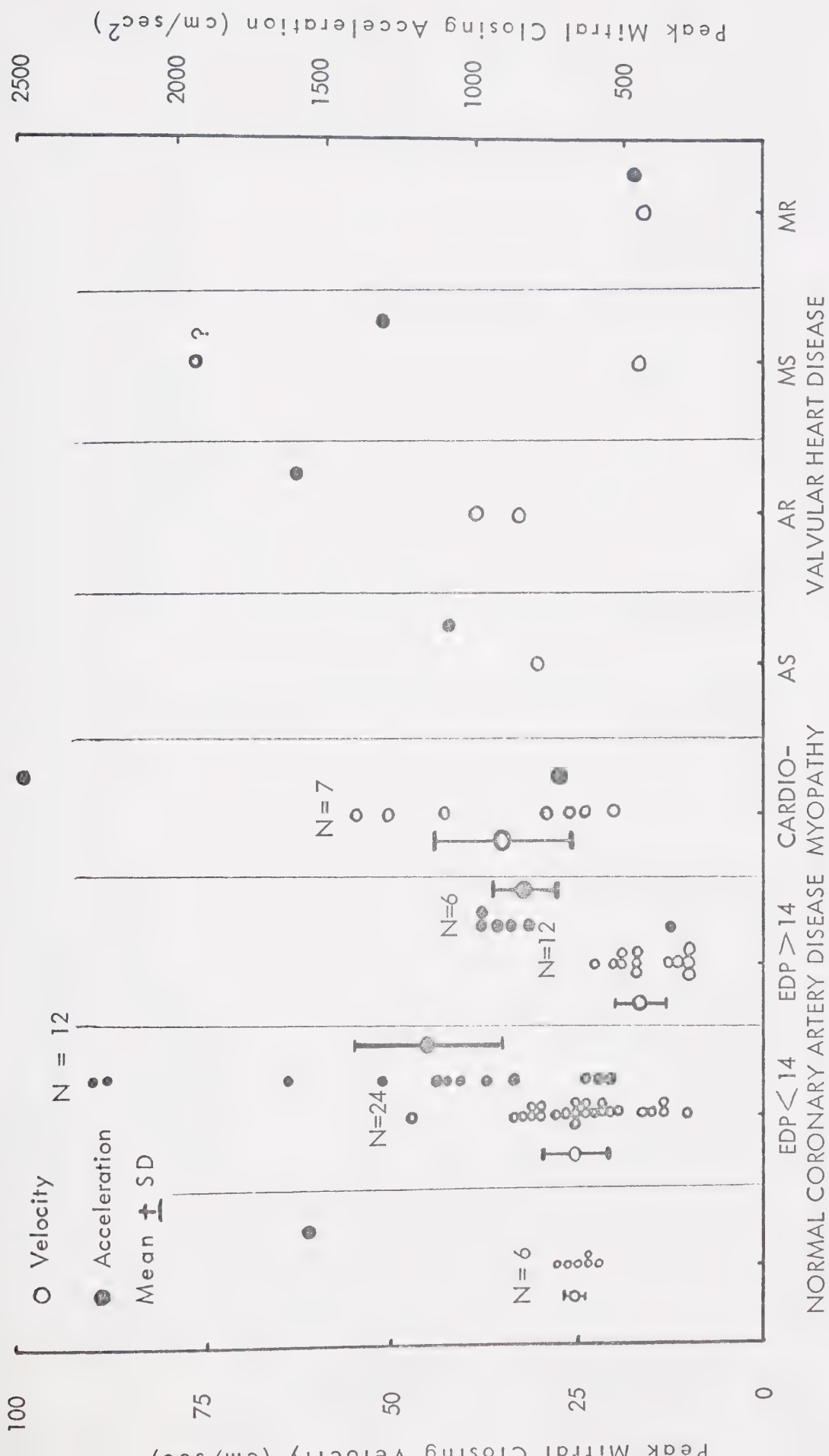


Figure 28: Grouping of Patients by Peak Mitral Closing Velocity and Acceleration and the Underlying Disease



ABBREVIATIONS: AS = Aortic Stenosis; AR = Aortic Regurgitation; EDP = Resting End-Diastolic Pressure (mmHg); MS = Mitral Stenosis; MR = Mitral Regurgitation; ? = Manual AC Slope

Figure 29: Relation Between Peak Mitral Closing Velocity and Acceleration and Resting Left Ventricular End-Diastolic Pressure in Coronary Artery Disease

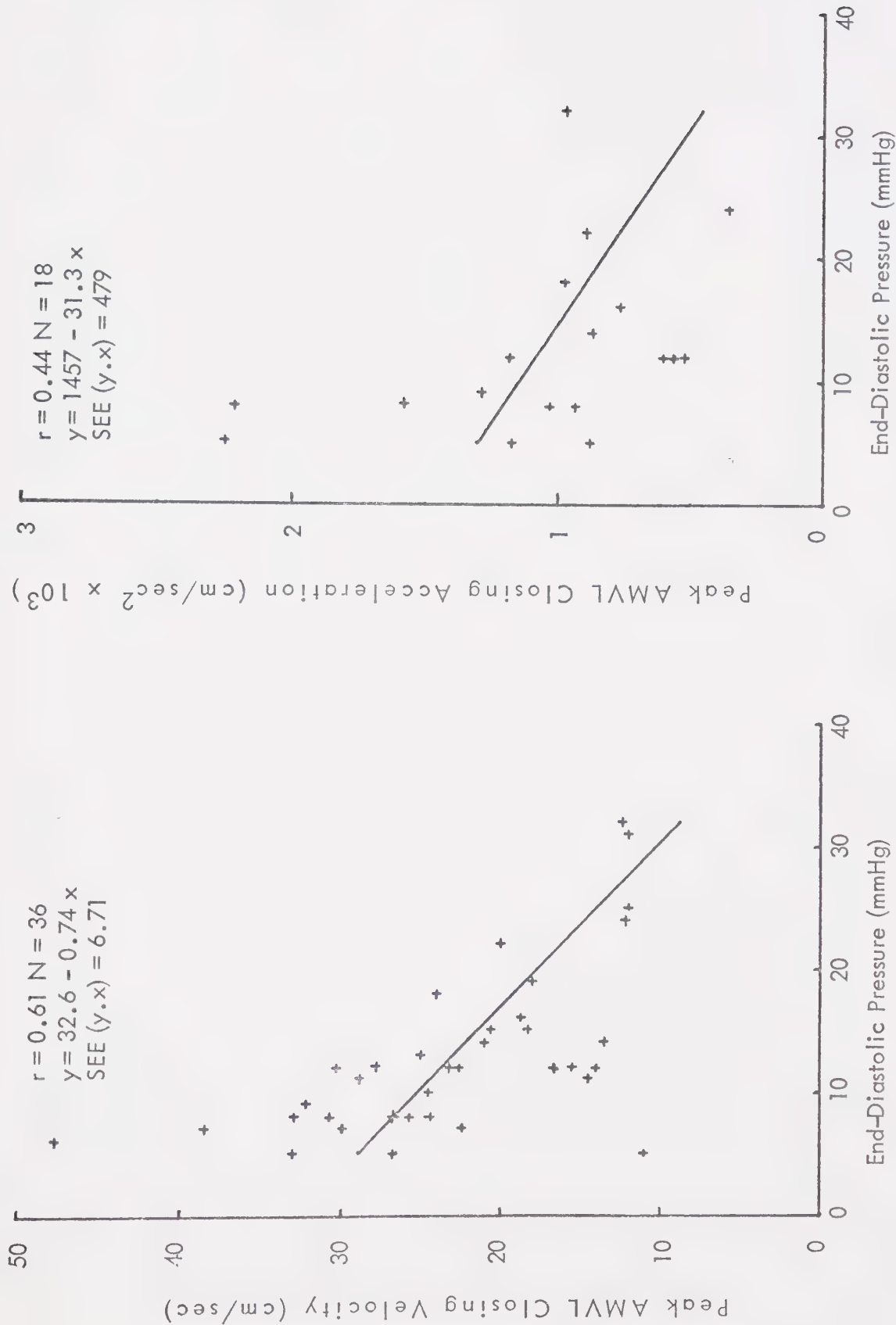


Figure 30: Relation of Peak Mitral Closing Velocity and Acceleration to Peak dp/dt in Man

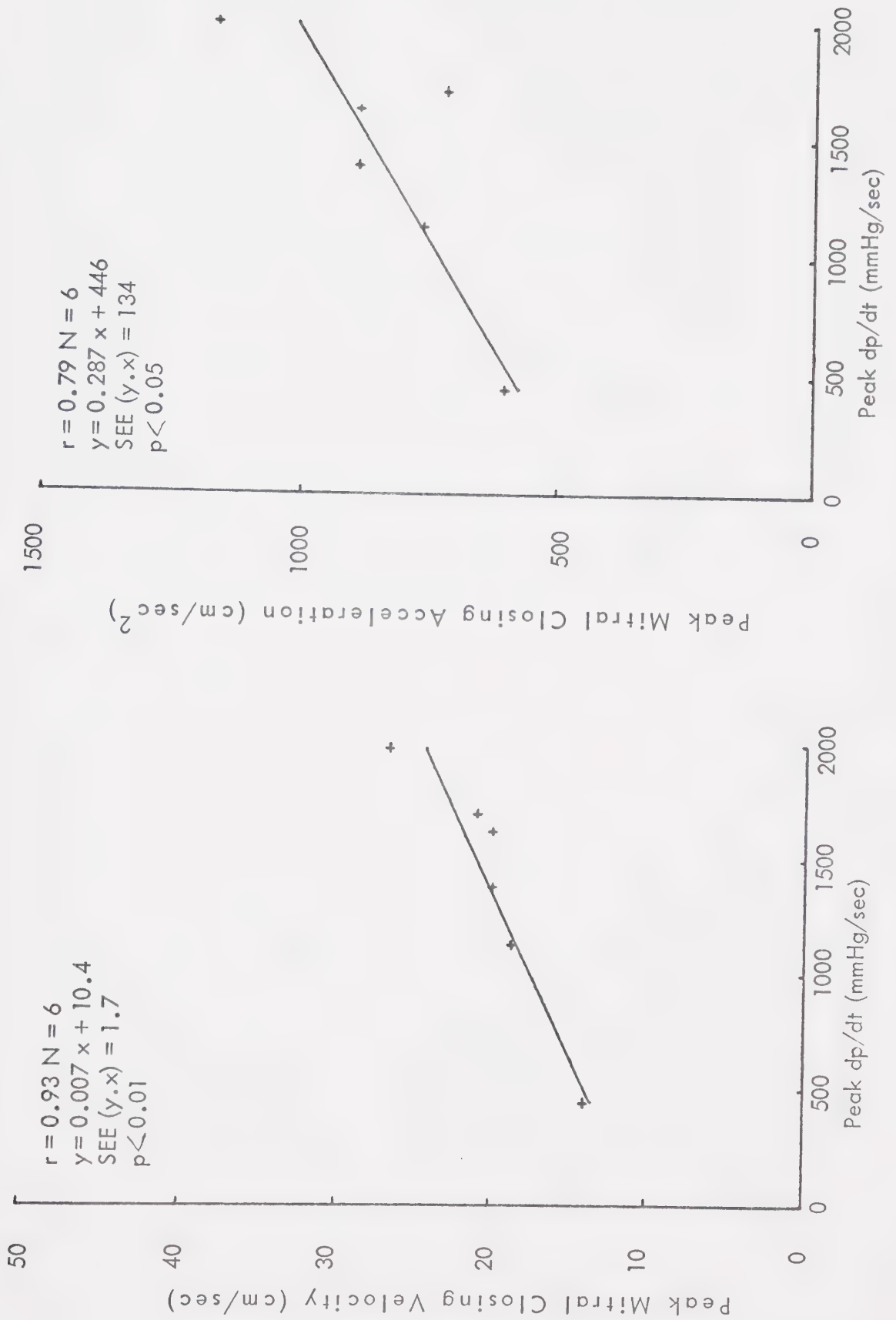
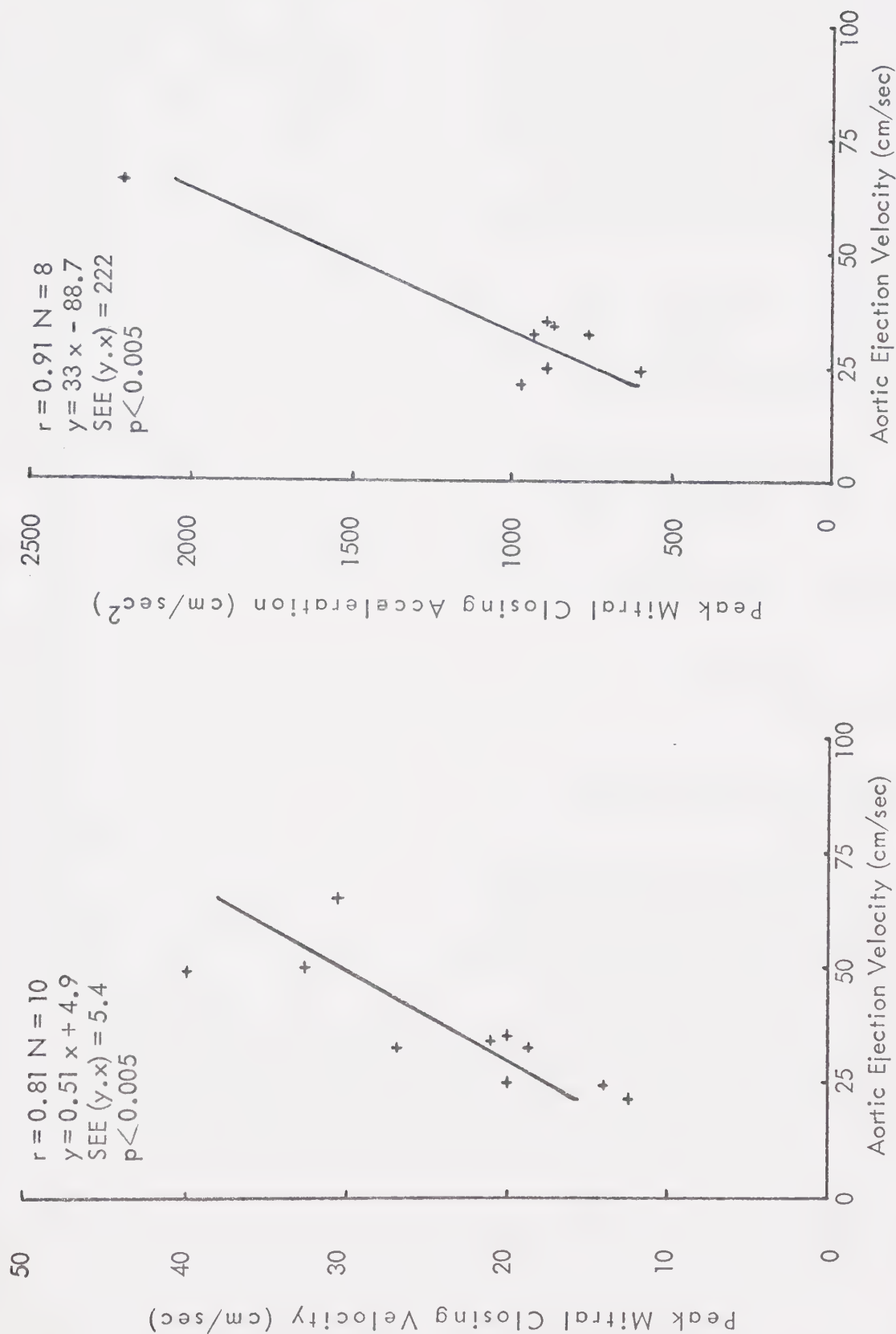


Figure 31: Relation of Peak Mitral Closing Velocity and Acceleration to Peak Aortic Ejection Velocity in Man



REFERENCES

1. Feigenbaum H: Echocardiographic examination of the left ventricle. *Circulation* 51:1, 1975
2. Feigenbaum H, Zaky A, Nasser WK: Use of ultrasound to measure left ventricular stroke volume. *Circulation* 35:1092, 1967
3. Feigenbaum H, Wolfe SB, Popp RL, Haine CL, Dodge HT: Correlation of ultrasound with angiocardiology in measuring left ventricular diastolic volume. *Am J Cardiol* 23:111, 1969
4. Feigenbaum H, Popp RL, Wolfe SB, Troy BL, Pombo JT, Haine CL, Dodge HT: Ultrasound measurements of the left ventricle. A correlative study with angiocardiology. *Arch Intern Med* 129:461, 1972
5. Popp RL, Harrison DC: Ultrasonic cardiac echography for determining stroke volume and valvular regurgitation. *Circulation* 41:493, 1970
6. Feigenbaum H: Clinical applications of echocardiography. *Prog Cardiovasc Dis* 14:531, 1972
7. Pombo JF, Troy BL, Russell RO Jr: Left ventricular volumes and ejection fraction by echocardiography. *Circulation* 43:480, 1971
8. Fortuin NJ, Hood WP Jr, Sherman E, Craige E: Determinations of left ventricular volumes by ultrasound. *Circulation* 44:575, 1971
9. Pombo J, Russell RO, Rackley C, Foster G: Comparison of stroke volume and cardiac output by ultrasound and dye dilution in acute myocardial infarction. *Am J Cardiol* 27:630, 1971
10. Murray JA, Johnston W, Reid JM: Echocardiographic determinations of left ventricular dimensions, volumes and performance. *Am J Cardiol* 30:252, 1972

11. Teicholz LE, Kreulen TH, Herman MV, Gorlin R: Problems in echocardiographic volume determinations (abstr). *Circulation* 46 (Suppl II): II-75, 1972
12. Fortuin NJ, Hood WP, Craig E: Evaluation of left ventricular function by echocardiography. *Circulation* 46:26, 1972
13. Sandler H, Dodge HT: The use of single plane angiocardiology for the calculation of left ventricular volume in man: *Am Heart J* 75:325, 1968
14. Cooper R, Karliner JS, O'Rourke RA, Peterson KL, Leopold GR: Ultrasound determinations of mean fibre-shortening rate in man. *Am J Cardiol* 29:257, 1972
15. Cooper RH, O'Rourke RA, Karliner JS, Peterson KL, Leopold GR: Comparison of ultrasound and cineangiographic measurements of the mean rate of circumferential shortening in man. *Circulation* 46:914, 1972
16. Paraskos JA, Grossman W, Saltz S, Dalen JE, Dexter L: A noninvasive technique for the determinations of velocity of circumferential fibre shortening in man. *Circ Res* 29:610, 1971
17. Ratshin RA, Rackley CE, Russell RO Jr: Quantitative echocardiography: Accuracy of ventricular volume analysis by area-length, linear regression and quadratic regression formulae (abstr). *Am J Cardiol* 35:165, 1975
18. Benzing G, Stockert J, Nave E, Kaplan S: Evaluation of left ventricular performance: Circumferential fibre shortening and tension. *Circulation* 49: 925, 1974
19. Quinones MA, Gaasch WH, Alexander JK: Echocardiographic assessment of left ventricular function: With special reference to normalized velocities. *Circulation* 50:42, 1974

20. Ludbrook P, Karliner JS, Peterson K, Leopold G, O'Rourke RA: Comparison of ultrasound and cineangiographic measurements of left ventricular performance in patients with and without wall motion abnormalities. *Br Heart J* 35:1026, 1973
21. Popp RL, Alderman EL, Brown OR, Harrison DC: Sources of error in calculation of left ventricular volumes by echography. *Am J Cardiol* 31:152, 1973
22. Lalani AV, Lee SJK: Echocardiographic measurement of cardiac output using the mitral valve and aortic root echo. *Circulation* 54:738, 1976
23. Lalani AV: Cardiac output and function by Echo. MSC Thesis 1976. University of Alberta, Edmonton, Canada.
24. Braunwald E, Ross J Jr, Gault JH, Mason DT, Mills C, Gabe IT, Epstein SE: Assessment of cardiac function. *Ann Intern Med* 70:369, 1969
25. Brutsaert DL, Sonnenblick EH: Cardiac muscle mechanics in the evaluation of myocardial contractility and pump function: Problems, concepts and directions. *Prog Cardiovasc Dis* 26:337, 1973
26. Rushmer RF: Summarizing comments. I. The Heart: Muscle and Pump. Proceedings of the third workshop on contractile behavior of the heart. Antwerp. *Europ J Cardiol (Suppl)* 4:169, 1976
27. Noble MIM, Trenchard D, Guz A: Left ventricular ejection in conscious dogs. I. Measurement and significance of the maximum acceleration of blood from the left ventricle. *Circ Res* 19:139, 1966
28. Reitan JA, Smith NT, Kadis B: A non-invasive correlate of ascending aortic blood flow acceleration. *Br J Anaest* 42:87, 1970

29. Jewitt D, Gabe I, Mills C, Maurer B, Thomas M, Shillingford J: Aortic velocity and acceleration measurements in the assessment of coronary heart disease. *Europ J Cardiol* 1:299, 1974
30. Bennett ED, Else W, Miller GAH, Sutton GC, Miller HD, Noble MM: Maximum acceleration of blood from the left ventricle in patients with ischemic heart disease. *Clin Sci Mol Med* 46:49, 1974
31. Chung DCW, Chamberlain JH, Seed RGFL: The effect of hemodynamic changes on maximum blood flow acceleration at the aortic root in the anaesthetized, open-chest dog. *Cardiovasc Res* 8:362, 1974
32. Gross G, Light LH: Non-invasive intrathoracic blood velocity measurement in the assessment of cardiovascular function. *Biomed Engin* 9:464, 1974
33. Kolettis M, Jenkins BS, Webb-Peploe MM: Assessment of left ventricular function indices derived from aortic flow velocity. *Br Heart J* 38:18, 1976
34. Abbott BC, Mommaerts WF HM: A study of inotropic mechanisms in the papillary muscle preparation. *J Gen Physiol* 42:533, 1959
35. Sonnenblick EH: Force-velocity relations in mammalian heart muscle. *Am J Physiol* 202: 931, 1962
36. Sonnenblick EH, Parmley WW, Urschel CW: The contractile state of the heart as expressed by force velocity relations: *Am J Cardiol* 23:488, 1969
37. Hill AV: The heat of shortening and the dynamic constants of muscle. *Proc Roy Soc London* 126:136, 1938

38. Braunwald E, Ross J Jr, Sonnenblick EH: Mechanisms of contraction of the normal and failing heart. Boston, Little Brown and Co, 1968, p.205
39. Ross J Jr, Covell JW, Sonnenblick EH, Braunwald E: Contractile state of the heart characterized by force-velocity relations in variably afterloaded and isovolumic beats. *Circ Res* 18: 149, 1966
40. Glick G, Sonnenblick EH, Braunwald E: Myocardial force-velocity relations studied in intact unanaesthetized man. *J Clin Invest* 44:478, 1965
41. Burns JW, Covell JW, Ross J Jr: Mechanics of isotonic left ventricular contraction. *Am J Physiol* 224:725, 1973
42. Peterson KL, Skloven D, Ludbrook P, Uther JB, Ross J Jr: Comparison of isovolumic and ejection phase indices of myocardial performance in man. *Circulation* 49:1088, 1974
43. Gault JH, Ross J Jr, Braunwald E: Contractile state of the left ventricle in man. Instantaneous tension-velocity-length relations in patients with and without disease of the left ventricular myocardium. *Circ Res* 22:451, 1968
44. Gleason WL, Braunwald E: Studies on the first derivative of the ventricular pressure pulse in man. *J Clin Invest* 41:80, 1962
45. Wallace AG, Skinner NS Jr, Mitchell JH: Hemodynamic determinants of the maximal rate of rise of left ventricular pressure. *Am J Physiol* 205:30, 1963
46. Mason DT, Sonnenblick EH, Ross J Jr, Covell JW, Braunwald E: Time to peak dp/dt : A useful measurement for evaluating the contractile state of the human heart (abstr). *Circulation* 32 (Suppl II): II-145, 1965

47. Mason DT, Sonnenblick EH, Covell JW, Ross J Jr, Braunwald E: Assessment of myocardial contractility in man: Relationship between the rate of pressure rise and developed pressure throughout isometric left ventricular contraction (abstr). *Circulation* 36 (Suppl II): II-183, 1967
48. Mason DT: Usefulness and limitations of the rate of rise of intraventricular pressure (dp/dt) in the evolution of myocardial contractility in man. *Am J Cardiol* 23: 516, 1969
49. Letac B, Cannon R, Hood WB, Lown B: Measurement of the second derivative of left ventricular pressure using a fiberoptic catheter. *Proc Soc Exper Biol Med* 127: 63, 1968
50. Nejad NS, Klein MD, Mirsky I, Lown B: Assessment of myocardial contractility from ventricular pressure recordings. *Cardiovasc Res* 5: 15, 1971
51. Veragut UP, Krayenbühl HP : Estimation and quantification of myocardial contractility in the closed-chest dog. *Cardiologia* 47:96, 1965
52. Covell JW, Taylor RR, Ross J Jr: Series elasticity in the intact left ventricle determined by a quick release technique (abst). *Fed Proc* 26:382, 1967
53. Covell JW, Ross J Jr, Sonnenblick EH, Braunwald E: Comparison of force-velocity relation and ventricular function curve as measures of contractile state of the intact heart. *Circ Res* 19:364, 1966
54. Gersh BJ, Hahn CE, Prys-Roberts C: Physical criteria for measurement of left ventricular pressure and its first derivative. *Cardiovasc Res* 5:32, 1971
55. Krayenbühl HP, Rutishauser W, Wirz P, Amende I, Mehmel H: High fidelity left ventricular pressure measurements for the assessment of cardiac contractility in man. *Am J Cardiol* 31: 415, 1973

56. Mason T, Spann JF Jr, Zelis R: Quantification of the contractile state of the intact human heart. *Am J Cardiol* 26:248, 1970
57. Hugenholtz PG, Ellison RC, Urschel CW, Mirsky I, Sonnenblick EH: Myocardial force-velocity relationships in clinical heart disease. *Circulation* 41:191, 1970
58. Beck W, Schrire V: Commentary. *Am J Cardiol* 30:188, 1972
59. Noble MIM: Problems concerning the application of concepts of muscle mechanics to the determination of the contractile state of the heart. *Circulation* 45:252, 1972
60. Gaasch WH, Cole JS, Quinones MA: Dynamic determinants of left ventricular diastolic pressure-volume relations in man. *Circulation* 51:317, 1975
61. Kreulen TH, Bove AA, McDonough MT, Sands MJ, Spann JF: The evaluation of left ventricular function in man. A comparison of methods. *Circulation* 51:677, 1975
62. Karliner JS, Gault JH, Eckberg D, Mullins CB, Ross J Jr: Mean velocity of fibre shortening: A simplified measure of left ventricular myocardial contractility. *Circulation* 44:323, 1971
63. Rushmer RG: Initial left ventricular impulse. A potential key to cardiac evaluation. *Circulation* 29:268, 1964
64. Spencer MP, Greiss FC: Dynamics of ventricular ejection. *Circ Res* 10:274, 1962

65. Levine HJ, Britman NA: Force-velocity relations in the intact dog heart.
J Clin Invest 43:1383, 1964
66. Spencer MP, Johnston FR, Denison AB Jr: Dynamics of the normal aorta.
Inertiance and compliance of the arterial system which transforms the
cardiac ejection pulse. Circ Res 6:491, 1958
67. Noble MM, Gabe IT, Trenchard D, Guz A: Blood pressure and flow
characteristics in the ascending aorta of conscious dogs. Cardiovasc Res 1:
9, 1967
68. Wilcken DEL, Charlier AA, Hoffman JIE, Guz A: Effects of alterations
of aortic impedance on the performance of ventricles. Circ Res 14:283, 1964
69. Noble MIM, Stubbs J, Trenchard D, Else W, Eisele JH, Guz A: Left
ventricular performance in conscious dog with chronically denervated heart.
Cardiovasc Res 6:457, 1972
70. Katz RL, Mills CJ: Use of a catheter tip electromagnetic velocity meter
to determine the cardiovascular effects of glucagon. Cardiovasc Res 5:62, 1971
71. Seed WA, Wood NB: Velocity patterns in the aorta. Cardiovasc Res 5:
319, 1971
72. Greenfield JC: Pressure gradient technic. Meth Med Res 11:83, 1966
73. Fry DL, Mallos AJ, Casper AGT: A catheter-tip method for measurement
of instantaneous aortic blood velocity. Circ Res 4:627, 1956

74. Benchimol A, Desser KB, Gartlan JL: Bidirectional blood flow velocity in the cardiac chambers and great vessels studied with the Doppler ultrasonic flowmeter. *Am J Med* 52:467, 1972
75. Ratshin RA, Royd CN, Rackley CE, Russell RO Jr: The accuracy of ventricular volume analysis by quantitative echocardiography in patients with coronary artery disease with and without wall motion abnormalities. (abstr) *Am J Cardiol* 33:164, 1974
76. Sweet RL, Moraski RE, Russell RO Jr, Rackley CE: Relationship between echocardiography, cardiac output, and abnormally contracting segments in patients with ischemic heart disease. *Circulation* 52:634, 1975
77. Bowyer AF, Jutzy RV, Coggin J, Crawford RB, Johns VJ: Contributions of ultrasound to the study of upright exercising man. *Am J Cardiol* 21:92, 1968
78. Carson P, Kantes L: Left ventricular wall movement in heart failure. *Br Med J* 4:77, 1971
79. Inoue K, Smulyan H, Mookherjee S, Eich RH: Ultrasonic measurement of ventricular wall motion in acute myocardial infarction. *Circulation* 43:778, 1971
80. Kraunz RF, Kennedy JW: An ultrasonic determination of left ventricular wall motion in normal man. Studies at rest and after exercise. *Am Heart J* 79:36, 1970
81. Kraunz RF, Ryan TJ: Ultrasound measurements of ventricular wall motion following administration of vasoactive drugs. *Am J Cardiol* 27:464, 1971

82. Wharton CF, Smithen CS, Sowton E: Changes in left ventricular movement after acute myocardial infarction measured by reflected ultrasound. *Br Med J* 4:75, 1971
83. Feigenbaum H, Popp RL, Chip JN, Haine CL: Left ventricular wall thickness measured by ultrasound. *Arch Intern Med* 121:391, 1968
84. Sjögren AL, Hytonen I, Frick MI: Ultrasonic measurements of left ventricular wall thickness. *Chest* 57:37, 1970
85. Troy BL, Pombo JF, Rackley CE: Ultrasonic measurements of left ventricular wall thickness and mass. (abstr) *Circulation* 42(Suppl III):III-38, 1970
86. Corya BC, Rasmussen S, Knoebel SB, Feigenbaum H: Echocardiography in acute myocardial infarction. *Am J Cardiol* 36:1, 1975
87. Franklin D, Sasayama S, McKown D, Kemper S, Ross J Jr: Ventricular wall thickness during acute coronary artery occlusion in conscious dogs. (abstr) *Circulation* 52 (Suppl II):II-65, 1975
88. Popp RL, Filly K, Brown OR, Harrison DC: Effect of transducer placement on echocardiographic measurement of left ventricular dimensions. *Am J Cardiol* 35:537, 1975
89. Edler I: Atrioventricular valve mobility in the living human heart recorded by ultrasound. *Acta Med Scan* 170 (Suppl 370):85, 1961
90. Edler I: Ultrasound cardiogram in mitral valve disease. *Acta Chim Scand* III:230, 1956.

91. Zaky A, Grabhorn L, Feigenbaum H: Movement of the mitral ring: a study in ultrasound cardiography. *Cardiovasc Res* 1:121, 1967
92. Laniado S, Yellin E, Kotler M, Levy L, Stadler J, Terdiman R: A study of the dynamic relations between the mitral valve echogram and phasic mitral flow. *Circulation* 51:104, 1975
93. Pohost GM, Dinsmore RE, Rubenstein JJ, O'Keefe DD, Grautham RN, Scully HE, Beierholm EA, Frederiksen JW, Weisfeldt ML, Daggett WM: The echocardiogram of the anterior leaflet of the mitral valve. *Circulation* 51:88, 1975
94. Rubenstein JJ, Pohost GM, Dinsmore RE, Harthorne JW: The echocardiographic determination of mitral valve opening and closure. Correlation with hemodynamic studies in man. *Circulation* 51:98, 1975
95. Laniado S, Yellin EL, Miller H, Frater RW: Temporal relation of the first heart sound to closure of the mitral valve. *Circulation* 47:1006, 1973
96. Duchak JM Jr, Chang S, Feigenbaum H: The posterior mitral valve echo and echocardiographic diagnosis of mitral stenosis. *Am J Cardiol* 29:628, 1972
97. Fisher JC, Chang S, Konecke LL, Feigenbaum H: Echocardiographic determination of mitral valve flow. *Am J Cardiol* 29:262, 1972
98. Pennock R, Kingsley B, Kawai N, Kimbiris D, Segal BL: Stroke volume and cardiac output measured by echocardiography. (abstr) *Am J Cardiol* 25:121, 1970

99. Konecke LL, Feigenbaum H, Chang S, Corya BC, Fischer JC:
Abnormal mitral valve motion in patients with elevated left ventricular diastolic pressures. *Circulation* 47:989, 1973
100. Edler I: Ultrasound cardiography. *Acta Med Scand* 370 (Suppl 170): 1, 1961
101. Joyner CR, Jr, Reid JM, Bond JP: Reflected ultrasound in the assessment of mitral valve disease. *Circulation* 23:503, 1963
102. Zaky A, Nasser WK, Feigenbaum H: A study of mitral valve action recorded by reflected ultrasound and its application in the diagnosis of mitral stenosis. *Circulation* 37:789, 1968
103. Zaky A, Steinmetz E, Feigenbaum H: Role of atrium in the closure of mitral valve in man. *Am J Physiol* 217:1652, 1969
104. Effert S: Pre and postoperative evaluation of mitral stenosis by ultrasound. *Am J Cardiol* 19:59, 1967
105. Parisi AF, Milton BG: Relation of mitral valve closure to the first heart sound in man. *Am J Cardiol* 32:779, 1973
106. Luisada AA, MacCanon D, Coleman B, Feigen LP: New studies on the first heart sound. *Am J Cardiol* 28:140, 1971
107. Quinones MA, Gaasch WH, Waisser E, Alexander JK: Reduction in the rate of diastolic descent of the mitral valve echogram in patients with altered left ventricular diastolic pressure-volume relations. *Circulation* 49:246, 1974

108. Decoodt PR, Mathey DG, Swan JHC: Abnormal left ventricular filling in coronary artery disease by automated analysis of echocardiograms. (abstr) *Circulation* 52 (Suppl II):II-133, 1975
109. Upton MT, Gibson DG, Brown DJ: Echocardiographic assessment of abnormal left ventricular relaxation in man. (abstr) *Circulation* 52(Suppl II): II-134, 1975
110. Upton MT, Gibson DG, Brown DJ: Instantaneous mitral valve leaflet velocity and its relation to left ventricular wall movement in normal subjects. *Br Heart J* 38:51, 1976
111. Feigenbaum H, Dillon JC, Haine CL, Chang S: Effect of elevated atrial component of left ventricular pressure on mitral valve closure.(abstr) *Am J Cardiol* 25:95, 1970
112. Yow MV, Reichek N: Left ventricular end-diastolic pressure and echocardiographic mitral valve closure. (abstr) *Circulation* 52(Suppl II):II-51, 1975
113. Bellhouse BJ: Fluid mechanics of a model mitral valve and left ventricle. *Cardiovasc Res* 6:199, 1972
114. Padula RT, Cowan GS Jr, Camishion RC: Photographic analysis of the active and passive components of cardiac valve action. *J Thorac Cardiovasc Surg* 56:790, 1968
115. Pridie RB, Oakley CM: Mechanism of mitral regurgitation in hypertrophic obstructive cardiomyopathy. *Br Heart J* 32:203, 1970
116. Wharton CFB, Lopez Bescos L: Mitral valve movement: A study using an ultrasound technique. *Br Heart J* 32:344, 1970
117. Brockman SK: Mechanism of the movements of the atrioventricular valves. *Am J Cardiol* 17:682, 1972
118. Gordon DA, Mathieu Y, Lipton I, Tsakiris AG: A study of mitral valve leaflet closure following isolated atrial contractions. (abstr) *Circulation* 49 and 50 (Suppl III): III-175, 1974

119. Henderson Y, Johnson FE: Two modes of closure of heart valves.
Heart 4:69, 1912
120. Sarnoff SJ, Gilmore JP, Mitchell JH: Influence of atrial contraction and relaxation on closure of mitral valve: Observations on effect of autonomic nerve activity. Circ Res 11:26, 1962
121. Rushmer RF, Finlayson BL, Nash AA: Movements of the mitral valve. Circ Res 4:337, 1956
122. Taylor DEM, Wade JD: The pattern of flow around the atrio-ventricular valves during diastolic ventricular filling. J Physiol 207:71, 1970
123. Taylor DEM: Mitral valve geometry and flow dynamics at varying heart rates in the dog. J Physiol 225:37, 1972
124. Dean AL Jr: The movements of mitral cusps in relation to the cardiac cycle. Am J Physiol 40:206, 1916
125. Luisada AA, MacCanon DM, Kumar S, Feigen LP: Changing views on the mechanism of the first and second heart sounds. Am Heart J 88:503, 1974
126. Shah PM, Kramer DH, Gramiak R: Influence of the timing of atrial systole on mitral valve closure and on the first heart sound in man. Am J Cardiol 26:231, 1970
127. Craige E, Burggraf G: Atrioventricular valve motion and the first heart sound in complete heart block. (abstr) Circulation 49 and 50 (Suppl III): III-86, 1974
128. Edler I, Gustafson A: Ultrasonic cardiogram in mitral stenosis. Acta Med Scand 159:85, 1957
129. Yoshitoshi Y, Sekiguchi H, Machii K, Kohashi Y, Shimizu S, Kuno H, Mishina Y, Ohta S: Measurement of the maximal velocity of mitral-valve closure and of the anterior ventricular wall movement by ultrasonic Doppler's method. Digest 6th Internat Conf Med Electr Biol Eng (Tokyo):35, 1965

130. Kingsley B, Linhart JW: Echocardiography. In, 'Advances in non-invasive diagnostic Cardiology', by Kingsley B, Linhart JW, Kantrowitz P. New Jersey, Charles B. Slack Inc, 1976, pp 95-161
131. Buynkozturk K, Kingsley B, Segal BL: The influence of heart rate, age and sex on the movements of mitral valve. *Acta Cardiologic (Brux)* T 27:427, 1972
132. Emerson R, Donnerstein R, Kronzon I, Schloss M, Glassman E: Maximal instantaneous mitral valve velocities measured with a digital echocardiographic tracking system. (abstr) *Am J Cardiol* 35:134, 1975
133. Sonnenblick EH, Napolitano LM, Daggett WM, Cooper T: An intrinsic neuromuscular basis for mitral valve motion in the dog. *Circ Res* 21: 9, 1967
134. Priola DV, Fellows SC, Moorehouse J, Sanchez R: Mechanical activity of canine mitral valve in situ. *Am J Physiol* 219:1647, 1970
135. Fenoglio JJ Jr, Pham TD, Wit AL, Bassett AL, Wagner BM: Canine mitral valve complex. Ultrastructure and electromechanical properties. *Circ Res* 31:417, 1972
136. Ratshin RA, Rackley CE, Russell RO Jr: Determination of left ventricular preload and afterload by quantitative echocardiography in man. *Circ Res* 34:711, 1974
137. Rankin LS, Moos S, Grossman W: Alterations in preload and ejection phase indices of left ventricular performance. *Circulation* 51:910, 1975
138. Quinones MA, Gaasch WH, Cole JS, Alexander JK: Echocardiographic determination of left ventricular-stress-velocity relations in man with reference to the effects of loading and contractility. *Circulation* 51:619, 1975

B30170